NEXT FRONTIER MIMO-OFDM BASED WIRELESS COMMUNICATION SYSTEM

Innovative Scientific Publication

Authors

Dr. Balram D. Timande

Dr. Hemant Vithalrao Hajare

Next Frontier MIMO-OFDM Based Wireless Communication System

Authors

Dr. Balram D. Timande

Associate Professor, Electronics & Telecommunication Engineering

Guru Nanak Institute of Engineering & Technology. Nagpur

Dr. Hemant Vithalrao Hajare

Principal

Guru Nanak Institute of Engineering & Technology. Nagpur

Published by

Innovative Scientific Publication, Nagpur

Published By

Innovative Scientific Publication

Nagpur (MS), India

Email: ijiesjournal@gmail.com

Ph: 7972481655

http://ijies.net/books

1st Edition: March, 2023

ISBN: 978-81-968730-4-2

Price: 400 INR

About the Authors

Dr. Balram D. Timande is working as an Associate Professor in the Department of Electronics and Telecommunication Engineering at Guru Nanak Institute of Engineering and Technology, Nagpur, Maharashtra, India. He graduated with a B.E. in Electronics Engineering from R.T.M.N.U., Nagpur University (M.S.), and obtained his postgraduate degree (M. Tech.) in Electronics and Telecommunication Engineering from C.S.V.T.U., Bhilai, C.G., India. He was awarded a Ph.D. in Electronics Engineering from MATS University, Raipur, C.G., India. With over 29 years of experience, Dr. Timande has been actively worked in Industry for more than 09 years and has been engaged in research and teaching activities for more than 20 years. He has published over 22 research papers in reputed, Scopus-indexed, and SCI-E international journals, and has presented numerous papers at national journals, National and International conferences. His primary areas of research interest include Embedded System Design, Wireless Communications, Ad-hoc Sensor Networks, and Industrial Instrumentation.

Dr. Hemant Vithalrao Hajare is working as the Principal at Guru Nanak Institute of Engineering and Technology, Nagpur, Maharashtra, India. He graduated with a B.E. in Civil Engineering and earned his postgraduate degree (M.Tech) in Hydraulics from Visvesvaraya Regional College of Engineering (VRCE), affiliated with R.T.M.N.U., Nagpur University (M.S.). He was awarded a Ph.D. in Civil Engineering from NEERI, RTMNU, Nagpur. With over 35 years of teaching experience, he also possesses administrative experience, having served as Principal, Dean of Academics, and Head of Department for more than 35 years.Dr. Hajare has been actively involved with various professional societies and has served on various statutory bodies of different universities. Engaged in research and teaching for over 20 years, he has published more than 40 research papers in reputed, Scopus-indexed, and SCI-E international journals. He has also presented numerous papers at national and international conferences. His primary areas of research interest include Hydraulic Engineering, Water Resources Engineering, and Irrigation Engineering.

PREFACE

This book contains basics of the MIMO-OFDM system which provide substantial growth in capacity and throughput along with reliability because of antenna diversity. To achieve this, the MIMO system doesn't require any extra bandwidth or transmission power, which is again in favor of the wireless system design. Thus the MIMO and OFDM systems are executing key roles in the existing as well as future generations to make them sophisticated and popular. Although there are many advantages of MIMO-OFDM systems, it is observed that the wireless channel even in a slow fading environment is vulnerable to different error rates like 'bit-error-rate (BER)', 'symbol-error- rates (SER)', and 'Frame-error- rates (FER)'. Similarly, this technology is also susceptible to inter-symbol and inter-carrier interferences because of high PAPR and failure of orthogonality in the OFDM system. The OFDM system also needs very accurate frequency synchronization between transmitter and receivers. This is because of the presence of closely placed narrow-band sub-carriers. The slight change in frequency may lead to carrier frequency offset (CFO). Many factors affect the synchronization like characteristics of devices manufactured by different manufacturers may not similar or may vary from the nominal specification, temperature, and aging effect may be the reason of CFO. Another reason for CFO is the relative motion between transmitter and receiver. This is known as the Doppler shift effect. However, the Doppler shift is much less than oscillators frequency still, it can degrade the quality of received signals. The CFO can destroy the orthogonality of sub-channels and lead to ICI. The effect of the above-listed factors resisting the advancement and applications of the future wireless system are motivating us to produce this research work in the form of book.

Chapter 1 under the heading of introduction, the history of wireless communication and the classification and features of the next-generation wireless system have been discussed. Background and overview of an OFDM system, MIMO system separately have been illustrated along with the merits and demerits of the combination of the MIMO-OFDM system which has been successfully employed in earlier wireless

systems (1G to 3G) and is being investigated and analyzed for the next-generation wireless system. The rest of the book is planned into different chapters summarized as follows;

Chapter 2 illustrates the review of the literature from the research articles by renowned researchers and academicians. The review process is classified according to various issues faced by MIMO-OFDM wireless communication systems, such as error rate performance, PAPR reduction, Capacity improvement, and Code-based performance evaluation of the MIMO-OFDM System. In each case, the methodologies used by the researcher and their results have been illustrated.

Chapter 3 deals with details on features, basic concepts, and design issues in MIMO-OFDM systems. Beginning from the basic single carrier modulation (SCM) system, the basic idea behind the OFDM system has been illustrated. The advantages of diversity concepts in the MIMO system have been explained, and finally, the basic architecture of the MIMO-OFDM system has been discussed.

Chapter 4 deals with problem identification and the methodology used for the fulfillment of proposed research work. This chapter is classified according to issues encountered in MIMO-OFDM wireless communication systems and each method has been illustrated using detailed mathematical expressions. Methodologies included in this chapter are BER performance and probability of error analysis using different constellation schemes; PAPR reduction methods using ICF and SLM schemes; performance investigation of MIMO-OFDM System over Multipath fading Channels; performance Evaluation of MIMO-OFDM System using transmit beamforming (Alamouti STBC scheme) and receive beamforming (MRC scheme). Channel capacity (ergodic as well as outage capacity) has been elaborated using proper mathematical expression.

Chapter 5 demonstrates the performance investigation of the proposed MIMO-OFDM wireless communication system, via simulation results of various methodologies used. This chapter includes the illustration of simulation results of the different algorithms employed for error rate improvement, PAPR reduction, and channel capacity enhancement.

Chapter 6 deals with the conclusion of the overall research work done and future scopes to the overall contribution of this book.

In particular, this book will be very useful for B.Tech. (Under graduates), M.Tech. (post graduates) and Ph.D. researchers in the field of next frontier wireless communication.

ACKNOWLEDGEMENT

"Writing a book is a journey that requires the support and encouragement of many individuals along the way. I am deeply grateful to everyone who has contributed to the creation of this Book."

First and foremost, I wanted to state from the bottom of my heart that, throughout the writing of this book I have received a great deal of support and assistance. I owe my heartfelt gratitude to my mentor Dr. Hemant V. Hajare, Principal GNIET, Nagpur. He provides me the benefit of his valuable time and exposure by rendering his precious knowledge and help during my journey of research. His patience, approach and unquestioning support, and trust in me have made this Book possible. I am delighted to introduce him as a co-author of this book since, his expertise was invaluable in formulating the research questions and methodology, MATLAB programming and simulation. I wanted to express my heartfelt gratitude for taking the time to proofread and correct the English grammar in my book. His meticulous attention to detail and expertise have truly enhanced the quality of the manuscript. His contributions have not only improved the clarity and readability of the text but have also helped to elevate the overall professionalism of the book. His dedication to ensuring accuracy and precision has been invaluable, and I am incredibly thankful for your assistance throughout this process. Your support and guidance have been instrumental in bringing this project to fruition.

Last but not the least; we cannot forget our friends and well-wishers who support me for the completion of this book. Finally, we are also gratified to our family members, and everyone around us who directly or indirectly contributed every bit in helping us to finish this book on time.

TABLE OF CONTENTS

Abstract

In today's modern era the speed of the mobile communication system plays an important role in human life. As numbers of customers and applications are rapidly increasing, there is a necessity for improvement in the speed of the network and high data rate capability for the optimum use of mobile applications. From the beginning of first-generation mobile communication, speed and throughput were the critical issues in the wireless communication system. That motivated researchers to improve the speed and throughput of the network. When 3G and 4G are not fulfilling the gap of speed in humans and their use, it is important to design an advanced 5G mobile communication system. 5G is intending to target a higher data rate capacity at high speed compared to the current 4G system, with a higher density of mobile broadband customers. The blend of Multiple-input multiple-output (MIMO) wireless technology with orthogonal frequency-division multiplexing (OFDM) is a highly efficient and popular technology that is still performing better in past and future generation wireless systems for achieving targets discussed above. Besides many advantages of MIMO and OFDM schemes, the wireless communication system using the MIMO-OFDM scheme faces many challenges, such as bit error rates (BER), inter-symbol interference (ISI), high peak to average power ratio (PAPR) which in turn breaks the orthogonality in the OFDM system causing inter-carrier interference (ICI). The information throughput or capacity of a wireless system can be improved by increasing the number of antennas at receiving and transmitting end but at cost of computational complexity. Also, in the MIMO system maintaining space between antennas is to have un-correlated fading paths and to reduce cross-correlation and inter-antenna interference.

Intending to grow accessible wireless systems able to meet the requests of information-intensive applications, the proposed technology dynamically in gaining radio frequency data transfer capacity. Along these lines, we must look to innovations to create more throughputs from existing data transfer capacity and expanding the channel capacity. In this research, various techniques for improving error rate and capacity or throughput using different constellation schemes along with different sets of antennas in the MIMO system such as transmit beamforming scheme (Alamouti STBC scheme), receive beamforming scheme (MRC scheme) have been employed, and analyzed for error rate performance. The STBC coding scheme is used to achieve better spatial diversity that improves the system performance in terms of data rate and

reliability. The iterative clipping and filtering scheme and selective mapping scheme along with cyclic prefixes are employed and analyzed for PAPR reduction to maintain the orthogonality and hence to avoid ISI and ICI in the proposed system. The simulation results in the result section depict that, to achieve the BER value of 10^{-4} the MRC Scheme with (1×2) and (1×4) antenna system outperforms the Alamouti STBC coded MIMO-OFDM scheme with (2×1) by SNR of 2 dB and 11 dB respectively. Similarly, the Alamouti STBC coded MIMO-OFDM scheme with (2×2) antenna system outperform MRC Scheme with (1×2)system by 4.8 dB SNR to achieve BER value of 10^{-4}, on the other hand, MRC Scheme with (1×4)system outperforms the Alamouti STBC coded MIMO-OFDM scheme with (2×2) system by SNR of 3 dB. The PAPR reduction performance of the proposed scheme using ICF techniques outperforms the SLM technique by 2.8 dB at the CCDF of 10^{-4}. Different antenna system $(M_T \times M_R)$ have been employed and analyzed and the results depict that increasing number of antennas at the transmitter and the receiver gives a substantial increase in the capacity of the wireless system, for example at the SNR of 20 dB, (2×2), (3×3) and (4×5) antenna system provides the channel capacity of 11.31, 16.77, and 24.74 b/s/Hz respectively.

List of Tables

List of Figures

List of Abbreviations / Symbols

3GPP	Third Generation Partnership Project
ADC	Analog-to-digital converter
AWGN	Additive White Gaussian Noise
BER	Bit Error Rate
BPSK	Binary Phase Shift Keying
CCDF	Complementary Cumulative Distribution Function
CDF	Cumulative Distribution Function
CDMA	Code Division Multiplexing Access
CF	Crest Factor
CFO	Carrier frequency offset
CIR	Channel Impulse Response
CP	Cyclic prefix
CSI	Channel State Information
DAB	Digital Audio Broadcast
DAC	Digital-to-analog converter
D-BLAST	Diagonal Bell Labs layered space–time
DCT	Discrete Cosine Transform
DFT	Discrete Fourier Transform
DMT	Discrete multi tone
DVB	Digital Video Broadcasting
EGC	Equal-gain combining
EM	Expectation maximization
FDM	Frequency Division Multiplexing
FDMA	Frequency-division multiple access
FFT	Fast Fourier Transform
FSK	Frequency shift keying
GA	Genetic Algorithm
GPRS	General Packet Radio Service
H-BLAST	Horizontal Bell Labs layered space–time
HSDPA	High Speed Downlink Packet Access

ICI	Inter Carrier Interference
IEEE	Institute of Electrical and electronics engineers
IDFT	Inverse discrete Fourier transform
IFFT	Inverse Fast Fourier Transform
IP	Internet protocol
ISI	Inter Symbol Interference
LAN	Local Area Network
LOS	Line of sight
LS	Least Square
LTE	Long Term Evolution
MAN	Metropolitan Area Network
MCM	Multicarrier Communication
MIMO	Multi-Input-Multi-Output
MISO	Multiple-input single-output
ML	Maximum Likelihood
MMSE	Mean Square Error Estimation
MRC	Maximal ratio combining
MSE	Mean Square Error
MUD	Multi User Detection
NLMS	Normalized least mean square
OFDM	Orthogonal Frequency Division Multiplexing
OFDMA	Orthogonal frequency-division multiple access
PAPR	Peak to Average Power Ratio
PDF	Probability Density Function
PSK	Phase shift keying
PTS	Partial Transmit Sequence
QAM	Quadrature Amplitude Modulation
QoS	Quality of service
QPSK	Quadrature Phase Shift Keying
RF	Radio Frequency
SCM	Single carrier modulation
SCO	Sampling clock offset
SDMA	Space Division Multiple Access

SER	Symbol Error Rate
SFBC	Space–frequency block code
SIMO	Single-input multiple-output
SISO	Single-input single-output
SLM	Selective Mapping
SM	Spatial multiplexing
SNR	Signal-to-noise ratio
STBC	Space–time block code
STC	Space–time code
STFBC	Space–time–frequency block code
STTC	Space–time trellis code
SVD	Singular value decomposition
TDMA	Time-division multiple access
UFMC	Universal filtered multi-carrier.
UWB	Ultra wideband
VBLAST	Vertical-Bell Laboratories Layered Space-Time
VoIP	Voice over Internet Protocol
WAN	Wide area network
Wi-Fi	Wireless Fidelity
Wi Max	Worldwide Interoperability for Microwave Access
WLAN	Wireless Local Area Network
ZF	Zero forcing
ZP	Zero padding

Chapter 1
Introduction

1.1 INTRODUCTION

Transmission of information or data or signals over meters to thousands of kilometers through space without using wired lines is known as wireless communication. Wireless communication is not only used for the communication between people but also things (IoT) and devices or systems. The applications of wireless are not only limited to the cellular telephonic system but also it is used for internet browsing, networking of working places or homes, internet of things (IoT), wireless devices used in computer systems, radiofrequency applications, GPS, etc.

1.1.1 History of wireless communication

The history begins with the theory of electro-magnetism. The transmission and acceptance of information, data signals, or symbols using the electromagnetic system is known as telecommunication. This definition was first given by ITU (International Telecommunication Union). The theory of electromagnetism was first invented by Hans Christian Oersted and Andre-Marie Ampere in the decade of 1820. Using electromagnetic theory, Joseph Henry and Samuel Morse established electrical telegraphy in 1832. In the US, the electrical telegraphy networks were used first in 1840. In 1864, James Clerk Maxwell introduced wireless propagation via electromagnetic waves and it was confirmed and verified by Heinrich Hertz in 1887. Marconi performed radiotelegraphy experiments, got a patent for the wireless system last decade of the 19th century between1895-1897. After 1897 things were not changed for many years, Americans referred to this transmission of information through the electromagnetic wave as a Radio, because transmitters were radiating the information using electromagnetic waves. Since the information or signals were transmitted with no wire link or wired connection between transmitter and receiver, British nationals were referring to this communication as wireless and in 1923 the BBC (British Broadcasting Company) was the first company who use the word

wireless. Things were transformed after 1923 because of advancements in integrated circuits since the wired telephony was fixed in one place and peoples were not free to use it anywhere. Also, the application of wired telephony was very limited. Thus mobile cellular system comes into existence in the decade of 1970s. This technology was friendly and workable for electronic mails, database accessing from remote places, and messaging services. In this era of the 1970s, Bell Laboratories had taken a foremost responsibility in the development of the novel mobile/cellular technology. Initially, NMT (Nordic Mobile Telephone) cellular system established closed cooperation between different operators (PTTs) in European countries. Later the US also agree on common standards and protocols of the analog AMPS system and captured 2/3rd mobile subscribers worldwide. The European PTT administrators agreed on a common protocol for cellular wireless networks in the 1980s referred to as GSM. The GSM is a French acronym for Groupe Special Mobile, the international group of European PTT administrators. The new standards for Pan-European digital mobile communication were developed in 1992 called a GSM cellular system. The advantage of common standards was that it allows international roaming across many European countries. Also, the key benefits of digital communication systems were transmission capacity per unit of the spectrum, encryption facility, data security, and the ability to combat wireless link impairments. A brief history of wireless communication can be viewed at a glance is shown in table 1.1.

1.1.2 New generation wireless technology overview.

Every generation of cellular services signifies a big contribution to the quality of services, speed, and capacity of information transmission. The journey of generation ‘G’ of cellular communication started with first-generation 1G in 1979. As the speed, capacity, bandwidth, and user applications increase because of advancements in technology, the generation of cellular telephony changed from the previous generation to the next generation. Table 1.1 shows the evolution of different generations of wireless technologies. The evolution of different generation wireless systems and the specification are depicted in table 1.2.Table 1.1 History of wireless communication.

Table 1.1 History of wireless communication

Year	Description
1866	Dr. Mahlon Loomis, patented a wireless transmission (22km)
1882	Amos Emerson Dolbear, patented wireless transmission system using telephone receiver, microphone and Induction coil.
1885	Thomas Edison patented electrostatic induction based wireless transmission system.
1895	Marconi generated and detected a coded message at a distance of 1.75 miles. Indian physicist, Dr. Jagadish Chandra Bose transmitted and received wireless signals using microwave devices.
1897	Marconi demonstrated a radio transmission system for 18 miles. Established first Wireless Telegraph and Signal Company.
1900	Tesla demonstrated a system for detecting an object using radio waves – (RADAR).
1918	Armstrong invented the Super-heterodyne Radio Receiver using 8 valves
1929	L. Cohen proposed resonant transmission line for radio reception. H.A. Affel and L. Espenscheid of AT&T/Bell Labs demonstrated the concept of coaxial cable for a FDMA multi-channel telephony system.
1932	International Telecommunications Union (ITU) formed and the word Telecommunication coined by ITU.
1933	Armstrong demonstrated Frequency Modulation (FM) and proposed FM radio in 1936.
1934	FCC (Federal Communications Commission) formed in US
1944	Time-Division Multiplexing (TDMA) was invented. Radio Research Lab developed radar countermeasures (jamming) in the 25 MHz to 6 GHz range.
1948	Shannon laid out the theoretical foundations of digital communications
1955	John R. Pierce proposed application of satellites for communications.
1969	The first digital radio-relay system begins its operation in Japan using 2 GHz operating frequency.
1974	FCC allocate 40 MHz for cellular telephony
1978	AT&T Bell Labs started testing a mobile telephone system based on cells.
1982	GSM (Group Special Mobile) established
1984	Initial deployment of AMPS cellular system.
1990	Formation of IEEE 802.11 Working Group to define standards for Wireless Local Area Networks (WLANs)
1993	CDMA (Code Division Multiple Access)
1994	PDCC (Personal Digital Cellular Operable) in Tokyo, Japan
1995	CDMA operable in Hong Kong
1996	Six Broad Band PCS (Personal Communication Services) licensed bands (120 MHz)
1997	Broadband CDMA constructed and 3rd generation mobile.
1999	WLAN systems, Bluetooth, using the 2.4 MHz spectrum.
1997	Release of IEEE 802.11 WLAN protocol, supporting 1-2 Mbit/s data rates in the 2.4 GHz ISM band
1999	Release of IEEE 802.11b WLAN protocol, supporting 1-11 Mbit/s data rates in the 2.4 GHz ISM band
1999	Release of IEEE 802.11a WLAN protocol, supporting 1-54 Mbit/s data rates in the 5 GHz ISM band
2003	Release of IEEE 802.11g WLAN protocol, supporting 1-54 Mbit/s data rates in the 2.4 GHz ISM band
2009	Release of IEEE 802.11n WLAN protocol, supporting up to 150 Mbit/s data rates in both the 2.4 GHz and 5 GHz ISM bands

Table 1.2 Evolution of different generations of wireless communication

Generation →	**1G**	**2G**	**3G**	**4G**	**5G**
Year of launching →	1979-80	1993	2001	2009	2018
Technology	AMPS (Advanced Mobile Phone System), NMT, TACS	GSM	WCDMA	LTE, WiMAX	MIMO, mm Waves
Access System	FDMA	TDMA, CDMA	CDMA	CDMA	OFDM, BDMA
Switching type	Circuit switching	Circuit switching for voice and packet switching for data	packet switching	packet switching	packet switching
Internet Service	No Internet	Narrow Band	Broad-Band	Ultra-Broadband	Wireless World Wide Web
Bandwidth	Analog communication	25 MHz	25 MHz	100 MHz	30GHz to 300 GHz
Speed	2.4 Kbps to 14.4 Kbps	64 Kbps	200 Kbps (IMT-2000) 21.6 Mbps (HSPA+)	100 Mbps (Walking) 1Gbps (Stationary)	More than 1Gbps

Advantages of next-generation (4th to 5th generation) technology:

1. High resolution
2. Bidirectional large bandwidth
3. Technology for subscriber supervision and security tools
4. Provides an enormous capacity (Gbps)
5. Easily upgradable from the previous generations
6. Provides uniform, uninterrupted, and consistent connectivity across the World

Disadvantages or limitations of next-generation (4th to 5th generation) technology:

1. It is very difficult to achieve the target of claimed speed due to lack of infrastructure, incompetent technological support worldwide.
2. The cellular phone which was designed for 3rd generation becomes useless in next generation (4th and 5th generation) wireless technology.

Applications of next-generation (4th to 5th generation) technology:

1. High-quality or resolution video streaming
2. Ultra-high transmitting and receiving speed
3. IoT, Internet of things
4. AI, Artificial Intelligence
5. Automobile advancements
6. Robotics
7. Healthcare or Patient care at remote places
8. Defense technology and many more

1.2 BACKGROUND AND MOTIVATION

1.2.1 Background of OFDM system

Today, there is an overwhelming need for high-speed data transfer and reliable wireless communication with high data rates to meet the demands of users and their applications such as video streaming, electronic mail, Internet browsing, bulk data transfer, and real-time applications. It is very challenging to provide such a reliable and high-speed network in a wireless environment that can transmit massive amounts of data from source to destination. Unlike wired communication, in the wireless environment, there are many obstacles in the transmission path, like trees, hills, monumental buildings, and many more which cause deterioration in the signal quality. In addition to the direct path (line of sight, LOS) of receiving, the transmitted signal reaches the receiver via multiple time-delayed paths because of refraction, reflection, and absorption from the different obstacles present in the wireless environment. Also, depending upon the distance between the base station and the mobile station, the transmitted signal is randomly attenuated because of absorption by several objects in the transmission path. Multiple replicas of the originally transmitted signal with random signal strength are received at the receiving station through multiple delayed paths. These replicas add up either constructively or destructively, causing a severe degradation in the system's signal quality performance. This is called fading in wireless communication. The fading of

the signal is shown in fig.1.1. The relative motion between transmitters and receivers in a fading environment results in an increase in the power spectrum. Similarly, the wireless medium is shared by multiple users and their applications, resulting in mutual interference between different users. In addition to the challenges faced by wireless links in a fading environment, wireless networks also have other significant issues such as bandwidth availability, transmission power constraints, hardware complexity, and overall system cost.

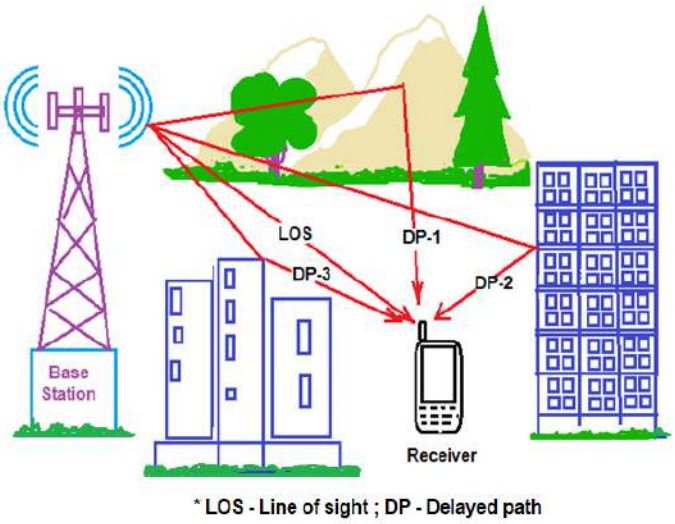

Fig. 1.1 Wireless propagation through a fading channel

In wireless systems, we have a limited spectrum in which it is very difficult to accommodate many users and their applications. One of the simpler solutions to improve bandwidth is to use higher-order modulation techniques; however, this solution can degrade signal quality compared to lower-order modulation if the transmitting power is not raised to a specific level. One of the most suitable and effective solutions for reliable communication over a wireless link is to apply various diversity techniques such as frequency, time, space, antenna, and modulation diversity. When a signal is transmitted through a wireless environment, only a small amount of signal power reaches the receiver due to path loss or fading effects. To overcome this problem, the most noticeable solution is to increase the transmitting power by using a special type of antenna system [1]. But there is a limit to the use of transmitting power in battery-operated devices. The equipment designed for low-power applications tends to be unable to accommodate network protocols and

sophisticated technologies to handle mobility. Similarly using specialized antenna systems to maintain QoS and high SNR can lead to increased hardware complexity and ultimately system cost. The application of an 'Orthogonal Frequency Division Multiplexing (ODFM)' scheme is important to reduce the after effects of channel fading. The basic block diagram of an OFDM transmitter and receiver is shown in fig. 1.2. The OFDM scheme is a 'multi-carrier modulating (MCM)' system where a wideband signal is divided into n number of narrow-band frequency flat signals to avoid frequency selective fading. In the OFDM scheme, individual narrow-band signals are referred to as sub-carriers. The orthogonal placing of the subcarriers in OFDM systems minimizes the possibility of 'inter-symbol interference (ISI)'. A 'single-carrier modulation (SCM)' system shown in fig 1.3 requires a guard signal between two adjacent symbols with a very complex equalization technique to avoid ISI. Whereas a multi-carrier modulation scheme like OFDM does not require any complex signal processing algorithms. Instead in the OFDM scheme simple IDFT/IFFT and DFT/FFT signal processing techniques can be efficiently used. In SCM, energy of each symbol is distributed over the whole bandwidth therefore; there is a minor effect on error probability. The output signal of SCM depicts a small crest factor; on the other hand, OFDM output depicts a Gaussian distribution [2], [3].

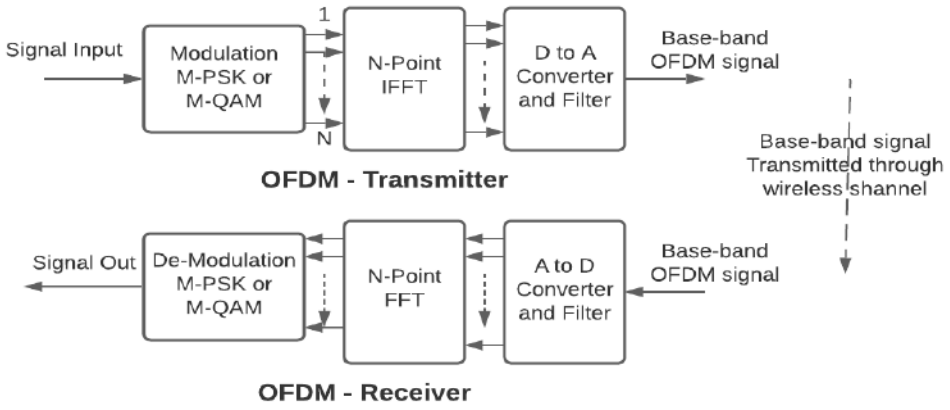

Fig. 1.2 Simple block diagram of OFDM transmitter and receiver

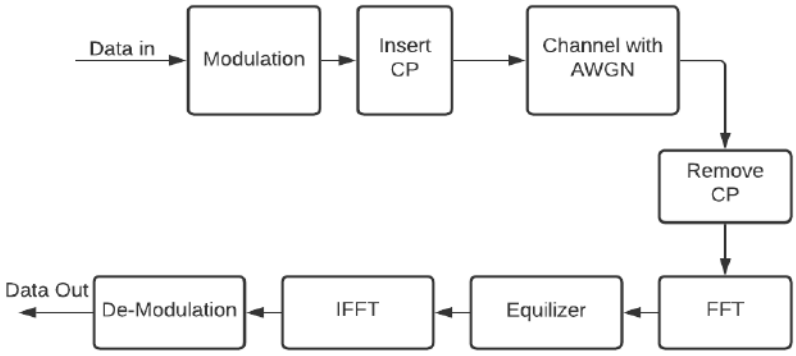

Fig. 1.3 Block diagram of SCM with frequency domain equalization

The single carrier system is susceptible to ISI because of the high data rate. To avoid ISI a symbol duration '*Tsym'* should be greater than the maximum symbol period $(\tau_{sym} > \tau_{max})$. Therefore to reduce the ISI symbol duration must be increased somehow. This can be done by introducing guard signals between neighboring symbols. For example, if the available bandwidth (W) is 1MHz, the symbol transmission rate is1 μs, and the maximum delay spread is 10 μs, then ISI will be occurred in at least 10 consecutive symbols. To avoid this duration of symbols to be transmitted must be greater than or equal to 10 μs. Thus to avoid the ISI guard band of a specific duration must be added between the symbols such that the total symbol period becomes greater than or equal to 10 μs. But, due to this extra overhead in the symbol period, the data rate is reduced [4].

The OFDM modulation technique is the most effective and efficient MCM technique [5] where the data signal is transmitted using 'N' numbers of orthogonally spaced sub-carriers. If 'W' is the available bandwidth, then the bandwidth of each subcarrier in OFDM system will be (W/N) [6]. Due to this fact, the OFDM system maintains the same data rate as the SCM due to the presence of multiple sub-carriers, despite the lower symbol transmission rate in OFDM. The most important feature of an OFDM system is that it is less sensitive to ISI, optimizes power and bandwidth, avoids complex equalization techniques, and provides high spectral efficiency. These characteristics make the OFDM system the most efficient solution for future wireless systems to meet the need for high speed and highly reliable communication [7].

1.2.1.1 Advantages and disadvantages of the OFDM system.

Advantages:

Following are the major advantages of the OFDM system;

1. It is able to combat ISI.
2. It is able to fight against ICI if orthogonality of the OFDM system is maintained.
3. It offers high spectral efficiency.
4. The OFDM system is robust against frequency selective fading compared to SCM.
5. In, OFDM offers low complexity using a ‘maximum likelihood (ML)’ decoder to provide better system performance.
6. One can integrate the OFDM system with the MIMO system to enhance the speed, capacity, and trustworthiness of the communication system.

Disadvantages:

1. Signal distortion occurs due to frequency mismatch between transmitter and receiver.
2. Practically in the OFDM system, channel variation may occur even at slow fading, which may destroy the orthogonality and become the cause of ICI.
3. The 'Cyclic Prefix (CP)' or guard signal added to each symbol to reduce ISI in the OFDM system decreases the data rates. Similarly, the equalization technique, space-time coding techniques used to reduce channel interference may increase the complexity.
4. High ‘peak to average power ratio (PAPR)’ in OFDM causes failure of orthogonality which results in ICI.

1.2.2 Background of the MIMO system

The deteriorating effect of multipath fading can be mitigated using antenna diversity or spatial diversity, which can be achieved using multiple transmitting and receiving antennas. Such antenna system is known as ‘multiple-input multiple-output (MIMO)’ systems. The key benefit of the MIMO system is to increase data rate

substantially and to improve system reliability by improving error rates probabilities. In the MIMO system above benefits can be achieved without using the additional increase in channel bandwidth or transmission power [8]. Different antenna diversity schemes are shown in fig.1. 4. In a MIMO system, hardware complexity and power requirements are major issues due to the need for separate radio frequency (RF) chains at each antenna of the transmitter and receiver. Furthermore, the RF chain operates in the same frequency band, so their isolation is essential for the proper functioning of the transmitter and receiver.

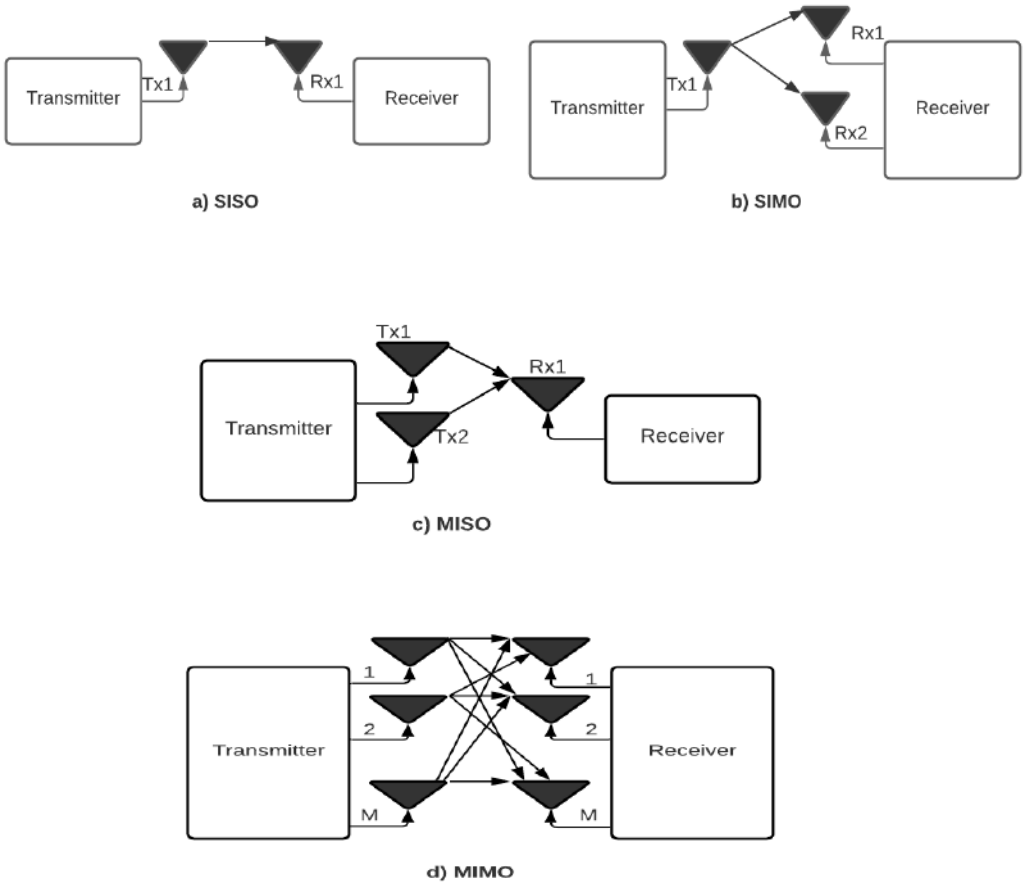

Fig. 1.4 Various antenna diversity schemes a) SISO, b) SIMO, c) MISO), d) MIMO

1.2. 3 Overview of the MIMO-OFDM system

As discussed in the above sections, today there is a substantial need for high speed and reliable wireless communication systems capable of providing multimedia services, such as high definition (HD) video streaming, ultra high-speed data

transfer, high security, and network enabled real time IoT control etc. In addition, virtual reality and multiplayer gaming are on the rise, requiring high-speed and energy-efficient systems as many devices today are battery-powered. To fulfill these demands, there is a need for substantial capacity, minimum interferences, zero packet loss, lower latency, and an energy-efficient wireless system [9]. Modern wireless systems like 'Ultra-Wideband (UWB)', 'space time-coded (STC)' systems such as 'space-time block- coded (STBC)' 'Space-time trellis-coded (STTC) 'space division multiple access (SDMA)', and beamforming MIMO systems offer significant gain. The future generation of wireless communication systems aims for providing all kinds of multimedia services. Undoubtedly, the ultra-high-speed and trustworthy wireless network providing ultra-high security against channel impairments in the fading environment requires further improved wireless system architectures [10]. The future wireless systems may comprise many wireless devices. The requirement of additional bandwidth to accommodate numerous applications may incur the challenge of exploitation of available spectral resources. Among various available technologies in the wireless system, the OFDM technology has many advantages and attracted the interest of researchers in this field. The merger of OFDM and MIMO technology has emerged as an efficient technology in the next-frontier wireless systems. However, the performance of the MIMO-OFDM system may be seriously affected because of various channel impairments as a result of fading, which results in many deleterious effects like packet loss and decoding failure [11]. Figure 1.5 depicts a simple architecture of the MIMO-OFDM system.

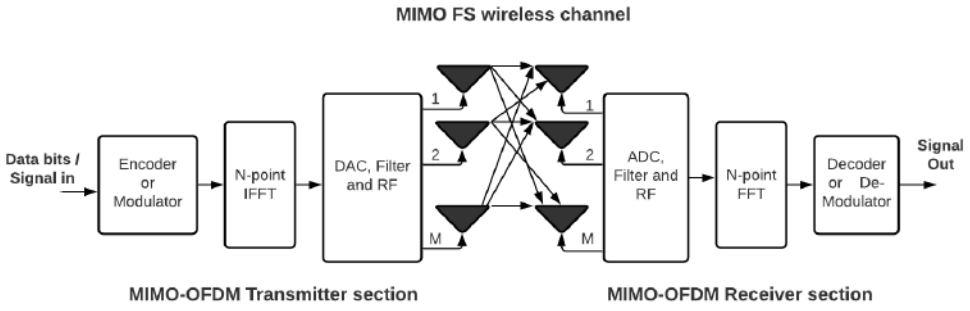

Fig. 1.5 Simple MIMO-OFDM block diagram

1.2.4 Motivation

Unprecedented growth in the advancement of wireless technology connects the entire world with ultra high-speed digital wireless communication. Due to this enormous growth in requirement of the ultra high speed the world is switching towards next-generation 5G technologies [12], [13]. Switching from the current generation to the next generation comes across many challenges while dealing with various wireless protocols and standards like IEEE 802.11a, IEEE 802.16a, etc. The primary objective of new generation technology is to optimize the resulting complexity of the combination of different schemes and algorithms. This combination is necessary to achieve ultra high speed with negligible error i.e. high quality of services and to make optimum use of available bandwidth etc. As discussed above in section 1.2.1., in a multipath fading environment the OFDM system is a promising technology that effectively combats ICI and ISI. In an OFDM system, the frequency selective fading channel is divided into several flat fading channels known as sub-channels or sub-carriers. All the subcarriers remain orthogonal to each other which make the OFDM system robust against ISI. Similarly, orthogonality can be retained by reducing PAPR, which results in reducing ICI. In Section 1.2.2., the basics of the MIMO system have been discussed which provide substantial growth in capacity and throughput along with reliability because of antenna diversity. To achieve this, the MIMO system doesn't require any extra bandwidth or transmission power, which is again in favor of the wireless system design. Thus the MIMO and OFDM systems are executing key roles in the existing as well as future generations to make them sophisticated and popular [14]. Further, the antenna diversity or spatial diversity provided by MIMO systems can be combined with other diversities for improving system performance. The spatial diversity can be combined with channel coding referred to as space-time coding to achieve new heights in wireless communication in terms of reliability and transmission rates [8]. Incorporating MIMO and OFDM technology prohibits the target wireless system from frequency selective fading without the application of complex equalizers. MIMO-OFDM is the gifted technology for the most trustworthy communication systems [11]. The MIMO-OFDM schemes using spatial diversity

and the high spectral efficiency provide remarkably high capacity, transmission rates, and robustness against channel impairments [15]. MIMO-OFDM system has been adopted in various standards Wi-Fi, LTE, and LTE Advanced or 3GPP, Wi-MAX, IEEE 802.16m, WLAN / IEEE802.11n [14], [16]. Although there are many advantages of MIMO-OFDM systems, it is observed that the wireless channel even in a slow fading environment is vulnerable to different error rates like 'bit-error-rate (BER)', 'symbol-error- rates (SER)', and 'Frame-error- rates (FER)'. Similarly, this technology is also susceptible to inter-symbol and inter-carrier interferences because of high PAPR and failure of orthogonality in the OFDM system. The OFDM system also needs very accurate frequency synchronization between transmitter and receivers. This is because of the presence of closely placed narrow-band sub-carriers. The slight change in frequency may lead to carrier frequency offset (CFO). Many factors affect the synchronization like characteristics of devices manufactured by different manufacturers may not similar or may vary from the nominal specification, temperature, and aging effect may be the reason of CFO. Another reason for CFO is the relative motion between transmitter and receiver. This is known as the Doppler shift effect. However, the Doppler shift is much less than oscillators frequency still, it can degrade the quality of received signals. The CFO can destroy the orthogonality of sub-channels and lead to ICI. The effect of the above-listed factors resisting the advancement and applications of the future wireless system are motivating to carry out this research work.

Many techniques, coding, and algorithms have been already used for the mitigation of error rates, PAPR, interferences like ISI and ICI and to enhance the speed, channel capacity, or information rates in wireless communication. However, the excellent features of MIMO and OFDM systems are not fully used. The methods used for the mitigation and improvement of the above-listed factors that limit the performance of the wireless systems can be improved further to achieve the optimum capability of the MIMO-OFDM wireless communication system. This research work is mainly focused and committed to improving the capability of a wireless link in terms of speed, channel capacity, and promising to minimize the different error rates and the most harmful factor PAPR in the OFDM system. The main objective of the

book is to analyze various algorithms or methods already being used on the various parameters, modulation schemes, and coding schemes for different antenna configurations. Our aim is to choose the best parameters for testing and analyzing the different schemes to obtain the best suitable results regarding improved capacity, reduced PAPR, and error rates.

1.3 OBJECTIVE AND SCOPE OF THE BOOK

1.3.1 Objective of the book.

The major objective of the book is to get better the overall performance of the proposed MIMO-OFDM wireless communication systems;

- To achieve better data rate or capacity by employing the spectral efficiency of the OFDM system and the spatial multiplexing (antenna diversity) of the MIMO system. To enhance the channel capacity or throughput without increasing transmission power.
- To mitigate various error rates, like BER SER and FER using MIMO system along with the schemes like MRC and Alamouti STBC coding.
- To reduce PAPR at the desired level without affecting the BER performance of the system.
- To reduce deleterious effects of ISI and ICI by maintaining orthogonality in the frequency selective fading environment

1.3.2 Scopes of the book.

The scope of the book is to explore the research methodologies regarding;

- The combination of MIMO and OFDM technology is employed to combat the frequency-selective fading effect in the wireless environment. The capabilities of these technologies are employed intelligently to preserve the orthogonality between the sub-carriers of the OFDM system to avoid ISI and ICI.
- The application of antenna diversity or spatial diversity for the improvement of error rates like BER, SER and FER as well as to enhance the channel capacity of

the wireless communication system. Particularly the receive diversity scheme (MRC scheme) and transmit diversity scheme (Alamouti scheme) are analyzed for BER performance and channel capacity improvement. Space-time coding such as space-time block code (STBC) and space-time trellis code (STTC) are used with the MIMO system for analyzing error rates.

- Different PAPR lessening methods for improving the PAPR performance in the OFDM system.

1.4 ORGANIZATION OF THE BOOK

In **chapter 1** under the heading of introduction, the history of wireless communication and the classification and features of the next-generation wireless system have been discussed. Background and overview of an OFDM system, MIMO system separately have been illustrated along with the merits and demerits of the combination of the MIMO-OFDM system which has been successfully employed in earlier wireless systems (1G to 3G) and is being investigated and analyzed for the next-generation wireless system. The rest of the book is planned into different chapters summarized as follows;

Chapter 2 illustrates the review of the literature from the research articles by renowned researchers and academicians. The review process is classified according to various issues faced by MIMO-OFDM wireless communication systems, such as error rate performance, PAPR reduction, Capacity improvement, and Code-based performance evaluation of the MIMO-OFDM System. In each case, the methodologies used by the researcher and their results have been illustrated.

Chapter 3 deals with details on features, basic concepts, and design issues in MIMO-OFDM systems. Beginning from the basic single carrier modulation (SCM) system, the basic idea behind the OFDM system has been illustrated. The advantages of diversity concepts in the MIMO system have been explained, and finally, the basic architecture of the MIMO-OFDM system has been discussed.

Chapter 4 deals with problem identification and the methodology used for the fulfillment of proposed research work. This chapter is classified according to issues

encountered in MIMO-OFDM wireless communication systems and each method has been illustrated using detailed mathematical expressions. Methodologies included in this chapter are BER performance and probability of error analysis using different constellation schemes; PAPR reduction methods using ICF and SLM schemes; performance investigation of MIMO-OFDM System over Multipath fading Channels; performance Evaluation of MIMO-OFDM System using transmit beamforming (Alamouti STBC scheme) and receive beamforming (MRC scheme). Channel capacity (ergodic as well as outage capacity) has been elaborated using proper mathematical expression.

Chapter 5 demonstrates the performance investigation of the proposed MIMO-OFDM wireless communication system, via simulation results of various methodologies used. This chapter includes the illustration of simulation results of the different algorithms employed for error rate improvement, PAPR reduction, and channel capacity enhancement.

Chapter 6 deals with the conclusion of the overall research work done and future scopes to the overall contribution of this book.

Chapter 2

Literature Survey

This chapter presents the technical background behind this research and a detailed survey of research articles based on system performance against various issues in the MIMO-OFDM wireless system.

2.1 BACKGROUND

The wireless communication background is very antagonistic. The signal propagated over a wireless channel is vulnerable to fading, channel interference, variation in amplitude, time delays, frequency offsets, and path loss effect, etc. Also, the scarcity of bandwidth in a wireless system is a big challenge in a wireless system. The next-generation wireless communication system should provide higher spectral efficiency, higher throughput, highly reliable with quality of services at low cost. New wireless schemes, such as UWB, advanced source, and channel encoding techniques STC, SDMA, beam forming, MIMO, and OFDM wireless systems are competent for offering substantial gain, delivering multimedia services that require high data rates. Undoubtedly, the high data rates, and high robustness against channel impairments, error rates, require competent wireless system architectures. OFDM is very popular in wireless systems since it is capable to provide high 'spectral efficiency (SE)' and effectively deal with multipath fading [17]. The blend of OFDM with spectrum efficient MIMO boosts up the OFDM as a good candidate to combat the challenges in the wireless system. In a MIMO-aided system, the high data rate and high channel capacity or data rates can be accomplished with the help of spatial diversity and Multiplexing techniques. The channel capacity is substantially increased due to antenna diversity. The MIMO-based system minimizes channel fading effects using various diversity techniques. OFDM offers multicarrier transmission over fading channels; this will be useful in minimizing 'inter-symbol interference (ISI)' problems and thus avoid the application of complex DSP algorithms for the same in the case of single-carrier transmission. Besides all the advantages of MIMO-OFDM schemes mentioned above, the wireless technology

using the MIMO-OFDM scheme faces many challenges and its performance is rigorously corrupted due to different channel interferences that lead to decoding failure that results in packet loss at the receiver [11].

2.2 LITERATURE SURVEY

MIMO-OFDM has been the most researched topic in the last decades. Many problems have been researched and mitigating techniques have been suggested. Still, there are some trade-offs and challenges to be addressed and improved. A literature review has been prepared based on the following challenges faced by the system designers of a wireless system.

1. Error Performance of the MIMO-OFDM System
2. PAPR Reduction in OFDM system
3. Channel Capacity of MIMO-OFDM System
4. Code-based performance evaluation of MIMO-OFDM System
5. MRC based performance evaluation of MIMO-OFDM System

2.2.1 Error performance of the MIMO-OFDM system

In the OFDM system, the subcarriers are orthogonal if and only if the peak of each subcarrier is aligned with the null point of the adjacent two subcarriers. Orthogonality of the subcarriers in the OFDM system is portrayed in fig. 2.1.

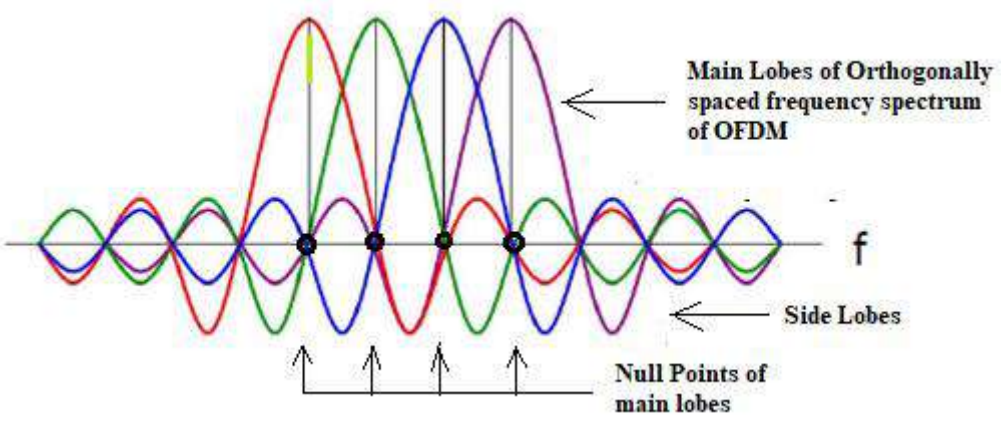

Fig. 2.1 orthogonally spaced OFDM signal in the frequency domain

The orthogonality is an important feature of the OFDM system that prohibits impairment like ICI since the orthogonality failure in OFDM causes an increase in ICI. In addition to high PAPR, the random frequency errors like imperfect synchronization between subcarriers, Doppler frequency shift, and local oscillator frequency difference between transmitter and receivers in the OFDM system are the main reasons for loss of orthogonality between subcarriers[18], which is responsible for ICI, 'multi-user interference (MUI)', and an increase in BER [19]. Similarly, the multipath propagation in the fading environment due to delayed signal replicas causes overlapping of signal energy with neighboring sub-channel that leads to ISI. One way to mitigate ISI is to introduce a pilot signal or cyclic guard interval or CP in each symbol. The filtered OFDM technique can be used to minimize the effect of interference in a multiuser environment. Although the length and roll-off factor of a filter can prohibit out of band radiation, the ISI and ICI increase at the same time. Attempt to insert a guard band of sufficient length to mitigate ISI and IUI (inter-user interference) will decrease the spectrum efficiency of OFDM [20]. When the OFDM symbol delay is greater than the maximum delay spread, the chances of occurrence of ISI can be significantly reduced [18]. The ICI can be mitigated by maintaining orthogonally in the OFDM system. Following are brief reviews of articles related to error rate reduction techniques.

Jayan and Nair (2018) in this article Filtered Orthogonal Frequency Division Multiplexing (F-OFDM), with a sub-band filtering approach are introduced. According to the traffic in the 5G network, different sub-bands are handled. The presentation of F-OFDM and conventional OFDM systems is analyzed in perspective to 'Power Spectral Density (PSD)' and BER. The experimental setup consists of VERILOG and the performance is investigated for different parameters. The PSD plot of the simulated results shows that the F-OFDM has smaller side-lobes compared to conventional OFDM which leads to improvement in spectral efficiency. The BER value for conventional OFDM and F-OFDM is found 4.0×10^{-6}at the SNR of 10 dB.

Alqahtani et al., (2019) proposed a next-generation MIMO-OFDM system. The authors suggested a new technique the rate less space-time block code (RSTBC) for eliminating the effects of channel impairments. The authors carry out an experiment using a (2×2) antenna configuration in the MIMO-OFDM system. A test bench using FPGA has been used to measure RSTBC. Results of BER performance depict that the experiment results are similar to simulation and analytical results. Considering the number of blocks = 1 to 18, QPSK modulation with the loss rate of 10% and 25% for the simulation of BER versus the number of blocks, the experimental and simulation BER value is 4.8×10^{-3} and 3.2×10^{-3} respectively at a 25% loss rate. Similarly at a 10% loss rate BER experimental and simulation value is 4×10^{-4} and 6.25×10^{-5} respectively for 8 blocks.

Nambi et al., (2018) proposed a new OFDM-IM method, where IM stands for index modulation to improve BER performance. They used lower order modulation techniques for lessening the error rates in a system**.** In this method, few bits are used for the selection of symbols and the remaining for the selection of index combinations. A group of subcarriers is selected and modulated as per incoming bitstreams. Simulation is carried out using the number of subcarriers N=128, symbol size M= 4 (proposed) and 8, 02 active subcarriers, symbol length n=4, and CP length of 16. At the spectral efficiency of 1.778 b/s/Hz and SNR of 20 dB, the BER value for OFDM-IM, M=8 is 4.5×10^{-3} and for proposed OFDM-IM, M=4 is 3.5×10^{-3} and 2.9×10^{-3} for OFDM with QPSK.

El-Abasi et al., (2015) presented an experimental setup for the verification of indoor wireless scenarios using the MIMO-OFDM-IA scheme with antenna selection. They employed two subcarrier selection criteria 1) Maximum sum rate (MSR) and 2) Minimum error rate (MER). Transmit antenna selection (TAS) is employed based on per subcarrier selection keeping distance $\lambda/2$ (λ = wavelength) between each node. The sum-rate (b/s/Hz) for per subcarrier selection maximum sum-rate and minimum error-rate at 20dB is found 22 and 21 b/s/Hz analytically. Similarly, the sum rate (b/s/Hz) for bulk selection maximum sum-rate and minimum error-rate at 20dB is found 22 and 18 b/s/Hz analytically. The BER value for bulk selection at maximum

sum-rate and maximum SNR is 3.5×10^{-2} and 4.5×10^{-2} at 10 dB analytically. Similarly, for per subcarrier selection, it is 1.5×10^{-4} and 7.5×10^{-5} analytically at 10 dB.

Rahmat et al., (2018) authors suggested that the ISI and BER performance can be improved if the missed symbols are predicted based on other symbols received in each OFDM signal under the deep fade scenario in Rayleigh fading channel. To achieve a high sampling rate a pre-coded OFDM scheme is employed and a new iterative receiving technique is utilized for the recovery of ideal symbols. Thus ISI and BER can be improved and the same has been depicted through simulation results. The simulation is carried out using 16-QAM, data block size K=32, number of subcarriers N=128, and oversampling factor of L=4. The BER value for 1, 10, and 100 iterations at sampling rate probability of ¼ and 15 dB SNR is 1.25×10^{-2}, 1.20×10^{-2} and 1.15×10^{-2}.

Arbi and Geller (2019) proposed an algorithm for the selection of two Rotated and Cyclically Q-Delayed (RCQD) QAM modulation is planned to optimize the BER. A blind SLM scheme is proposed to improve PAPR. For the 64-QAM modulation at a 10 dB SNR over Rayleigh fading channel the symbol error rate is 0.29×10^{-4}. The BER values for the blind detection and hard ML estimation over the Rayleigh fading channel at 15 dB SNR is 2.8×10^{-2}. For 16 QAM and 4 QAM modulation, the BER value at 15 dB SNR is 7.0×10^{-3} and 1.25×10^{-3} respectively.

Bento et al., (2019) proposed M-PSK modulation with magnitude modulation techniques and pulse shaping filters for the improvement of BER. A Gaussian model is employed to estimate the error distortion distribution due to magnitude modulation (MM) used for BER evaluation. Here two cases are considered, first BER is analyzed over the AWGN channel analytically. Second, BER is analyzed for the time-dispersive channel using MM, with an equalization technique in the frequency domain at the receiver. The analytical results prove that the BER analysis is accurate.

Giannopoulos and Paliouras (2008) suggested a 'partial transmit sequence (PTS)' scheme for the reduction of PAPR, which is responsible for an increase in power consumption as well as degrading BER performances. The BER analyzed over the

AWGN channel for different SNR values and considering the effect of DAC and the PA performance on the transmitted signal. The PTS scheme reduces IBO need is by 1 dB in case of SNR > 6 dB without affecting BER. The proposed PTS scheme reduces power consumption considerably up to 22% without any harmful degradation in BER performance. Authors also show that by decreasing the resolution of DAC by 1 bit, the power consumption is reduced by 50%.

Yang et al., (2019) proposed a filtered OFDM (F-OFDM) scheme for the mitigation of ISI, ICI, IUI, and BER. An optimized F-OFDM model with proper filtering parameters and guard signal of proper bandwidth is employed for uplink asynchronous F-OFDM system. Simulation results show proposed F-OFDM scheme outperforms the conventional OFDM scheme in terms of spectrum efficiency. The following parameters are used for simulation: Size of FFT = 2048/1024, CP length 60, Modulation scheme 64 QAM, and sub-band filter as Kaiser Window FIR filter. At 15 dB SNR the BER value is about 8.0×10^{-4}. The spectrum efficiency is about 5.2 to 5.5 b/s/Hz for 20 iteration and above. The spectrum sufficiency is about 4.5 to 5.5 b/s/Hz at the SINR of 20 dB.

Wang et al., (2017) proposed a 'Polynomial cancellation coded (PCC -OFDM)' and 'universal filtered multi-carrier (UFMC)' techniques are combined to reduce the amplitudes of side-lobes in (OFDM) spectrum to combat ICI in 5G network. In this article, the authors analyzed signal to interference plus noise (SINR) ratio versus BER presentation. The proposed scheme improves the ICI and ISI performance but at the cost of spectral efficiency and computational complexity. To reduce the computational complexity author further proposed a new scheme overlap and add (OA-UFMC) using an infinite IIR filter bank. Simulation results show BER analysis over AWGN and Rayleigh fading channels for conventional OFDM, UFMC, and PCC-OFDM schemes considering 10 or 50 sample time offset. It is observed that there is no considerable degradation in BER for PCC OFDM even at 50 samples which shows the proposed scheme can mitigate ICI significantly. At 15 dB SNR, over Rayleigh fading channel, the BER value for OFDM and PCC-OFDM at 10 and 50 samples using 16 QAM and QPSK modulation is comparable and it is 8.0×10^{-3} and 9.0×10^{-3} respectively. Similarly, for the UFMC scheme at10 and 50 samples

using BPSK or QPSK, the BER is 8.0×10^{-3} and 1.3×10^{-2} respectively. Over AWGN channel at the SNR of 10 dB for UFMC at 10 and 50 samples using BPSK or QPSK, the BER is 5×10^{-6} and 4.0×10^{-5}. For the conventional OFDM scheme for the same condition, the BER is 4.0×10^{-5} and 10^{-4} respectively. For PCC-OFDM the BER at 10 dB SNR and 10 or 50 samples is 1.85×10^{-3} using 16-QAM modulation, whereas for QPSK it is the same as UFMC that is 5×10^{-6}.

Wu and Li (2019) proposed a simple and efficient with less complex computation for the mitigation of ICI. The result shows a considerable increase in SINR output. The length of CP is used such that it is equal to delay spread to avoid system overhead. The settling time of automatic gain control (AGC) is chosen greater than the remaining portion of CP which is not overlapped with ISI otherwise orthogonality of subcarriers will be lost and that leads to ICI.

Hao et al., (2016) proposed a less complex algorithm for the mitigation of ICI in the MIMO-OFDM system based on the linear time-varying channel estimation. Simulation using QPSK and 16QAM constellation schemes demonstrate that 2 dB SNR gain is achieved at the un-coded BER is 10^{-3} and the normalized Doppler frequency is 0.1. For the simulation following parameters are considered, BW=1Mz, number of subcarrier K=1024, maximum Doppler shift = 100Hz, 02 transmit antennas, and 4,8 and 12 receive antennas over Rayleigh fading channel.

Fu et al., (2007) proposed a two-stage equalizing technique for the mitigation of ICI and MUI in OFDM. Tomlinson-Hiroshima-precoding (THP) is used as the first nonlinear stage which is used to reduce the spatial ISI and the second stage is the low complex MMSE equalization technique which is used to lessen ICI. The simulation result proves that the proposed method reduces the BER by 10%. The MIMO-OFDM system with a multiuser scenario using 4-QAM, 64 subcarriers, 4 or 8 transmitting antennas, and 6 tap Rayleigh fading channels is considered for BER analysis. At 15 dB SNR value 4 transmit antennas and 4 users the BER is 7.5×10^{-3} with a proposed equalizing or pre-coding scheme for different values of the frequency offset. Similarly for the same condition for 4 users and 8 transmitting antennas the BER at 15 dB SNR is 6.5×10^{-5}.

2.2.2 PAPR reduction in OFDM system

For faithful signal transmission, the amplitudes of the signal should lie under the linear region of power amplifiers (PA) used in transmitters. Reliable communications mostly depending upon the faithful amplification of transmit power using power amplifiers. If amplitudes of transmitting signal cross the range linearity of PA leads to pushing the PA in a nonlinear region, where it behaves non-linearly and leads to out of band radiation. In the OFDM system, the logical summation of the signal from all N subcarriers at IFFT in the time domain produces very high peak power in an OFDM signal. When such a high peak power is fed to the input of PA, it is unable to accommodate the input power and hence enters into saturation region causing nonlinear amplification of input signal leads to out of band radiation. The ratio of peak signal power to the average signal power is known as 'peak to average power ratio (PAPR)' and it is increased due to the above said reason. High PAPR value in the OFDM is one of the major issues and it must be reduced to have reliable wireless communication. Many PAPR lessening methods are available but it is found that these schemes reduce the PAPR at the cost of an increase in BER and computational complexity [7]. The following sections give brief reviews about various PAPR reduction techniques suggested by different authors.

Xing et al., (2020) proposed a less complex companding technique for PAPR lessening in OFDM system over AWGN channel using QPSK modulation scheme. This reduction scheme outperforms other companding schemes by 3 to 5 dB SNR while achieving a BER of 10^{-4}. For c=0 and A= 1.414, 1.67, 17.34 the PAPR values measured from simulation results are 3.4, 4.25, and 5.1 dB respectively at the CCDF of 10^{-3}.

Tang et al., (2020) proposed a hybrid scheme of iterative clipping and filtering scheme and enhanced non-linear companding scheme. Simulation is carried out using parameters, the number of subcarriers 256; 16 QAM modulation; oversampling factor =4; clipping ratio 1.5 to 1.8; clipping level 3; shape factor s = 60, the normalization factor v= 0.72 to 0.87. The simulation results depict that the projected ICF scheme is very close to ENC in terms of PAPR and for clipping ratio of 1.5 & 1.8 the PAPR

value is found to be 4.25 dB and 5.4 dB respectively at the CCDF of 10^{-3}. At 10 dB SNR the BER is recorded as 7.0×10^{-3} and 4.0×10^{-3} for CR=1.5 and 1.8 respectively.

Bao et al., (2016) developed the PAPR reduction technique based on the Bayesian approach using the surplus 'degree of freedom (DoF)' of the transmit array. Further, they suggested the 'generalized approximate message passing (GAMP)' embedded into the variational 'expectation-maximization (EM0' framework scheme to reduce the computational complexity in the suggested methodology. The proposed EM-TGM-GAMP algorithm for the number of iterations 20 and 200 shows that the PAPR is reduced to greater than 11 dB compared to 'zero-forcing (ZF)' algorithms at the CCDF of 1%. Similarly, the PAPR presentation of the suggested scheme is 2 dB, 3.2 DB less than the PAPR performance of the FITRA algorithm at 2000 iteration and clipping algorithm respectively. The above said presentation of the suggested scheme is achieved at the cost of 2.5 dB and 1.7 dB loss of SNR gain at SER value of 10^{-3} compared to ZF and FITRA schemes.

Rateb and Labana (2019) proposed a PAPR diminution technique based on linear signal coefficients and analyzed different performance metrics. The author shows through analytical and simulation results that PAPR can be reduced effectively without any considerable change in BER at the cost of a little reduced data rate. At 1024 subcarriers, the PAPR is recorded below 7.4 to 6.9 dB with a 1% to 2% fall in data rate. Also, it is observed that by an increasing number of subcarriers the value of PAPR varies slightly. The proposed technique achieves results where PAPR is less than 6 dB, 6.5 dB, 6.9 dB, and 7.4 dB, for spectral efficiency of = 90%, 95%, 98% and 99%.

Gokceli et al., (2019) proposed an 'iterative clipping and error filtering (ICEF)' scheme for PAPR minimization. In this scheme, the noise is controlled flexibly and filtered within the transmitter pass-band. The results are demonstrated in the milieu of the 5G wireless network. At CCDF of 1% the PAPR value is reduced to 8.35dB, 6.3dB and 6 dB with 1,2,20 iterations. The PAPR of the original signal was 9.4 dB at CCDF of 10^{-3}.

Anoh et al., (2017) -1, introduced the 'iterative clipping and filtering (ICF)' scheme for the reduction of PAPR in OFDM signal. The author uses the 'Lagrange multiplier (LM)' for the optimization to reduce the number of iterations, and the MMSE method to improve the BER presentation. The approach suggested by the author performs better compared to the conventional ICF method. Results show at CCDF of 1% and 03 iterations (Clip), PAPR reduced to 4.2 dB from 10.2 dB PAPR of original signal without optimization. Whereas using optimization the PAPR value reduces to 0.9 dB from the original PAPR value. The BER value at the SNR of 10 dB is found to be 1.0×10^{-2} using optimization and 9.0×10^{-2} without using optimization.

Anoh et al., (2017) -2, proposed the novel a root-based μ -law companding (RMC) method for PAPR minimization. In this method amplitude of the OFDM signal is expanded and compressed simultaneously unlike the conventional MC scheme. The proposed scheme outperforms all other MC schemes and gives PAPR = 3.2 dB at the CCDF of 10^{-3}. The BER value of the proposed scheme at 10 dB SNR is 1.2×10^{-2} achieved.

Kim (2019) proposed a novel OFDM-IM scheme, which uses an index of active subcarriers. In this scheme dither signals are added to the inactive subcarriers to lessen the PAPR. Simulation results show the PAPR reduced to 5.9 dB from 9.6 dB (original) at CCDF of 1%. The BER value is found to be 10^{-2} at 20 dB SNR.

Tang (2019) proposed the clipping-noise compression technique for the minimization of PAPR in the OFDM system. Here the transmitted signal is modified using clipping and noise compression in the time domain. The proposed scheme shows PAPR equals to 4.8 dB, 4.6dB, and 4.4 dB for $\mu = 2$, 3, and 10 respectively at CCDF of10^{-3}. For the clipping ratio of 6 dB and 3 dB, the BER value of the proposed scheme is found to be 2×10^{-3} and 6.5×10^{-3} respectively.

Gupta et al., (2019) proposed selected mapping (SLM) technique for lessening the PAPR. Authors use discrete cosine transform (DCT) for optimizing PAPR in transmitted OFDM signal. At CCDF of 0.001% and phase sequences U = 16, 32, 64 and 128, number of subcarriers 128 and 4-PSK modulation, a notable gain of 1.36, 1.25, 1.4, and 1.27 dB respectively is obtained. For the condition stated above, at the

CCDF of 10^{-3}, the lowest PAPR value for U= 8, N=128 and 4 PSK modulation, U = 128, N = 128, and 4-PSK, U = 8, N = 64, and 4-PSK, U = 128, N = 32, and 4-PSK is measured as 7.7dB, 6.3 dB, 7.2 dB and 5.0 dB.

Amhaimar et al., (2018) introduced a partial transmit sequence (PTS) scheme with a novel swarm intelligence algorithm, also referred to as fireworks algorithm (FWA) is employed to mitigate PAPR. The suggested scheme achieves less PAPR with lower computational complexity. The proposed PTS-FWA gives the best PAPR result compared to another algorithm like 'simulated annealing (SA)', 'standard particle swarm optimization (PSO)', and 'genetic algorithm (GA)', and SLM scheme. At the CCDF of 10^{-3}, the PAPRs values observed are 7.1 dB, 5.2 dB, 5.879 dB, 4.421 dB, 4.948 dB, 4 dB, and 10.66 dB for the SLM scheme, PTS, GA, SPSO, SA, FWA, and original OFDM signals, respectively.

Gao et al., (2018) suggested iterative PTS combined with clipping method for lessening the PAPR. The proposed scheme portrays better PAPR performance compared to the PAPR performance by individual PTS and Clipping method. At CCDF of 10^{-3} PTS method alone reduces PAPR to 7.75 dB, Clipping method alone reduces PAPR to 6.4 dB, and combined iterative PTS-clipping method reduces PAPR to 5.25 dB. Also, the proposed method reduces the computational complexity.

Francisco Sandoval (2017) introduced a hybrid technique combining modified code repetition (MCR) and SLM scheme with clipping. The simulation is carried out using the number of subcarriers 512, 50% cyclic prefix, the oversampling factor of 1, and BPSK modulation over the AWGN channel. The simulation result shows the PAPR reduces to 3.4dB at the CCDF of 10^{-3} and the BER value of 1.0×10^{-4} is achieved at the SNR of 7 dB.

Wang et al., (2015) proposed an 'iterative companding transform and filtering (ICTF)' method of PAPR minimization and BER improvement. It is proved that the suggested ICTF scheme outperforms the conventional ICF method. It is also shown that the ICTF method presents the best BER performance without de-companding at the receiver. Simulation results after 3 iterations the proposed ICTF-LST (linear symmetrical transform) and ICTF-TPWC (two piecewise compandings) shows PAPR of 6.5 dB and 5.25 dB respectively at CCDF of 10^{-3}. Also, the ICTF-TPWC

scheme with 3 iterations provides an SNR gain of 1.2 dB compared to the conventional ICF method after 8 iterations to achieve BER of 1.0×10^{-4}.

Wang and Wu (2019) proposed a 'tone reservation (TR)' scheme based on 'signal to clipping noise ratio (SCR)' for PAPR mitigation. It is found that the suggested scheme mostly suffers from a low convergence rate. To improve the above problem author suggested multiple scaling SCR (MS-SCR) scheme. The above problem is improved at the cost of an increase in computational complexity. From the simulation result, it is observed that proposed technique for the clipping ratio 3, 2, and 1 dB, the PAPR is reduced to 6.1 dB, 5.1dB, and 4.6 dB respectively at the CCDF of10^{-3}. The BER result for the proposed MS-SCR scheme with CR=2 and 4 is 8.0×10^{-3} and 3×10^{-4} respectively at the SNR of 10 dB.

Ni et al., (2016) proposed a new 'adaptive tone reservation (ATR)' technique for the minimization of PAPR in the multiuser MU-MIMO-OFDM system. Analytically PAPR value found between 5.1 dB to 10.5 dB. Simulation results show that the achievable PAPR is 6.8 dB at the CCDF of 10^{-3} and clipping ratio 2.2 dB.

2.2.3 Channel capacity of MIMO-OFDM system

In recent years and the coming future, the application of wireless mobile communication is dramatically increasing. At the same time number of users is also rapidly increasing that needs a high data rate, high speed, highly reliable wireless link to fulfill demands of the future communication on the wireless link [41], [42]. To increase the wireless link capacity one of the most popular techniques is to employ the MIMO antenna system which consists of multiple transmitting and receiving antennas [43]. The MIMO system utilizes multiple antennas to provide antenna diversity at transmitter and receiver and more degree of freedom to transmit and receive several data streams by exploiting spatial multiplexing and thus increase the channel capacity [44]. The channel capacity can be increased linearly by increasing the number of transmitting and receiving antennas in the MIMO system. Moreover, the MIMO system provides a reliable communication link in a fading environment [45], [46]. In the MIMO system, the capacity can be enhanced without utilizing extra bandwidth and transmit power by the factor, $min(M_T, M_R)$ where

'M_T' and 'M_R' are the number of transmitting and receiving antennas. [15]. A merger of MIMO technology with an OFDM system and their simple implementation offers high spectral efficiency, high channel capacity, highly reliable link, minimum interference between sub-bands or subcarriers, and improved error performance in fading environment [47-48]. Many techniques have been adopted to improve the capacity of the wireless link and some of the research articles in this field have been surveyed in the following paragraphs.

Anoh et al.,(2019), used 'quasi-orthogonal (QO)' 'space-time block code (STBC)' MIMO technique including beamforming to improve BER as well as data rates. The result shows the BER performance of STBC and SVD detection with single-directional beamforming using 16-QAM constellation and 2×1 antenna system is 1.6×10^{-1} and for 4×1 antenna system is found to be 1.9×10^{-2} at 10 dB SNR. The data rate of the SVD based QO-STBC-MIMO system at 10 dB SNR is 6.2 bits/s/Hz for 2×1 antenna configuration. After elimination of interference, the additional gain of 3 dB is achieved at 10^{-4} BER. Hadamard-based QO-STBC provides data rates, up to 6 bits/s/Hz.

Sahoo and Sahoo (2019) investigated the channel capacity performance of the time-varying MIMO channel model using a sparse model based on the 'diffusion least-mean-square (DLMS)' algorithm. The performance is measured in both urban and suburban milieu. The experiments are performed on I-METRA, IEEE802.11 & 3GPP channel models using STBC. The estimated CSI is employed to determine channel capacity. The experimental results show that using the AC-DLMS algorithm at 15 dB SNR the channel capacity for IEEE 802.11 channel, I-METRA channel, and 3GPP channel is measured to be 14 bps, 18.8 bps, and 17.2 bps respectively. At the SNR of 20 dB, the capacity for the same channels is found to be 18 bps, 22.2 bps, and 20.8 bps respectively.

Aggarwal and Bohara (2018) proposes a nonlinear 'dual-band (DB)' 'multi-user (MU)' MIMO-OFDM system to evaluate SER and the average capacity over the Rayleigh fading channel. The authors show that the preprocessing employed before transmission can be used to minimize 'inter-user interference (IUI)' in a linear DB-MU-MIMO-OFDM system. Following parameters are used for simulation of HPA

based DB-MU-MIMO-OFDM nonlinear system; The number of subcarriers N = 1024 and the cyclic prefix length = 256, users =4, IBO=5dB For, and total transmit power of 5, 10, and 15 dB, the overall capacity is found to be 10,18 and 24 bits/s/Hz respectively.

Kundu and Hughes (2017) Authors determined the channel capacity of broadband MIMO-OFDM systems using coupled receiving antennas considering 'uniform circular array (UCA)' and 'Uniform linear array (ULA)'. Upper and lower bounds have been placed over the best capacity which is achievable and realizable with the frequency-selective matching of receiving antennas. Results show the channel capacity has been surprisingly improved in presence of perfect matching and coupling of receiving antennas. The frequency of selective matching is increased with an increase in SNR. The frequency-selective-lower bound outperforms the frequency non-selective matching by 14 to 32 % in the case of a 2×2 antenna system and 26 to 44% in the case of 4×4 for CSI at receiver. Similarly for full CSI, it is found that FS exceeds FNS by 14 to 23% and 20 to 29% for the same antenna systems.

Chen (2012) proposed a full correlation scheme for measuring MIMO channel capacity in the reverberation chamber. The model proposed by the author can measure the ergodic capacity accurately but not the outage capacity. 6×3, 4×3, and 2×3 antenna systems are used to measure ergodic capacity in the reverberation chamber and it is measured as 6 bits/s/Hz, 5 bits/s/Hz, and 4 bits/s/Hz at 10 dB SNR, whereas at the SNR 25 dB it is found to be 20 bits/s/Hz, 17 bits/s/Hz, and 12 bits/s/Hz.

Choudhury and Gibson (2007) investigated channel capacity and outage probability over Rayleigh fading channel. The CSI at the receiver as well as the transmitter is known. It is shown that average capacity probability is not affected considerably whereas the average distortion of source information increases with SNR. The simulation result shows the probability of distortion at 5dB SNR is 0.7. By increasing the SNR value to 15 dB the overall distortion is reduced and the probability of getting average distortion is 0.9.

Torabi et al., (2006) demonstrated the effect of erroneous CSI on the error performance, outage probability, and channel capacity of the MIMO-OFDM system. They consider the SFBC-OFDM scheme and adaptive modulation to determine the 'spectral efficiency (SE)' under imperfect CSI at the transmitter. Simulated results for perfect CSI (0% error) the capacity is found to be 26.5 bits/s/Hz. At 1%,5% and 10% CSI error for 3x3and 8x8 antenna system the channel capacity is measured as 13.5, 10, 8 bits/s/Hz and 36.6, 26.5, 21 bits/s/Hz respectively. The BER value for SFBC-OFDM with QPSK modulation for 3x3 antenna system is 3.0×10^{-6} at 5% CSI error and 10 dB SNR.

2.2.4 Code based MIMO-OFDM System

Although the MIMO-OFDM is a highly accepted technology in wireless communication, some factors such as Computational Complexity, power constraints, ICI, and the system cost may limit the efficacy of the system [60]. Recently different technologies have been employed for combating the many issues in the next-generation wireless communication systems such as 'maximal ratio combining (MRC)', STBC, and/or 'Space-time Trellis code (STTC)' aided MIMO-OFDM system, Alamouti STBC system, and so on. In the following sections, some articles related to these technologies are reviewed.

2.2.4.1 Performance evaluation of STBC coded MIMO-OFDM System

Adejumobi and Pillay (2019) employed 'cyclic structured STBC coded spatial modulation (STBC-CSM) for the cyclic rotation of active pairs transmitting antennas to transmit Alamouti codes obtained from two sets of modulation for the improvement of the spectral efficiency (SE) of the proposed system. Also, the authors show that 'media-based modulation (MBM)' using RF mirrors provides a noteworthy enhancement in the error rate presentation of the STBC-CSM system. A low complexity ML detector is employed for the proposed MBM-STBC-CSM and MBM-STBC-SM system which reduces the computational complexity by 41% with a significant BER performance.

Zhang et al., (2020) introduced a new CSI estimation scheme for STBC based MIMO-OFDM system in a time-varying environment. They employed 'adaptive multi-frame averaging (AMA)' and 'improved mean square error optimal threshold (IMOT)' systems for the estimation of CSI precisely without adding complexity and hence to improve the system performance. Results represent that the proposed schemes can achieve better system performance in terms of BER. At the BER of 10^{-2} the AMA-IMOT method has an SNR gain of about 0.5 dB to 2.7 dB compared to the 'threshold-based selection (TBS)' method. Similarly, at the Doppler spread of 20 Hz, the AMA-IMOT method achieves an SNR gain of 0.3 dB to 2.4 dB compared to TBS methods at the BER of 10^{-3}.

Wu et al., (2019) introduced a novel STBC scheme with rectangular differential spatial modulation (RDSM) for the MIMO system to improve error performances of the MIMO-OFDM system. The authors merged STBC and RDSM to achieve the benefits in system performance and to eliminate shortcomings of the conventional DSM scheme. The proposed RDSM-STBC scheme outperforms the DSM method which is depicted in simulation results. BER performance of proposed method using BPSK and QPSK modulation and ML detectors for 4×2 and 8×2 antenna system at the SNR between 10 dB to 20dB is found almost similar and in the range of 10^{-2} to 10^{-5}.

Tang et al., (2020) proposed an STBC-MIMO-OFDM scheme with antenna systems of 2×2 and 4×4, employing Kalman filter for estimation of MIMO channels. Here the CSI is estimated iteratively using the Kalman Filter equation. At the BER of 10^{-1} for Doppler spread of 20 Hz, the proposed KF method provides SNR gain of 1.2 dB, 1.3 dB, and 2.3 dB compared to SVD, DFT, and LS methods, respectively. At the BER of 10^{-3}, the proposed KF method provides an SNR gain of about 0.8 dB and 2.0 dB SNR compared to DFT and LS methods, respectively. The proposed method provides better BER performance of STBC MIMO-OFDM system over CDT1 channel at 10 dB SNR with Doppler frequency shifts of 80 Hz is about 2.4×10^{-2} and 9.0×10^{-3} for 2×2 and 4×4 antenna configuration respectively.

Shao et al., (2019) presents STB coded full-duplex relaying spatial modulation technique (STBC-SM-FDR). Here source and destination functions in half-duplex

mode whereas relay node functions in a full-duplex mode and transmits the information bits along with STBC code words. The authors investigated the BER and Channel capacity of STBC-SM-FDR and found that the proposed scheme gives better BER results with less complexity. At 20 dB SNR for a transmission rate of 5 bits/s/Hz, the BER value equals 6.0×10^{-3} for 4 transmit antennas. For 8 transmit antenna it is about 10^{-5} at 4 bits/s/Hz transmission rate. Channel capacity at 20 dB SNR for 4×2 and 6×4 configuration is 5.2 and 5.7 bits/s/Hz.

Raut and Jalnekar (2019) proposed a novel Dolphin-Rider-Optimization (DRO) optimization technique for the STBC-MIMO-OFDM system is employed. The performance of the proposed system has been analyzed over Rayleigh and Rician channels and 03 types of constellations BPSK, QPSK, and QAM. The Proposed scheme is found more effective using BPSK modulation with minimal BER of $3.78 \times 10-7$ and a maximal throughput of 0.875.

Dehri et al., (2019) proposed and analyzed the new blind digital modulation classification algorithm for the STBC-MIMO-OFDM system in presence of frequency offset and channel estimation error. The major scope of their article is the design of the estimator and its impacts on the blind classification capability. The simulation results proved that the proposed algorithm is robust against CFO, CSI errors, and impulsive noise. The suggested system functions well at low SNR too.

Xiao et al., (2017) proposed an STBC-MIMO-DSM (differential spatial modulation) scheme, which utilizes hybrid concepts of the STBC and the DSM to exploit diversity benefits of MIMO-STBC, without any knowledge of channel estimation. Novel antenna matrixes with sparse RF chains are employed and then it is extended to large-scale MIMO systems. Both analytical and simulation results portrayed the proposed techniques are capable of outperforming the existing DSM and differential Alamouti schemes with considerable performance gains. At 15 dB SNR, BER = 1.8×10^{-5} , 2.2×10^{-4} and 4.8×10^{-3} for BPSK, QPSK, and 8 PSK modulation and with N_t= 4 and N_r = 2.

Kumar and Saxena (2014) proposed STBC coded MIMO system with a high code rate. Different modulation schemes have been employed in the semi-blind digital environment. The simulation results show the performance is very near to the

scheme using known CSI estimation. At 10 dB SNR the BER value for Alamouti model at ½ code rate, diversity 1, a semi-blind scheme using QPSK modulation and 16- QAM modulation for the antenna configurations (1) 3×3 is about 4.0×10^{-5} and 4.1×10^{-3}. (2) 4×4 QPSK is about 1.4×10^{-7} and 2.0×10^{-3}. With increasing code rate beyond ½, suddenly BER values dropped between 10^{-1} and 10^{-2} for both antenna configuration and the constellations with the same parameters except code rate.

2.2.4.2 Performance evaluation of Alamouti STBC coded MIMO-OFDM System

The capacity and information rates can be enhanced over fading channel by providing spatial diversity using multiple transmitting and receiving antennas in a MIMO system. The STBC is a very efficient method of accomplishing transmits diversity [8]. By adapting the switching strategy for the transmit antenna selection, the average feedback requirement can be reduced and the probability of average error rate can be enhanced [67].

Alamouti in 1998, introduces transmit diversity using two transmit antennas ($M_T = 2$) and one receive antenna ($M_R = 1$). The proposed Alamouti scheme provides diversity similar to the 'maximal ratio combining (MRC)' scheme using ($M_T = 1$) and ($M_R = 2$) antennas. According to the author, the proposed scheme can be generalized with 02 transmit and M number of receive antennas which can provide 2M diversity. The simulation results show a comparison between BER values for Alamouti and MRC scheme using different antenna systems over the Rayleigh fading channel using the BPSK modulation scheme. At 15 dB SNR the BER values for the MRC scheme with 1×2 and 1×4 antenna system is 2.0×10^{-4} and 7.5×10^{-4} and for Alamouti scheme with 2×1 and 2×2 antenna system is 1.5×10^{-7} and 2.0×10^{-6}. The above results are obtained without any extra bandwidth, channel information, and additional computational complexity compared to MRC.

Roopa and Shobha (2019) proposed the Alamouti and OSTBC coding techniques for the BER reduction of a MIMO system with a 2×2 configuration. The simulation is carried out using BPSK modulation over Rayleigh fading channel. The simulation

result shows the BER value for the OSTBC scheme at 10 dB SNR is 8.0×10^{-5}. For the same environment, the BER values for the Alamouti scheme with 2×1 and MRC scheme with 1×2 is found to be 5.5×10^{-3} and 1.6×10^{-3}

Mishra and Kulat (2018) demonstrated a novel reduced feedback scheme for the analysis and comparison of BER performance, and outage probability in a MIMO system. The performance comparison of the proposed scheme with the conventional TAS scheme has been presented in this article. Simulation is carried out using BPSK modulation and the results depict that the proposed scheme optimally reduces BER values. At 14dB SNR for N_t = 3, 6, 9, and 12 the BER is found to be 1.25×10^{-3}, 5.0×10^{-5}, 6.0×10^{-6} and 1.2×10^{-6} respectively.

Dlodlo et al., (2018) proposed differential STBC expansion and trellis coding for improving the bandwidth efficiency using two transmit antennas. STBC expansion is carried out by using transformation of the unitary matrix. The proposed method transmits more information bits in each block of STC compared to the conventional DSTBC scheme. Using 16-QAM modulation proposed scheme accomplishes a 12.5% hike in bandwidth efficiency. The simulation result depicts the BER performance as follows. The 'conventional differential detection (CDD-STBC)' scheme and the proposed TC-DSTBC scheme using 16-QAM constellation with the transmission rate of 4 b/s/Hz and 4.5 to 5 b/s/Hz at 15 dB SNR is observed to be similar that is 4.0×10^{-3}. The same BER performance for64 QAM modulation is observed at 21 dB SNR. Thus the former schemeusing16 QAM outperforms the later scheme by the SNR gain of 6 dB. Similarly, in the case of bandwidth efficiency also the scheme using 16 QAM outperforms the scheme using 64 QAM.

Nandi and Nandi (2017) employed the Alamouti STBC code for the improvement of BER performance in the MIMO-OFDM system. The simulation results show BER values at 10 dB SNR for different modulation techniques such as BPSK, QPSK, and 16 QAM about 5.0×10^{-5}, 2.0×10^{-4} and 4.0×10^{-3} respectively. Similarly, the BER values at 10 dB SNR for the MRC scheme (theoretical) and Alamouti scheme (theoretical and simulated) are found to be 5.5×10^{-3}, 1.75×10^{-3} and 1.0×10^{-4} respectively.

Pattanayak et al., (2017) investigated a multi-user MU-MIMO-STBC system with imperfect CSI at different SNR values. The authors used Alamouti STBC codes to enhance transmit diversity for the improvement of reliability. For simulation 2×2 antenna configuration, BPSK modulation, over Rayleigh fading channel, the number of user K= 2,4,8, cyclic prefix length 16, and minimum mean square error combiner at the receiver are used. The BER value of 1.5×10^{-4} , 2.8×10^{-4} , 4.5×10^{-4} for K= 2, 4, 8 users at 15 dB SNR.

2.2.5 MRC based performance evaluation of MIMO-OFDM System

Lee (2018) proposed an MRC scheme over imperfect channel estimation to investigate the ergodic capacity and outage capacity in a MIMO system. The author employs the duel selection method, which is user selection and transmitting antenna selection for this purpose. The numerical results portray that the proposed MRC method enhances the capacity with the number of receiving antennas and users, also the outage probability is restricted. From the simulation results, it is depicted that the ergodic capacity of the proposed MRC scheme with 2×1 for the number of user K=1 and K=2 at 10 dB SNR is 3.7 and 4.25 bits/s/Hz respectively. The outage probability of 10^{-3} is achieved at 12 dB and 20 dB SNR for a target capacity of 2 bits/s/Hz and number of users K=2 and K=1. The outage capacity at 10 % outage, for K=1 at 10 dB SNR is 2.5 bits/s/Hz, the same outage capacity can be achieved at SNR= 7 dB for K=2 users.

Luong and Ko (2018) proposed OFDM-IM (index modulation) with MRC and greedy detector for the investigation of BER and error probability. They show that the proposed scheme performs similarly as MRC -ML (maximum likely hood detector) at low complexity. Simulation is carried out using BPSK and QPSK modulation, 1 active sub-carrier of 2 or 2 active subcarrier of 4 subcarriers, one transmit, and 2, 4, 6 and 8 receive antennas. For MRC-GD with perfect CSI, 4 subcarriers, 2 active subcarriers, and QPSK modulation at 10 dB SNR, the average error probability is 2.5×10^{-2} , 2.5×10^{-4} and 4×10^{-6} for L= 2, 4, 6 receive antennas. Similarly, for MRC at receiver with imperfect CSI, L= 2, 4, and 6

receive antennas the BER at 10 dB SNR is 1.8×10^{-2}, 6.0×10^{-4} and 2.8×10^{-5} for L= 2, 4, 6 receive antennas.

Beaulieu and Zhang (2017) introduced a novel asymmetrical power twin branch, Nakagami-0.5 linear diversity combining scheme. Analytical solutions for average error probability and outage probability are determined. For 'selection combining (SC)' and 'equal gain combining (EGC)' at an error rate of 10^{-2} there is a loss of 1dB. At the error rate of 2×10^{-1} to 2×10^{-3}, the SC and EGC have 1 dB SNR loss compared to MRC. This indicates at the cost of small SNR loss complexity of MRC can be avoided.

Misra et al., (2017) proposed MRC and EGC schemes for the improvement in BER and MRT schemes for lessening the PAPR in the MIMO-OFDM system. Results of the proposed scheme are compared with SLM and PTS scheme. Considering 2 and 3 receive antennas BER performance for MRC and EGC scheme is compared. It is found that for BER performance offered by both the scheme is comparable and it is about 2.0×10^{-3} and 2.0×10^{-4} at the SNR of 10 dB over the Rayleigh fading channel. At the BER value of 10^{-3} for 1×2 and 1×4 the SNR for MRC 12.4 dB and 4 dB respectively, and the EGC scheme is 12.5 dB and 4 dB respectively. For the number of channel tap L=4, the PAPR value for the MRT scheme is about 5.25 dB at the CCDF of 10^{-3}. The PAPR value using PTS scheme for the number of sub-blocks V=16 is about 6.9 dB at CCDF of 10^{-3}. The result from the simulation of the SLM scheme for the phase vectors U= 4,8, and 16 it is seen that the probability of PAPR greater than 6 dB using the SLM scheme is 75%, 60%, and 35% respectively.

Das and Subadar (2017) presented an MRC scheme with two-wave diffuse power (TWDP) fading channels for BER improvement in MIMO systems. Simulation has been carried out using 16-QAM modulation upon fading parameters. At 10 dB SNR for 2 and 3 receive antenna BER value of 6.5×10^{-4} and 3.5×10^{-5} is observed. Similarly, for 8- QAM and 4- QAM, the BER values for 2 and 3 receive antennas are found the same as 16-QAM for the same fading parameters.

Tiwari and Saini (2014) proposed MRC diversity and STBC coding for the analysis of BER performance. Different modulation schemes like 16-QAM, BPSK, and

QPSK have been used over Rayleigh, Nakagami-m, and Rician fading channels for the analysis. The BER values for Alamouti STBC using 2×1 antenna system, 16-QAM, BPSK, and QPSK over Rayleigh Channel at 20 dB SNR are 1.5×10^{-2}, 5.0×10^{-5}, and 4.9×10^{-4} respectively. Over Rician fading channel for the same criteria, the BER at 20 dB is 4.0×10^{-4}, 2.5×10^{-4}, and 9.0×10^{-3} respectively. For m = 0.5 over the Nakagami-m channel, the BER values for the Alamouti STBC scheme using 16-QAM, BPSK, and QPSK is 6.0×10^{-2}, 2.9×10^{-3}, and 10^{-2}. The BER values for the MRC scheme over the Rayleigh fading channel at 10 dB SNR with 1×2 and 1×4 are 1.9×10^{-3} and 2.0×10^{-6} for BPSK, 10^{-2} and 2.0×10^{-4} for QPSK, and 1.0×10^{-1} and 3.2×10^{-2} for 16 QAM modulation. The BER values for the MRC scheme over the Rician fading channel at 10 dB SNR with 1×2 and 1×4 are 7.0×10^{-4} and 5.0×10^{-6} for BPSK, 6.5×10^{-3} and 10^{-4} for QPSK and 1×10^{-1} and 2.3×10^{-2} for 16 QAM modulation. The BER values for the MRC scheme for the Nakagami-m fading channel at m=0.5 and 10 dB SNR with 1×2 and 1×4 are 1.0×10^{-2} and 5.0×10^{-4} for BPSK, 4.0×10^{-2} and 3.0×10^{-3} for QPSK and 1.2×10^{-1} and 6.5×10^{-2} for 16 QAM modulation.

Ahn (2009) proposed a MIMO-MRC scheme for the analysis of outage probability and symbol error rates (SER) over Rayleigh fading channels. The average SER and the outage probability are analyzed for BPSK modulation. The outage probability at SINR 10 dB for 2×2, 3×2, 4×2, 4×3, and 4×4 is 5.0×10^{-1}, 4.0×10^{-2}, 1.0×10^{-2}, 2.0×10^{-3}, and 3.0×10^{-4}. The average SER value at 15 dB SINR for 2×2, and 4×2 is about 7.0×10^{-5}, and 2.5×10^{-7}.

2.2.6 Comparative analysis of literature survey at a glance

In this section, the literature review is portrayed in tabulation form. In this presentation, the research articles from the year 2015 onwards are considered. From the tables, it is very easy to analyze different issues of the wireless communication system. Table 2.1 to table 2.6 depicts the analysis of various issues like different error rates, PAPR, data rate, etc.

Table 2.1 Error rate performance using various modulation schemes

S.No.	Authors	Year	Technology & parameters used for simulation	SNR	Bit Error Rates/Symbol Error rates	
1	*Ali H. Alqahtani et.al.*	2019	Rate-less space-time block code (RSTBC); Experimental setup using FPGA, 2×2 antenna system; number of subcarriers 64; Number of symbols 1000; QPSK modulation; Number of RSTBC blocks L= 1,2,4,6,8	at 10 % loss rate	L=1	0.5
					L=2	5×10^{-2}
					L=4	5×10^{-3}
					L=6	5×10^{-4}
					L=8	$0.625 \times 10^{-}$
2	*Tarak Arbi and Benoit Geller*	2019	Two RCQD algorithms with QAM constellations is proposed BER reduction, over Rayleigh fading channel; with M-QAM modulation,256 subcarriers, and blind detection or hard ML detection.	SNR= 10 dB	M=64	7.5×10^{-2}
					M=16	3.5×10^{-2}
					M=4	9.5×10^{-3}
3	*Meijie Yang et al.*	2019	Filtered OFDM (F-OFDM) scheme; Size of FFT 2048/1024, CP length 7% of symbol length, Modulation scheme 64 QAM.	SNR= 10 dB	2.5×10^{-2}	
4	*S. Abhijith Nambi et.al*	2018	OFDM-IM method; number of subcarriers 128; symbol size and length =4; Cp length=16; QPSK modulation	SNR= 10 dB	5.0×10^{-2}	
5	*Gopika Jayan and Aswathy K. Nair*	2018	F-OFDM; BPSK modulation; 50 resource blocks.	SNR= 10 dB	4.0×10^{-6}	
6	*Alireza Rahmat et al.*	2018	A pre-coded OFDM scheme is employed; N=128 subcarriers, and L=4 oversampling factor, symbol size 32, modulation 16-QAM, 10 iterations of an iterative receiver at sampling rate probability of ¼	SNR= 10 dB	3.25×10^{-2}	
7	*Shendi Wang et al.*	2017	PCC -OFDM and UFMC techniques; Rayleigh fading channel; BPSK, QPSK, and 16 QAM modulation	SNR= 10 dB	Rayleigh fading	2.5×10^{-2} to 2.8×10^{-2}
					AWGN channel	4.0×10^{-5} to 5.0×10^{-6}
8	*Hengyao Bao et al.*	2016	The Bayesian approach using the surplus degree of freedom of the transmit array. EM-TGM-GAMP algorithm is proposed for the number of iterations 20; the number of antennas 100 at BS, 10 single users; Number of symbols 128; 16 QAM modulation technique.	SER @ SNR= 10 dB	Clipping	1.9×10^{-2}
					FITRA	4.8×10^{-4}
					ET-TGM-GAMP	10^{-3}
9	*Mohammed El-Abasi et al.*	2015	MIMO-OFDM-IA (Interference alignment**)** scheme with antenna selection; CP length 16; the number of subcarriers 64; users 03 and 3×2 antenna system; Per-subcarrier antenna selection scheme at max-sum-rate and max-SNR.	SNR= 10 dB	Max Sum-rate	1.5×10^{-4}
					Max SNR	7.5×10^{-5}

Table 2.2 Error rate performance of STBC coded MIMO-OFDM System

S.No.	Authors	Year	Technology & parameters used for simulation	Bit Error Rates/Symbol Error rates @ SNR=10dB		
1	*Mingtong Zhang et al.*	2020	The STBC based MIMO-OFDM system in a time-varying environment with CSI estimation scheme; AMA and IMOT schemes are employed, Parameters: 2×2 antenna configuration, number of subcarrier = 1280, CP length =256, QPSK modulation, Doppler spread between 20 Hz to 160 Hz.	Static channel	TBS	1.5×10^{-3}
					AM AIM OT	1×10^{-3}
				Static channel with DS =80 Hz	TBS	2.0×10^{-3}
					AM AIM OT	1.5×10^{-3}
2	*Ruiguang Tang et al.*	2020	The STBC-MIMO-OFDM scheme with 2×2 and 4×4 configurations of antenna systems employing Kalman filter for estimation of MIMO channels.	2×2 , DS = 80 Hz		2.4×10^{-2}
				4×4 , DS = 80 Hz		9.0×10^{-3}
3	*Babatunde S. Adejumobi and Narushan Pillay*	2019	STBC-CSM; MBM modulation using RF mirrors; less complex ML detector is employed to reduce complexity; BER performance is analyzed for MBM-STBC-CSM, Nt = 3, Nr = 2, 16-QAM, RF mirror (mrf) = 2 and MBM-STBC-SM, Nt = 4, Nr = 2, M = 16, mrf = 2.	16 QAM, 3×2, MBSTBC-CSM		2.6×10^{-3}
				16 QAM, 4×2, MBSTBC-SM		2.4×10^{-3}
4	*Chaowu Wu et al.*	2019	A novel STBC scheme with rectangular differential spatial modulation (RDSM); BER performance for BPSK, QPSK, and ML detector; 4×2 and 8×2 configuration, transmission rate between 2 to 3 bpcu	BPSK and ML	4×2	2.5×10^{-3}
					8×2	9.0×10^{-3}
				QPSK and ML	4×2	1.8×10^{-2}
					8×2	4.8×10^{-2}
5	*Yanzhang Shao et al.*	2019	STB coded full-duplex relaying spatial modulation technique (STBC-SM-FDR);ML detector; 4×2 and 8×6 antenna configuration with 2 active transmits antennas; transmission rate 4 bits/s/Hz and 5 bits/s/Hz for $\lambda = 1$, using QPSK modulation.	STBC-SM-FDR (4×2)		1×10^{-1}
				STBC-SM-FDR (8×6)		3×10^{-2}
6	*Shital N. Raut, Rajesh M. Jalnekar*	2019	A novel hybrid optimization technique, the Dolphin-Rider-Optimization (DRO) is utilized for the STBC-MIMO-OFDM scheme; over the Rayleigh channel; using BPSK, QPSK, and QAM modulation.	BPSK	BER	2.5×10^{-5}
				QPSK		
				QAM		
				BPSK	SER	6.0×10^{-6}
				QPSK		
				QAM		
7	*Lixia Xiao et al.*	2017	The STBC-MIMO-DSM (differential spatial modulation) scheme; BPSK, QPSK, and 8 PSK modulation and with N_t= 4 and N_r = 2.	BPSK		8.0×10^{-4}
				QPSK		7.8×10^{-3}
				8PSK		4.2×10^{-2}

Table 2.3 Error rate performance of Alamouti STBC coded MIMO System

S.No.	Authors	Year	Technology & parameters used for simulation	Bit Error Rates/Symbol Error rates @ SNR=10dB	
1	*Siavash M. Alamouti*	1998	Alamouti scheme with 2×1 and 2×2 antenna configuration; BPSK modulation over Rayleigh fading channel.	Alamouti (2×1)	1.0×10^{-5}
				Alamouti (2×2)	1.3×10^{-4}
				MRRC (1×2)	1.9×10^{-3}
				MRRC (1×4)	6.0×10^{-3}
2	*Roopa M. and Dr. B.N. Shobha*	2019	The Alamouti and OSTBC coding technique for BER minimization, 2x2 configuration, BPSK Modulation scheme over Rayleigh fading channel	OSTBC coding (2×2)	8.0×10^{-5}
				Alamouti STBC (2×1)	5.5×10^{-3}
				MRC (1×2)	1.6×10^{-3}
3	*Sudhir Kumar Mishra and Kishor Damodar Kulat*	2018	A novel reduced feedback rate scheme for transmit antenna selection (TAS) scheme; BPSK modulation scheme; BER is analyzed for a different set of transmit antennas Nt = 3, 6, 9, and 12.	Nt = 3	1.25×10^{-3}
				Nt = 6	5.0×10^{-5}
				Nt = 9	6.0×10^{-6}
				Nt = 12	1.2×10^{-6}
4	*B. Dlodlo et a.l*	2018	Differential STBC expansion and trellis coding (TC-DSTBC) for improving the bandwidth efficiency using two transmit antennas; BER performance is analyzed using M-QAM modulation (M=16 and 64) scheme, over Rayleigh fading channel. No chaneel information is at the receiver, Nt =2 and Nr=4, Viterbi decoder,	TC-DSTBC for 16QAM	4.0×10^{-2}
				TC-DSTBC for 64QAM	1.4×10^{-1}
5	*S Nandi and A Nandi*	2017	Alamouti STBC coded MIMO-OFDM system. BER values are analyzed for different modulation schemes; BER values comparison between MRC and Alamouti scheme presented.	BPSK	5.0×10^{-5}
				QPSK	2.0×10^{-4}
				16QAM	4.0×10^{-3}
				Theoretical (Tx=1, Rx=2, MRC)	5.5×10^{-3}
				Theoretical (Tx=2, Rx=1, Alamouti)	1.75×10^{-3}
				Simulated (nTx=2, nRx=2, Alamouti)	1.0×10^{-4}
6	*Prabina Pattanayak et al.*	2017	Multi-user MU-MIMO-STBC system with imperfect CSI; BPSK modulation, the number of user K= 2, 4, 8, cyclic prefix length 16, and MMSE combiner at the receiver is used over Rayleigh fading channel; 2×2 antenna configuration.	K = 2	1.7×10^{-2}
				K = 4	1.3×10^{-2}
				K = 8	9.8×10^{-3}

Table 2.4 Error rate performance of MIMO System using MRC scheme

S.No	Authors	Year	Technology & parameters used for simulation	Bit Error Rates/Symbol Error rates @ SNR=10dB		
1	*Thien Van Luong and Youngwook Ko*	2018	The OFDM-IM (index modulation) with MRC and greedy detector (GD) for the investigation of BER and error probability; BPSK and QPSK modulation; one transmit, and 2, 4, 6 and 8 receive antennas; for BPSK modulation, 2 Subcarriers and 1 active subcarrier, and QPSK modulation, 4 Subcarriers, and 2 active subcarriers.	BPSK (perfect CSI)	BER Nr=2	2.5×10^{-3}
					BER Nr=4	1.0×10^{-5}
				BPSK (Imperfe-ct CSI)	BER Nr=2	6.0×10^{-3}
					BER Nr=4	6.0×10^{-5}
				QPSK (perfect CSI)	IEP Nr=2	2.5×10^{-2}
					IEP Nr=4	2.5×10^{-4}
					IEP Nr=6	4.0×10^{-6}
				QPSK (Im-perfect CSI)	BER Nr=2	1.8×10^{-2}
					BER Nr=4	6.0×10^{-4}
					BER Nr=6	2.8×10^{-5}
2	*N. C. Beaulieu and Yixing Zhang*	2017	Different combining schemes including MRC with unequal power dual branch, over Nakagami-m where m=0.5, BPSK modulation	SC		5.5×10^{-2}
				EGC		5.5×10^{-2}
				MRC		4.5×10^{-2}
3	*Ms. Manisha Misra et al*	*2017*	The MRC and EGC schemes for the improvement in BER and PAPR reduction in MIMO-OFDM system; for N=10000 subcarriers, channel taps L = 4, number of transmit antennas = 8	MRC	1×2	2.2×10^{-3}
					1×4	1.6×10^{-3}
					1×8	1.0×10^{-4}
				MRC over Rayleigh fading	1×2	1.7×10^{-3}
					1×3	1.4×10^{-4}
				EGC	1×2	2.2×10^{-3}
					1×4	1.2×10^{-3}
					1×8	2.0×10^{-4}
				EGC over Rayleigh fading	1×2	2.0×10^{-3}
					1×3	2.0×10^{-4}
4	*Pampee Das and Rupaban Subadar*	2017	MRC scheme with two-wave diffuse power (TWDP) fading channels for BER improvement in MIMO systems. Considering 1×2 and 1×3 antenna configuration with 16 QAM modulation scheme	16-QAM, 8-QAM, 4-QAM	1×2	6.5×10^{-4}
					1×3	3.5×10^{-5}

Table 2.5 PAPR reduction performance in OFDM system

S.No.	Authors	Year	Technology & parameters used for simulation	PAPR in dB @ CCDF= 10^{-3}		Remark	
1	*Zhitong Xing. et al.*	2020	A low complexity companding schemes; AWGN channel; QPSK modulation.	C = 0 A=1.414,	3.4 dB	BER @SNR 10 dB	4×10^{-4},
				C = 0 A=1.67	4.25 dB		2.5×10^{-4}
				C = 0 A=17.34	5.1 dB		1×10^{-4}
2	*Bo Tang et al.*	2020	ICF method with ENC scheme, 256 subcarriers , 16 QAM modulation; oversampling factor =4; clipping ratio 1.5 to 1.8; clipping level 3; shape factor s = 60, v= 0.72 to 0.87	ICF and ENC CR=1.5	4.25 dB	BER @SNR 10 dB	7×10^{-3}
				ICF and ENC CR=1.8	5.4 dB		4×10^{-3}
3	*Tarak Arbi and Benoit Geller*	2019	The blind detection in an SLM scheme is used to improve PAPR; Rayleigh fading channel; with 64-QAM modulation; subcarriers=1024; sub-blocks= 16	9.7 dB		Tone Reservation	
				7 dB		PTS	
				8.9 dB		Clipping (10 iteration)	
				8.6 dB		Blind detection for SLM	
4	*Ahmad M. Rateb and Mohamed Labana*	2019	Low-complexity techniques like SLM, PTS and ICF for PAPR reduction are analyzed over AWGN channel, 16-QAM and 64-QAM modulations , and 1024 subcarriers	9.8 dB		SLM	
				8.3 dB		PTS	
				7.2 dB		Clipping	
				6.0 to7.0 dB		Linear scaling of coefficients	
5	*Selahattin Gokceli et al.*	2019	ICEF scheme. Bandwidth 20 MHz; Total number of subcarriers 2048; QPSK, M-QAM constellations (M=16 and 64), for iterations = 1, 10,and 20	8.35 dB		1 Iteration	
				6.3 dB		10 Iteration	
				6 dB		20 Iteration	
6	*Kee-Hoon Kim*	2019	A novel OFDM-IM scheme; Modulation 16-QAM; clipping ratio 5; iteration=2; subcarrier N=128; length of sub-block = 4; Number of active subcarriers k= 2	6.7 dB		BER @10 dB SNR	7.0×10^{-2}
7	*Bo Tang*	2019	Clipping-noise compression technique with μ -law algorithm; Number of subcarriers 256; modulation = 16 QAM; over sampling factor =4; Number of iteration =3 ; clipping ratio = 3 and 6 dB; μ =10	C.R. =3	4.4 dB	BER @10 dB SNR	6.5×10^{-3}
				C.R.=6	6.35dB		2×10^{-3}
				ICF-Technique for CR=3,6	4.8 & 7.1 dB		3.8×10^{-2} & 2.8×10^{-3}
8	*Prabal Gupta et al.*	2019	SLM technique with discrete cosine transform (DCT) for optimizing PAPR; Modulation: 4-PSK, Phase sequences U=128, N=32 subcarriers	5.7 dB		-- -- --	

S.No.	Authors	Year	Technology & parameters used for simulation	PAPR in dB @ CCDF= 10^{-3}		Remark	
9	*Jingqi Wang and Wen Wu*	2019	TR scheme based on SCR; and MS –SCR scheme used for optimization; 16-QAM modulation; Number of subcarriers 256; Tone reservation T=32; oversampling rate 4; Clipping ratio =4,3,2,1	S-SCR for CR=2	7.5 dB	BER @10 dB SNR	5.0×10^{-4}
				MS-SCR for CR=2	5.1 dB	BER @10 dB SNR	0.8×10^{-3}
10	*Lahcen Amhaimar et al.*	2018	PTS scheme with an FWA algorithm, 2×1 and 4×1 antenna system, QPSK, 52 subcarriers, 104 random OFDM symbols, oversampling factor L = 4, over AWGN channel, number of sub-blocks = 2; 4; 6; 8	5.2 dB		Con. PTS	
				4 dB		PTS-FWA	
				7.1 dB		SLM	
11	*Fan Gao et al.*	2018	Iterative PTS combined with clipping method; OFDMA scheme with 256 points IFFT, number of blocks 3000 and sub-blocks 'V'	PTS	7.8 dB	Sub-block V = 4	
				Clipping	6.4 dB	4-Clip & filter	
				PTS-Clipping	6.2 dB	V = 4, 4-Clip & filter	
				IPTS	5.25 dB	V = 4,Iterative PTS & Clipping	
12	*Francisco Sandoval*	2017	A hybrid technique combining modified code repetition (MCR) and SLM scheme with clipping; number of subcarriers 512, 50% cyclic prefix, the oversampling factor of 1, number of phase sequences 8 and BPSK modulation over the AWGN channel.	MCR-SLM	3.4 dB	BER @10 dB SNR	4.8×10^{-6}
13	*Kelvin Anoh et al.*	2017 -1	Clipping and filtering (ICF) method; AWGN channel, QPSK modulation, 128 samples, 512 subcarriers, No CP, MMSE optimization	1-clip; with & without optimization	1.9 &5.5dB	BER @10 dB SNR	2.5×10^{-3} & 1×10^{-2}
				2-clip; with & without optimization	1.25 &4.7 dB		-- --
				3-clip; with & without optimization	1.0 &4.5 dB		1×10^{-2} & 9×10^{-2}

S.No.	Authors	Year	Technology & parameters used for simulation	PAPR in dB @ CCDF= 10^{-3}		Remark	S.No.
14	*Kelvin Anoh et al.*	2017-2	Root-based μ -law companding (RMC) method; Number of subcarriers 512; symbols =128, QPSK modulation, oversampling factor=4; $\mu = 30$;	3.2 dB		BER @10 dB SNR	1.2×10^{-2}
15	*Ms. Manisha Misra et al*	2017	MRT, MRC, and EGC schemes are used in the MIMO-OFDM system for the PAPR reduction, subcarriers N=10000, channel taps L = 4	MRT	5.25 dB	For Channel tap =4	
				PTS	6.9 dB	For sub-blocks =16	
				SLM	> 6.0 dB	75 % of time, for number of phase vector U=4 ,8, 16	
16	*Chunxing Ni et al.*	2016	ATR technique; Number of subcarriers 1024; number of peak reduction tones (PRT) = 64, clipping ratio =2.2, user =10 antennas =100; and 4-QAM modulation	ATR	6.8 dB	--	--
17	*Hengyao Bao et al.*	2016	The Bayesian approach using the surplus degree of freedom of the transmit array. EM-TGM-GAMP algorithm is proposed for the number of iterations 20; the number of antennas 100 at BS, 10 single users; Number of symbols 128; 16 QAM modulation technique.	Clipping	4.9 dB	SER @ 10 dB SNR	1.9×10^{-2}
				FITRA	3 dB		4.8×10^{-4}
				ET-TGM-GAMP	2.6 dB		10^{-3}
18	*Yong Wang et al.*	2015	ICTF with linear symmetrical transform and two piecewise companding method; the number of subcarriers=1024; QPSK modulation; oversampling ratio = 4; 10^6 random OFDM frames; 03 iterations; over AWGN and multipath fading channels; 25% CP length.	ICTF-LST with 3 iteration	6.5 dB	BER @10 dB SNR	0.5×10^{-3}
				ICTF-TPC with 3 iteration	5.25 dB	BER @10 dB SNR	3.0×10^{-5}

Table 2.6 Channel capacity performance in MIMO-OFDM

S.No.	Authors	Year	Technology & parameters used for simulation	BER @ 10dB SNR			Data Rates bits/s/Hz @ 10 dB SNR	
1	Yanzhang Shao et al.	2019	STB coded full-duplex relaying spatial modulation technique (STBC-SM-FDR); ML-detector, 4×2 and 8×6 antenna configuration with 2 active transmits antennas; transmission rate 4 bits/s/Hz and 5 bits/s/Hz; $\lambda = 1$ z; QPSK modulation.	STBC-SM-FDR (4×2)		1×10^{-1}	2.15 bits/s/Hz	
				STBC-SM-FDR (6×4)		3×10^{-2}	2.55 bits/s/Hz	
2	*Kelvin Anoh et al.*	2019	QO-STBC-MIMO technique; standard SVD bases detection with one-directional beamforming using 16-QAM constellation; 2×1 antenna system	SVD	2×1	1.6×10^{-1}	SVD 2×1	6.2 bits/s/Hz
				std STBC	2×1	6.5×10^{-2}		
				SVD	4×1	1.9×10^{-2}	SVD 8×1	6.8 bits/s/Hz
				std STBC	4×1	4.1×10^{-3}		
3	*Madhusmita Sahoo and Harish Kumar Sahoo*	2019	The time-varying MIMO channel model using a sparse model based on the DLMS (diffusion least-mean-square) algorithm; 2×2 antenna configuration; 16 QAM, AWGN channel, STBC code diversity; Capacity tested for IEEE802.11, I-METRA, and 3 Gpp channels.	I-MET.	2×2	--	9.9 bits/s/Hz	
				IEEE 802.11	2×2	--	6.0 bits/s/Hz	
				3-Gpp	2×2	--	8.5 bits/s/Hz	
4	*Parag Aggarwal and Vivek Ashok Bohara*	2018	A nonlinear dual-band MU- MIMO-OFDM system; subcarriers = 1024, users = 4, CP=1/4, IBO=5dB; overall capacity is measured against 4 users for transmitting power P_T = 5 dB to 15 dB.	SER	6×2	5.5×10^{-1}	P_T = 10 dB	18 bits/s/Hz
				SER	3×1	6.0×10^{-1}	P_T = 15 dB	24 bits/s/Hz

Table 2.7 Ergodic capacity, Outage capacity and outage probability performance

1	*Donghun Lee*	2018	MRC scheme over imperfect channel estimation to investigate the ergodic capacity and outage capacity in a MIMO system; transmit antenna selection and user (K) selection is combined for 2×1 MIMO system	**Data rates/ Capacity and Outage capacity**			
				Ergodic capacity (K=1)			3.7 bits/s/Hz
				Ergodic capacity (K=2)			4.25 bits/s/Hz
				Outage capacity at 10% outage (K=1)			2.5 bits/s/Hz
				Outage capacity at 10% outage (K=2)			3.3 bits/s/Hz
				Outage probability @10 dB SNR for (K=1)			6.5×10^{-2}
				Outage probability @10 dB SNR for (K=2)			4×10^{-3}
2	*Lopamudra Kundu and Brian L. Hughes*	2017	Broadband MIMO-OFDM systems with the frequency-selective matching of receiving antennas; antenna configurations 2×2 and 4×4; Carrier frequency = 900 MHz, No. of subcarriers= 64; considering UCA and ULA at the receiver	**Data rates/ Capacity and Outage capacity**			
				UCA	2×2	Capacity	4.5 bits/s/Hz
					4×4		8.0 bits/s/Hz
					2×2	Outage capacity	4.4 bits/s/Hz
					4×4		7.8 bits/s/Hz
				ULA	2×2	Capacity	5.0 bits/s/Hz
					4×4		7.0 bits/s/Hz

2.2.7 Summary of the literature survey

The literature survey is focused on various issues encountered in MIMO-OFDM unwired communication system. This survey has been carried out for analyzing some noteworthy issues such as error rates, PAPR, channel impairments, and information or data rate (capacity), etc. From the survey of literature during the last 05 years, it is observed that effective and significant to combat one or more issues have been suggested by many researchers. Considering SNR of 10 dB for measuring BER, PAPR, and Data rates, the following are some findings from the literature survey.

1. It is observed that the error rate presentation of the MIMO-OFDM system over the AWGN channel is better than that of over Rayleigh fading channel. Also, the error rate performance of the MIMO-OFDM system using the lower-order (BPSK/QPSK) modulation method is better as compared to higher-order (M-QAM) modulation techniques.

2. The results of most of the schemes suggested by different researchers depict that over the AWGN channel the error rate (BER) values are in the range of 10^{-5} to 10^{-6}. On the other hand, the BER values over the Rayleigh fading channel is recorded as in the range of 10^{-2} to 10^{-3}. For example, the F-OFDM scheme by Jayan and Nair (2018), using BPSK modulation over the AWGN channel give BER of 10^{-6}. The same system suggested by Yaang et al., (2019), using 64 QAM modulation over the Rayleigh fading channel gives a BER value of 2.5×10^{-2}. A similar result is observed using PCC-OFDM and UFMC scheme suggested by Wang et al., (2017), that is BER value over AWGN and Rayleigh fading channel are 5.0×10^{-6} and 2.8×10^{-2} using QPSK modulation respectively.
3. For STBC coded MIMO OFDM systems the BER result is improved even over the Rayleigh fading channels. For example, the STBC-MIMO-OFDM system with DR-optimization by Raut and Jalnekar (2019), gives BER and SER values in the range of 10^{-5} to 10^{-6}, the STBC-MIMO-DSM scheme by Xiao et al.,(2017) gives BER value of 10^{-4} , the STBC coded MIMO OFDM systems by Zhang et al., (2020); Ruiguangtang et al.,(2020); Adejumobi and Pillay (2019), gives the BER value of 10^{-3}.
4. For Alamouti STBC coded MIMO system by Roopa and Shobha (2019); Mishra and Kulat (2018); Nandi and Nandi (2017), the BER values are recorded in the rage of 10^{-3} to 10^{-5} for BPSk / QPSK modulation techniques. It is also observed that by increasing the number of transmit antennas the BER values can be further reduced to less than 10^{-6}.
5. For the MIMO-OFDM scheme with MRC using BPSK/QPSK modulation, by Mishra et al.,(2017); Das and Subadar (2017); OFDM-IM-MRC by Luong and Ko (2018), the BER value is recorded in the rage of 10^{-3} to 10^{-5} over Rayleigh fading channel. By increasing the number of receiving antennas the BEr BER value decreases.
6. The PAPR performance of iterative clipping and filtering (ICF) scheme in an OFDM system is found better as compared to others techniques such as PTS, SLM, ICTF, TR, etc. The PAPR value for; companding scheme by Xing et al., (2020), 3.5 dB to 5.0 dB; SLM scheme by Gupta et al., (2019), 5.7 dB; PTS scheme with FWA algorithm by Amhaimar et al., (2018), 5.2 dB; IPTS scheme by Gao et al.,(2018),

5.25 dB; Hybrid MCR-SLM scheme by Sandoval (2017), 3.4 dB; Root based micro-law companding (RMC) scheme by Anoh et al., (2017-1), 3.2 dB; ICF technique by Tang et al., (2020), 4.25 dB to 5.4 dB at C.R. = 1.5 and 1.8 and the BER is maintained to 4.0×10^{-3} ; ICF technique by Anoh et al.,(2017-2), 4.5 dB with 3.0 clips and BER = 9.0×10^{-2}; ICF technique by Bao et al.,(2016), 4.9 dB with BER = 1.9×10^{-2}.

7. It is also found that by increasing the transmit antennas in a MIMO system, the channel capacity or data rates are linearly increases but at the cost of an increase in error rates (BER). For the QO-STBC-MIMO scheme by Anoh et al., (2019), for 2×1 and 4×1, the data rates are 6.2 and 6.8 bits/s/Hz respectively; the MIMO system with DLMS algorithm by Sahoo and Sahoo (2019), the data rates found between 6.0 to 9.9 bits/s/Hz at different standards, using 2×2 configuration; the broadband MIMO-OFDM system using frequency selective matching at the receiver by Kundu and Hughes (2017), data rates = 5.0 bits/s/Hz and 8 bits/s/hz for 2×2 and 4×4 antenna configurations.

2.2.8 Need for further Research

From the literature survey of last 5 years it has been observed that the BER reduced in the range of 10^{-5} to 10^{-6} using various modulation schemes, channel coding schemes, and antenna selection and combining schemes. Here there is a scope to lessen the BER below the level mentioned above over AWGN channel and Rayleigh fading channel. To get rid of the most deleterious effects of PAPR in the OFDM system different algorithms have been used by many researchers and they have reduced the PAPR to significant value. However, there is further scope for reducing the PAPR without adding complexity and cost of the system and most important without increasing BER significantly. As far as the capacity of data transfer is concerned, enhancing capacity by implementing more antennas in the MIMO system is not a proper solution, since it may results in high power consumption and the cost and complexity of the system. So there is a scope to choose such an algorithm and combination of antennas in the MIMO system which not only increases the capacity but also lessens the error rates of the system as well as power consumption and hardware complexity.

Chapter 3

MIMO-OFDM Systems

3.1 OFDM CONCEPT AND DESIGN CHALLENGES

This chapter includes fundamentals/concepts, benefits, limitations, and design challenges of the OFDM system. In this new era the high speed, high capacity or data rate, and reliable wireless communications is the utmost requirement to support various application on mobile, internet of things, web browsing, secure and confidential data transfer and so on. An OFDM system is the most efficient and popular scheme used in wireless communication in the last decade. And till date OFDM is the best choice for providing errorless communication over the wireless link. The OFDM is the multi-carrier modulation system that significantly outperforms the conventional single-carrier system.

3.1.1 Background

Unlike wired communication, in the case of wireless environment transmitted signals are received at the receiver terminal through multiple paths after brief delays between each copy due to reflection, refraction, and attenuation from various objects like forest/trees, hills/mountains, huge buildings, etc. These delayed multiple copies of the transmitted signal result in serious performance degradation of the wireless communication system. The phenomenon is also known as fading. If "T" is the symbol duration of transmitted signal and "T_m" is the maximum delay among all delayed replicas of the transmitted signal at the receiver then normalized delay spread is given by Eq. 3.1.

$$D = {T_m}/{T} \quad \text{... (3.1)}$$

If D << 1 or the symbol period is too greater than the maximum delay spread " T_m", the channel is known as flat fading channel. The flat fading channel doesn't incur inter-symbol interference (ISI). On the contrary, if D>>1 or $T < T_m$, the channel is

known as a multi-path fading channel. In such an environment there is a strong possibility of the occurrence of inter-symbol interference [8].

3.1.2 Single-Carrier (SCM) versus Multicarrier Modulations (MCM)

SCM utilizes only one frequency for transmitting any data signal. It has been used in several wireless communication systems like 1G, 2G, 3G, and in the uplink of 4G systems. Due to many advantages, SCM systems are still utilized in 4G communication standards, for example, SC-FDMA. The SC-FDMA is one of the best technologies employed for the uplink in the 'long-term-evaluation (LTE)' standard. The system functional block diagram of SC-FDMA is as shown in fig 3.1

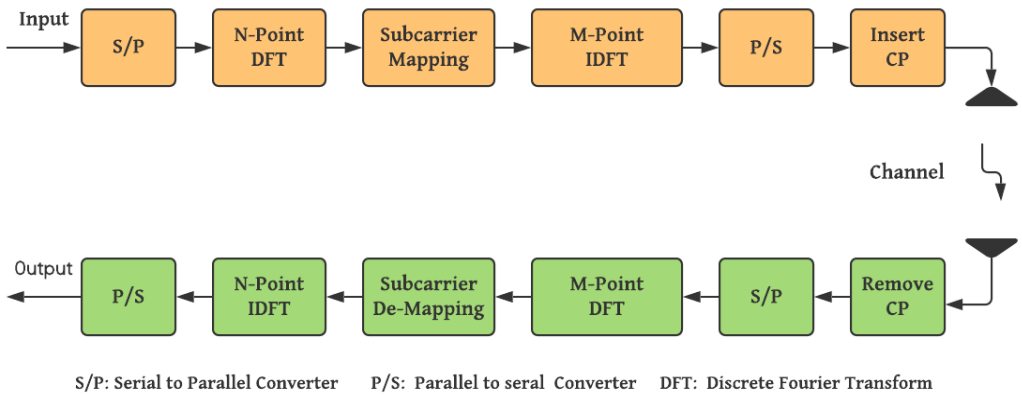

Fig. 3.1 System functional block diagram of SC-FDMA

The SC-FDMA wireless system uses *N*-point 'Discrete-Fourier-Transform (DFT)' and *M*-point 'Inverse-Discrete-Fourier-Transform (IDFT)' modules, where N is always less than M. Due to this feature occurrence of PAPR is greatly minimized or produce very little PAPR during signal transmission. The insertion of the cyclic prefix of proper length makes easy channel equalization in the frequency domain [77].

Advantages of SCM:

1. The PAPR in SCM is very less compared to MCM. This property of SCM is very important for a stable, errorless, interference less and reliable

communication system. SCM is generally used in low-cost devices exploited in wireless communication systems.

2. SCM systems are less susceptible to phase noise and frequency shift, which is helpful for time and frequency synchronization in the wireless system.

Disadvantages of SCM:

1. The SCM systems performance in terms of spectral efficiency is deeply degraded in presence of multipath fading which is obvious in today's wireless system.
2. In SCM the bandwidth is high and symbol duration is small hence they more sensitive to frequency selective fading channels which results in ISI.
3. To avoid ISI in SCM very complex multi-tap channel equalizer is needed which in turn makes the SCM system complex and costly.

In the MCM system, the whole channel frequency is split into many subcarriers. The high-rate input signal to be transmitted is sliced into many low-rate signals equals to the number of subcarriers and is transmitted on the subcarriers in parallel.

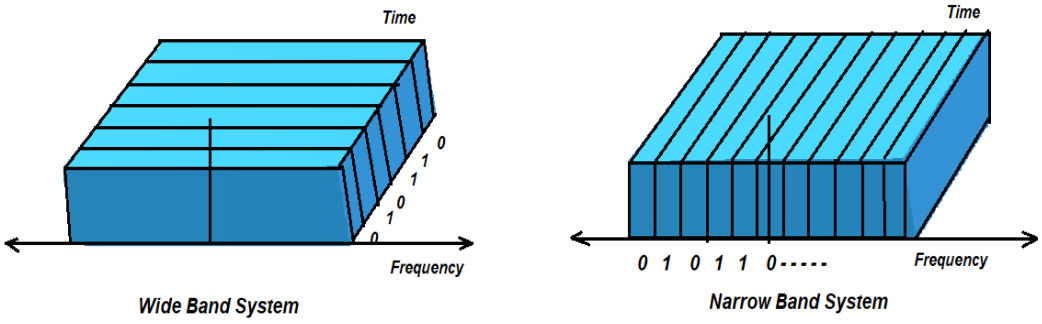

(a) (b)

Fig. 3.2 (a) Wideband transmission in SCM (b) Narrow band transmission in MCM

From fig. 3.2 it is obvious that the symbol duration in MCM is larger than the symbol duration in SCM. In case SCM as the symbol duration is too less than the maximum delay spread, the system is susceptible to ISI. Whereas in MCM the symbol duration is too greater than the maximum delay spread due to the multi-path

fading channel and hence the MCM system is more robust against ISI. The frequency selective channel in the case of SCM is now becoming a flat fading channel in the case of MCM due to the segmentation of wideband into narrowband subcarriers. Because of the ability to combat the effects of multipath fading, MCM systems have become more popular in wireless systems. The MCM system was first introduced by Randel et al. (2006) with the data rate of 1Gbits/s over 100 m polymer optical fiber (POF). The data rate achieved by Randel at that time was just double the highest data rates achieved earlier over the same fiber length. For the above experiment 80 subcarriers, each with the bandwidth of 2 MHz without any guard band were used [78].

MCM technology is plagiaristic of frequency-division multiplexing (FDM). Presently MCM are used in DSL MODEMs and DAB/DVB broadcast system. In MCM normally FFT technology is used for signal transmission over multiple independent subcarriers with equal narrow bandwidth. However, MCM technology is less susceptible to ISI, still, the performance of MCM degraded slightly due to the ISI. The ISI in MCM can be reduced by inserting guard bands between the two symbols [79]. One of the drawbacks and the most critical issue in MCM is the presence of PAPR. Due to the increase in PAPR most linear components such as PA and DAC/ADC in the MCM system behaves nonlinearly which causes in-band distortion and out of band radiation. This results in a breakdown of orthogonality, incur interference between adjacent subcarriers (ICI), and major loss in SNR. To reduce the effect of PAPR, linearization techniques can be used to increase the linearity of the system but at the cost of an increase in complexity and the system cost [15], [80]. If 'D' is the difference between PAPR of MCM and SCM and 'N' is the number of subcarriers in MCM then, the difference 'D' is given by

$$D=10\log N \quad \text{dB} \qquad \text{... (3.2)}$$

The SNR loss in MCM system is given by Eq. 3.3

$$\text{SNR loss in dB} = 10\log\left(\frac{L_b+L_c-1}{L_b}\right) \text{ dB} \qquad \text{... (3.3)}$$

Where, L_b = original block length, L_c = length of channel response and $L_b + L_c - 1$ is extended symbol length.

3.1.3 Frequency division multiplexing (FDM)

In an FDM system, the available bandwidth of a single channel is split into N number of sovereign frequency channels that allow users to transmit their signal on different frequency channels within the same bandwidth. Using different modulation techniques N number of different information signals is translated using N number of independent frequency channels. All the modulated signals are combined to form a composite signal using linear summing circuits. Now the resulting composite signal is ready to transmit over the wireless channel. The carrier signals with frequencies $F_1, F_2, F_3, \ldots\ldots\ldots F_N$ used for transmission are known as sub-carriers. The composite signal to be transmitted over N subcarriers is shown in fig. 3.3

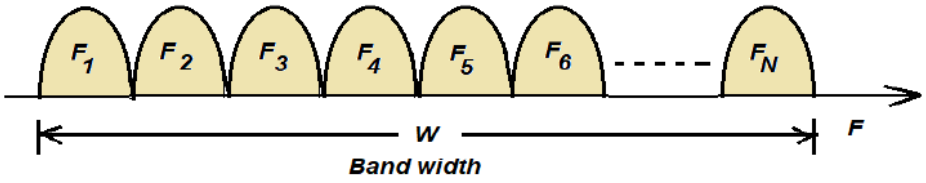

Fig. 3.3 Composite signal transmission

At the receiver, all the independent information signals are separated using filters and demodulated to achieve the original information signals. Now if the subcarriers are very close to each other as depicted in fig 3.3, there is a high probability of having inter-channel interference or cross talk. The ICI or Cross-talk is a partial overlapping between the neighboring channels as shown in fig. 3.4.

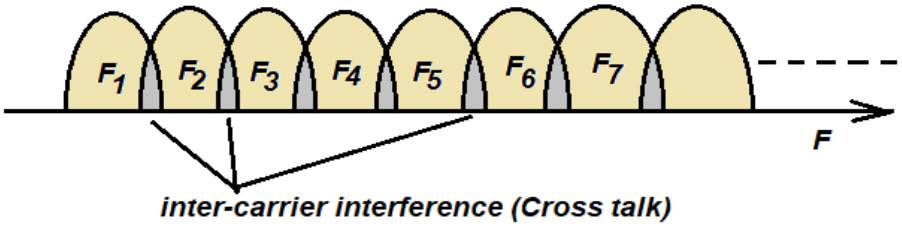

Fig. 3.4 Inter-carrier interference between adjacent channels

The chances of incurring ICI can be minimized by inserting narrow bands between two neighboring channels as shown in fig. 3.5, is known as guard bands. Thus using the FDM technique independent information signals can be transmitted safely without ICI.

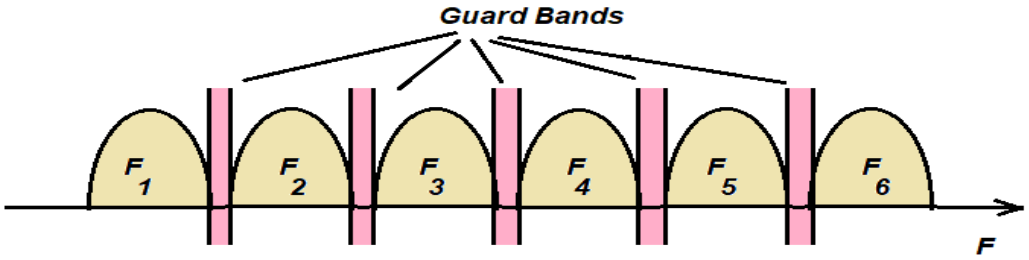

Fig. 3.5 Guard band between neighboring channels

Advantages of FDM:

1. There is no need for synchronization between receiver and transmitter.
2. More than one information signal can be safely transmitted.
3. Easy demodulation.
4. Due to the slow fading channel, only one channel may be affected.

Disadvantages of FDM:

1. FDM channels may be affected in presence of wide-band fading.
2. Due to more number of demodulators in FDM, the power consumption as well as system complexity increases.
3. Due to the insertion of guard bands, a large bandwidth is required to accommodate all the channels.
4. In presence of the guard band also there is a chance of cross-talk.

3.1.4 OFDM Systems

There are two types of MCM namely 'multi-carrier-code division multiple access (MC-CDMA and OFDM'; 'using time-division multiple access (TDMA)'. In MC-CDMA to distinguish different users, they are multiplexed with orthogonal codes. Multiple users can access the MC-CDMA system simultaneously; however, different users are allocated with numerous codes where data is present in either time domain or frequency domain. In OFDM-TDMA different users are allocated in time slots to transmit or receive data. It can use all higher-order (M = 4 to 256) M-QAM modulation along with lower-order modulations like BPSK and QPSK [82].

The OFDM system can adopt many communication standards like 3GPP Long Term Evolution (LTE), Wi-Max, IEEE 802.11a/g/n (Wi-Fi), IEEE 802.16a MAN, LAN, 'Digital Audio Broadcasting (DAB)' and 'Digital Video Broadcasting (DVB)', European DVB and 'Asymmetric Digital Subscriber Line (ADSL)' and many more [81].

The OFDM is an MCM that was first proposed in 1966. OFDM splits the single broadband channel into many parallel sub-channels like the MCM system. If 'W' is the overall available bandwidth of OFDM and 'N' subcarriers or sub-channels then the subcarrier bandwidth is $\left({}^{W}/_{N}\right)$. Each subcarrier has a different frequency and the frequency of each subcarrier is an integer multiple of a fundamental frequency.

In general, the multicarrier transmission in OFDM includes a set of modulators each at a different carrier frequency. The transmitter section combines the output of all the modulators and produces a composite signal for transmission. Consider X_k (k = 0, 1, 2, 3……., N-1) as a complex number output of the modulation used and it consists of N bit data. Assuming T_s as OFDM symbol period and the carrier frequency of k^{th}subcarrier $f_k = {}^{k}/_{T_s}$, the complex output of a transmitter is given by

$$x(t) = \sum_{k=0}^{N-1} X_k \, e^{j2\pi f_k t} \qquad \text{... (3.4)}$$

For discrete signal putting $t = nT_o$, where T_o is the symbol period of the original signal, and is equal to ${}^{T_s}/_{N}$ if N is the number of subcarriers. Therefore, $t = {}^{nT_s}/_{N}$, and sample index n = 0,1,2……N-1. Therefore the above expression in a discrete domain can be written as,

$$x(nT_o) = \sum_{k=0}^{N-1} X_k \, e^{j2\pi f_k nT_o} \qquad \text{... (3.5)}$$

$$x(nT_o) = \sum_{k=0}^{N-1} X_k \, e^{j2\pi \frac{k\, nT_s}{T_s\ N}} \qquad \text{... (3.6)}$$

Therefore the OFDM signal is given by

$$x_n = x(nT_o) = \sum_{k=0}^{N-1} X_k \, e^{j2\pi \frac{nk}{N}} \qquad \text{... (3.7)}$$

The above expression is similar to the expression of N-point IDFT except that the multiplication factor (1/N). If the number of subcarriers is a power of two then many

efficient and fast algorithms are available for the implementation of IDFT. Thus OFDM is the best suitable technology in today's wireless communication [82].

The system architecture of OFDM is shown in Fig. 3.6. In the OFDM system, a stream of serial data is modulated using BPSK/ QPSK/ M-QAM modulation technique to map source data to a complex number. The complex value is specifying the amplitude and phase of the sinusoid at the mapped constellation point for the corresponding subcarrier. The serial to parallel converter is used to convert serial complex data stream into the parallel data stream where the stream of serial data input is split into the stream of 'K' low rate parallel data or symbols.

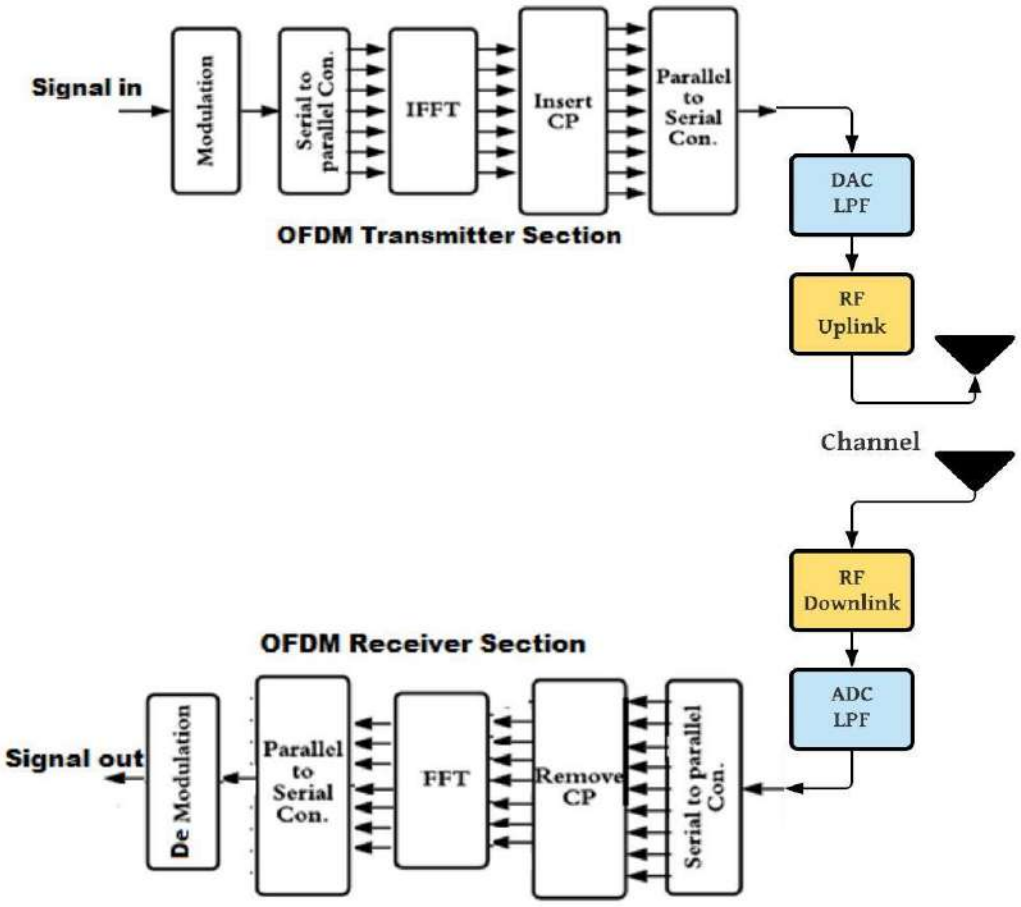

Fig. 3.6 System architecture of OFDM

Now each parallel sub-channel carries one complex number symbol in the frequency domain. The K symbols are then passed through N-point IFFT. The IFFT receive N symbols from the K symbols and each symbol has a symbol period of 'T_s' where $(T_s = {}^{N}/_{W})$ and produces N orthogonal sinusoids over N subcarriers. Each subcarrier has a different frequency which is an integer multiple of a fundamental frequency. The input to an IFFT in the frequency domain is transformed into the time domain. The output of IFFT is the logical summation of all N orthogonal sinusoids or N orthogonal sub-carriers which is known as one OFDM symbol. A guard band or cyclic prefix of a specific length is inserted at the beginning of each output symbol from the IFFT to prohibit the possibility of ISI between adjacent sub-carriers. Now the parallel stream of data including cyclic prefix is converted into the serial data stream in the time domain which is further passed through analog device DAC and LPF filter for RF up-conversion before transmitting over RF channel. The transmitted signal is received through receiving antenna and it is down-converted for further processing the signal. The received signal is then passed through ADC and LPF to convert it into digital form. The digital output signal is converted into parallel form to remove cyclic prefixes from each symbol that was inserted before the transmission of the signal. The output of the serial to parallel (S to P) converter is nothing but the original OFDM symbol after removal of the CP, and it is passed through N-point FFT. The FFT block is employed to converts the input signal from the time-domain to frequency-domain which is further converted into the serial form using a parallel to serial (P to S) converter. The serial output from the P to S converter is demodulated to obtain the original information or data stream. The presence of fast and efficient IFFT and FFT algorithms at transmitter and receiver makes the OFDM a very popular system providing high spectral efficiency. Inserting CP in each symbol increases the symbol period such that the symbol period T_s becomes greater than the multipath delay spread " T_m ". This minimizes the probability of incurring ISI in the OFDM system, but at the cost of reduced data rates.

Advantages of OFDM Scheme

1. *Combating ability against ISI:* In OFDM based wireless communication system the inter-symbol interference has a deleterious effect on system performance. If the bandwidth of the OFDM symbol is too less than the coherence bandwidth or the OFDM symbol duration is too greater than the original symbol duration the ISI can be mitigated. This can be done by adding the CP which is nothing but the last sample of the previous symbol added at the beginning of the next symbol.
2. *Combating ability against ICI:* The OFDM systems are time-limited and not band-limited, so these systems may suffer from out-of-band radiation. The large picks in an OFDM lead to out-of-band radiation which may break the orthogonality of the OFDM system and further result in ICI. The effect of ICI can be mitigated by reducing the high PAPR and thus maintaining the orthogonality.
3. *High spectral efficiency:* In the OFDM system the available bandwidth 'W' is split into several flat fading sub-channels or subcarriers. All the subcarriers are orthogonally spaced that is the frequency spectrum of each subcarrier spectrum intersects at the zero-crossing level of the spectrum of the neighboring subcarrier. Although the spectra are overlapped with each other the signal can be easily demodulated by extracting subcarriers using orthogonality. Thus overlapped and multiplexed spectrums of subcarriers allow us to improve the spectral efficiency.
4. *Robust against frequency selective fading effects:* OFDM divides the overall channel bandwidth into multiple fat fading channels (sub-bands or sub-carriers) with narrow bandwidth. Thus the OFDM system offers immunity against the effects of frequency selective fading.
5. *Complexity and flexibility:* The OFDM systems are less complex, flexible, adaptive, and robust compared to SCM. In OFDM, the maximum likelihood (ML) decoding technique offers low complexity with improved quality of services.

6. *Simple channel equalization:* since all the subcarriers are orthogonal, the OFDM system requires a simple signal processing algorithm and only one tap equalizer. This reduces computational complexity in the OFDM system.
7. *Merger of MIMO and OFDM system:* The OFDM system can be integrated with the MIMO system to achieve the benefits of both OFDM and MIMO systems together, such as the Speed, capacity, and reliability of the communication system.

Disadvantages of the OFDM scheme

1. Signal distortion due to frequency mismatch between transmitter and receiver.
2. OFDM is susceptible to carrier frequency offset (CFO) and drift compared to SCM.
3. Computation complexity increases by increasing the number of subcarriers.
4. Practically in the OFDM system, channel variation may occur even at slow fading, which may destroy the orthogonality and becomes the cause of ICI.
5. To reduce ISI in the OFDM system, it is required to add CP which in turn reduces the data rates, use of equalization technique, space-time coding, and other schemes adds computational complexity in the system.
6. The most deleterious issue in the OFDM system is the high PAPR which further results in ICI. An attempt to reduce PAPR results in an increase in BER.

3.1.5 Orthogonality in OFDM

The ICI can be mitigated by maintaining the orthogonality in the OFDM system [15]. Considering the time-limited complex exponential signal $\{e^{j2\pi f_k t}\}$, k =0----N-1 which represents various subcarrier at a frequency $f_k = {}^{k}/_{T_s}$, where $0 \leq t \leq T_s$, where T_s is the OFDM symbol period without a guard signal. The signals in OFDM are orthogonal if and only if the integral of the products for their common period is null. Therefore,

$$ {}^{1}/_{T_s} \int_0^{T_s} e^{j2\pi f_k t}\ e^{-j2\pi f_i t} dt \ = \ {}^{1}/_{T_s} \int_0^{T_s} e^{j2\pi \frac{k}{T_s} t}\ e^{-j2\pi \frac{i}{T_s} t} dt \qquad \text{... (3.8)} $$

$$= {}^{1}/_{T_s} \int_0^{T_s} e^{j2\pi \frac{k-i}{T_s} t}\, dt \quad \text{... (3.9)}$$

$$= \begin{cases} 1 & \forall \text{ integer } k = i \\ 0 & \text{otherwise} \end{cases} \quad \text{... (3.10)}$$

For the 'N' subcarriers, the symbol period T_o ($T_o = {}^{T_s}/_{N}$) of original signal; the discrete signal can be obtained by putting $t = nT_o = {}^{nT_s}/_{N}$, where n = 0,1,2……N-1. Therefore the above expression in the discrete domain can be written as,

$$\frac{1}{N} \sum_{n=0}^{N-1} e^{j2\pi {}^{k}/_{T_s} nT_o}\, e^{-j2\pi {}^{i}/_{T_s} nT_o} = \frac{1}{N} \sum_{n=0}^{N-1} e^{j2\pi {}^{k}/_{T_s} \frac{nT_s}{N}}\, e^{-j2\pi {}^{i}/_{T_s} \frac{nT_s}{N}} \quad \text{... (3.11)}$$

$$= \frac{1}{N} \sum_{n=0}^{N-1} e^{j2\pi \frac{(k-i)\, n}{N}} \quad \text{... (3.12)}$$

$$= \begin{cases} 1 & \forall \text{ integer } k = i \\ 0 & \text{otherwise} \end{cases} \quad \text{... (3.13)}$$

3.1.6 OFDM System Design Challenges and issues

To design any system, a comprehensive understanding of the role of critical parameters and their effects on the system performance is necessary. Following are some system design challenges in OFDM systems:

- **Available bandwidth:** The available bandwidth in a wireless network is always a critical issue since it limits the number of subcarriers to be implemented in the OFDM system. The number of subcarriers to be accommodated in a given bandwidth is further reduced due to the addition of guard bands or cyclic prefixes to mitigate ISI.
- **Required bit rate:** The system should be able to provide high speed and data rates to support today's multimedia applications and the huge number of users and their applications.
- **Tolerable delay spread:** Selection of CP length is also a critical issue since the delay spread experienced indoor and outdoor is not equal. So the CP length should be selected carefully according to the maximum possible delay spread.

- **Doppler values:** Doppler shift is another critical issue in wireless communication since the user on running vehicle experiences very high Doppler shift compared to the pedestrian.

Following are the critical design parameters that need to understand in an OFDM system,

- **The number of subcarriers:** In presence of a large number of subcarriers in OFDM, the synchronization at the receiver end becomes highly complicated.
- **The symbol duration and Guard signal period (CP interval):** To fight against multipath fading effects, the symbol duration needs to be increased by inserting CP of proper length such that no significant amount of energy will be lost. Ideally, the length of CP should be 2 to 4 times the RMS value of maximum delay spread.
- **Subcarrier spacing:** It is a very significant parameter to mitigate ISI; spacing should be suitable for easy synchronization. Subcarrier spacing is mainly depending upon the channel bandwidth and number of sub-channels [4].

3.2 DIVERSITY CONCEPTS

In wireless communication, the diversity technique is utilized for finding a highly un-correlated or independent channel for faithful communication. In wireless communication, several delayed replicas of the transmitted signal may be received due to scattering, reflection, and refraction of the originally transmitted signal from the various objects present in the wireless environment. The basic idea is at least one or a few of the received replicas having good SNR values to be considered. Thus the instantaneous or average SNR can be improved significantly. In a small-scale fading environment, if two antennas are separated from each other by a fraction of a meter, one of them may receive a stronger signal compared to the other antenna. So choosing the antenna with a strong and best quality signal at the receiver the effect of small-scale fading can be mitigated. This technique is called antenna diversity.

The large-scale fading due to shadowing caused by variation in the surrounding also degrades the system performance severely. Assuming 'M' independent diversity branches carrying the same information signals. The signal and additive noise at each branch is identically and independently Rayleigh distributed. Figure 3.7 shows 'M' diversity branches carrying the same information, where b is the transmitted bit; $S_1 = \alpha_1 E_b^{1/2} b + n_1$; $S_2 = \alpha_2 E_b^{1/2} b + n_2$ ----------; $S_M = \alpha_M E_b^{1/2} b + n_M$, E_b is the bit energy; α_i is the fading complex envelop on i^{th} branch and n_i is AWGN noise on i^{th} branch. Let Instantaneous SNR on i^{th} branch $\gamma_i = {E_b}/{\sigma^2} \cdot \alpha_i^2$, where ${E_b}/{\sigma^2}$ is the SNR without fading. Therefore the average SNR on each branch, where α is Rayleigh distributed and α^2 is exponentially distributed,

$$\Psi = {E_b}/{\sigma^2} \cdot E\{\alpha_i^2\} \quad \text{... (3.14)}$$

Therefore γ_i is exponentially distributed with PDF

$$P(\gamma_i) = \frac{1}{\psi} e^{-\gamma_i/\psi} \quad , \quad \gamma_i \geq 0 \quad \text{... (3.15)}$$

The probability that a single branch has SNR less than some threshold value γ_T is,

$$P(\gamma_i \leq \gamma_T) = 1 - e^{-\gamma_T/\Psi} \quad \text{... (3.16)}$$

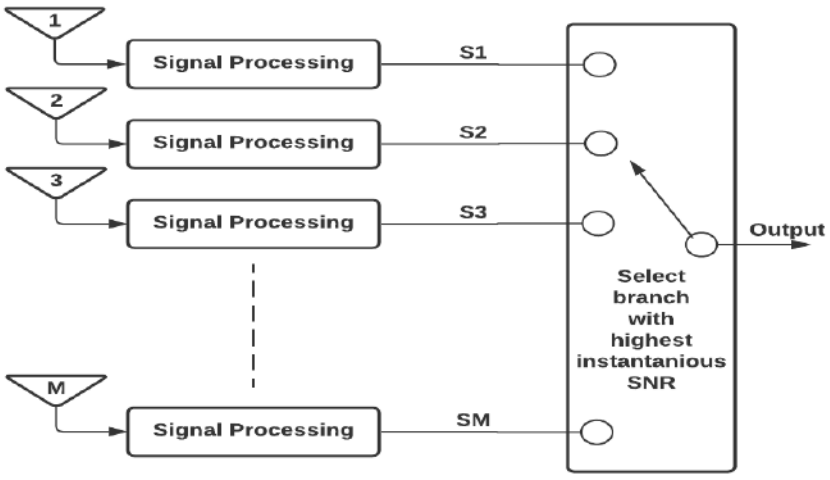

Fig. 3.7 'M' diversity Branches

For selecting the diversity branch with maximum instantaneous SNR, the probability that the diversity branches from M branches receiving SNR less than the threshold SNR value is

$$P_M(\gamma_T) = P[\gamma_{sel} \leq \gamma_T] \quad \text{... (3.17)}$$

$$= P[{}^{max}_{i}\{\gamma_i\} \leq \gamma_T] \quad \text{... (3.18)}$$

$$= P(\gamma_i \leq \gamma_T).P(\gamma_2 \leq \gamma_T) \dots \dots P(\gamma_M \leq \gamma_T) \quad \text{... (3.19)}$$

Therefore,

$$P_M(\gamma_T) = \left[1 - e^{-\gamma_T/\Psi}\right]^M \quad \text{... (3.20)}$$

Similarly, the probability that one or more branches having SNR greater than the threshold SNR value is

$$P_M(\gamma_T) = P[\gamma_{sel} \geq \gamma_T] = P[{}^{max}_{i}\{\gamma_i\} \geq \gamma_T] \quad \text{... (3.21)}$$

$$= [1 - P_M(\gamma_T)] \quad \text{... (3.22)}$$

$$= 1 - \left(1 - e^{-\gamma_T/\Psi}\right)^M \quad \text{... (3.23)}$$

Now average SNR of the selected branch is given by

$$\hat{\gamma}_{sel} = E[{}^{max}_{i}\{\gamma_i\}] \quad \text{... (3.24)}$$

$$= \int_0^\infty [1 - P_M(\gamma_T)]d\gamma \quad \text{... (3.25)}$$

$$= \int_0^\infty \left[1 - \left(1 - e^{-\gamma_T/\Psi}\right)^M\right] d\gamma \quad \text{... (3.26)}$$

$$= \int_0^\infty \left\{1 - \left[\sum_{i=0}^{M}(-1)^i \binom{M}{i} e^{-i\gamma/\Psi}\right]\right\} d\gamma \quad \text{... (3.27)}$$

$$= \sum_{i=1}^{M}(-1)^{i-1} \binom{M}{i} \int_0^\infty e^{-i^{\gamma}/\Psi}\ d\gamma \quad \text{... (3.28)}$$

$$= \Psi \sum_{i=1}^{M}(-1)^{i-1} \left[\frac{M!}{i!(M-i)!}\right] \frac{1}{i} \quad \text{... (3.29)}$$

$$\hat{\gamma}_{sel} = \Psi \sum_{i=1}^{M} \frac{1}{i} \quad \text{... (3.30)}$$

Thus the average SNR improvement offered by the diversity selection technique is,

$$\frac{\hat{\gamma}_{sel}}{\Psi} = \sum_{i=1}^{M} \frac{1}{i} \quad \text{... (3.31)}$$

From the above expression of average improvement in SNR due to diversity selection we conclude that the average SNR always increases with an increasing number of diversity branches but at the cost of a decrease in diversity gain. No additional power is needed, easy to implement provided the signals are to be monitored faster than the fading. However, this is not an optimal diversity scheme since all the M branches are not exploited simultaneously.

Diversity is the most effective and efficient technique which can accomplish reliable communication and fulfills the need of today's warless communication applications. Types of diversity schemes are

- Frequency diversity
- Time diversity
- Modulation diversity and
- Antenna diversity

Frequency Diversity: transmission of information signal at different carrier frequencies offers frequency diversity. For example, the OFDM system where symbols are transmitted over several subcarriers at different frequencies. The idea behind transmitting information at different frequency bands is that the fading doesn't affect all the channels equally and good average SNR may be received through at least one or more channels. The frequency diversity technique is mainly used to avoid frequency selective fading effects which are very harmful to the quality of communications [83].

Time Diversity: The main intention of using time diversity is to enhance the robustness of the system against all kinds of impairments. The time diversity can be achieved by sending the same information in 'M' different time slots such that the separation between two consecutive time slots is greater than or equal to the coherence time of the channel. The time diversity can be achieved by sending similar information on M independent branches in M time slots. The duration of each independent time slot is greater than or equal to the coherence time of the

channel. The time diversity in the next generation communication systems is implemented through the interleaving of transmitted symbols and different channel codes [84].

Few examples of channel coding:

- Convolution and block coding
- Trellis coding
- Multilevel coding
- Bit interleaved coding
- Turbo coding, parity check coding, and coded modulation techniques.

Modulation Diversity: To achieve reliable communication with minimum error rates and maximum data rate different modulation techniques can be used, for example; M order PSK and QAM, spatial modulation, index modulation, and so on. This is known as modulation diversity. High data rates and better spectral efficiency can be achieved using modulation diversity [81], [85].

Antenna Diversity: Antenna diversity or spatial diversity can be achieved by employing more than one antenna at the transmitter and receiver section of the OFDM system. It is the most popular, robust, and convenient method to fight against various deleterious effects of fading. Multiple transmitting antennas transmit the same information at a single frequency and multiple receive antennas receive several delayed copies of the originally transmitted signal independently through non-correlated fading paths. MIMO system is the best example of antenna or spatial diversity. The main purpose of spatial diversity is to improve data rates and error rates in a fading environment. In this case, multiple antennas are located $\lambda/2$, (λ = wavelength) apart from each other to minimize inter antenna interference (IAI).

Different diversity schemes and be merged to obtain enhanced performance of the system, for example, 1) 'Space-time coding (STC)', it is the combination of channel coding with spatial diversity. This technique offers a better solution for realizing reliable and impaired immune systems. 2) STBC and STTC coding schemes are

used to achieve the best spatial diversity. Among these two codlings, STBC achieves the best reliability, whereas STTC achieves the best data rates.

3.3 MULTI-INPUT MULTI-OUTPUT (MIMO) SYSTEMS

MIMO systems are the key technology that enhances the channel capacity or information rate and maintains the reliability of the wireless communication system. It consists of multiple antennas at receiver and transmitter as shown in fig.3.8.

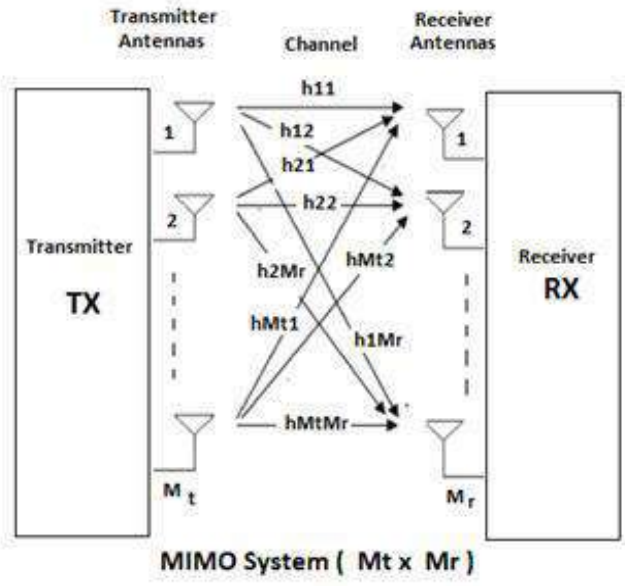

Fig. 3.8 Multi-input multi-output antennas system

The primary objective of multiple antennas in the MIMO scheme is to enhance data rates and improve BER. Also in cellular networks, they are used to support beamforming to enhance overall network capacity to accommodate a large number of users and their applications [15]. The MIMO system offers spatial diversity, which leads to an increase in the data rates and reliability of the system. In MIMO systems multiple antennas can be employed in many different ways at both transmit and receive ends. Multiple antennas at the transmitter provide transmit diversity which leads to providing the best reliability but not the improved data rate. Data rates are still comparable to the SISO system.

Alternatively, if the independent un-correlated signals are transmitted via different transmit antennas can achieve a higher channel capacity at the cost of poor reliability. Spatial diversity is the space diversity rather than time or frequency diversity since it uses an RF channel for simultaneous multiplexing of several parallel streams of information at a single frequency with no extra transmitting power. In MIMO system the space between two adjacent antennas is maintained at-least $\lambda/2$, where λ is the wavelength and it is given by $\lambda = c/f_c$. The main objective of maintaining space between antennas is to have un-correlated fading channels, to diminish cross-correlation and 'inter-antenna interference (IAI)'. In the MIMO system combinations of coding schemes like STBC and STTC can be used to achieve spatial diversity that improves the system data rate and reliability performance. Among these STC schemes, one provides the best reliability whereas the other provides the best data rates.

Assuming that $x_1, x_2, x_3, \ldots\ldots, x_t$ are the symbols transmitted via 1, 2, 3… t transmit antennas and $y_1, y_2, y_3, \ldots\ldots, y_r$ are the received symbols through 1, 2, 3… r receive antennas. Now if $\vec{x}$ and $\vec{y}$ are the 't' and 'r' dimensional transmit and receive vectors, then the MIMO channel matrix is,

$$\begin{bmatrix} y_1 \\ y_2 \\ y_3 \\ . \\ . \\ y_{r-1} \\ y_r \end{bmatrix} = \begin{bmatrix} h_{11} & h_{12} & \ldots\ldots\ldots & h_{1t} \\ h_{21} & h_{22} & \ldots\ldots & h_{2t} \\ & & \vdots & \\ h_{r1} & h_{r2} & \ldots\ldots\ldots & h_{rt} \end{bmatrix} * \begin{bmatrix} x_1 \\ x_2 \\ x_3 \\ . \\ . \\ x_{t-1} \\ x_t \end{bmatrix} + \begin{bmatrix} n_1 \\ n_2 \\ n_3 \\ . \\ . \\ n_{r-1} \\ n_r \end{bmatrix} \quad \ldots (3.32)$$

If H is the $r \times t$ dimensional channel matrix, the above equation in vector form can be written as

$$\vec{y} = H\vec{x} + \vec{n} \quad \ldots (3.33)$$

The MIMO system supports several communication standards such as IEEE 802.11, 802.16, and 3GPP. IEEE 802.11used in Wi-Fi (Wireless Fidelity), and the IEEE 802.16 standard is used in Wi-MAX. The latest version of IEEE 802.11 such as IEEE 802.11n supports data rates of 100 Mbps [8].

Diversity gain: In the MIMO system, the signal can be transmitted or received with diversity. Receiver diversity is used to reduce fading effects and transmit diversity is used to enhance capacity compared to the SISO system. Transmit diversity in a MIMO system with space-time coding like STBC and STTC is used for transmitting independent, un-correlated information signals. It is an efficient method of improving communication reliability and information rates [79].

3.4 MIMO-OFDM SYSTEM

Figure 3.9 show basic MIMO-OFDM system architecture with M_T transmitting and M_R receiving antenna system. The MIMO-OFDM is a multi-diversity technology providing time, frequency, antenna, and space or spatial diversity which promotes to improve system performance over a wireless network in a multipath fading environment.

As discussed earlier the OFDM system is a competent technology used in future or next frontier wireless systems. The efficient FFT and IFFT algorithm in the OFDM system makes it a very efficient and effective system providing high spectral efficiency, and also provide immune system against different types of channel impairments like ISI, ICI, and error rates. Similarly, the MIMO antenna system provides spatial diversity (transmit and receive diversity) that supports different communication standards to provide the best data rate or channel capacity suitable to numerous cellular/wireless applications which require high speed, high capacity, and reliable wireless system. Another aim of the next frontier system is to optimize the system complexity due to the integration of different technologies and algorithms. To face various challenges of the next-generation system, the alliance of MIMO and OFDM technologies is playing an important role.

Concatenation of MIMO system with OFDM schemes offers a significant improvement over, the requirement of bandwidth, power constrain, spectral efficiency, quality of services, reliability, and throughput to fulfill the needs of today and next frontier wireless communication system. In addition, the MIMO-OFDM system can attenuate frequency selective fading effects and avoid the application of

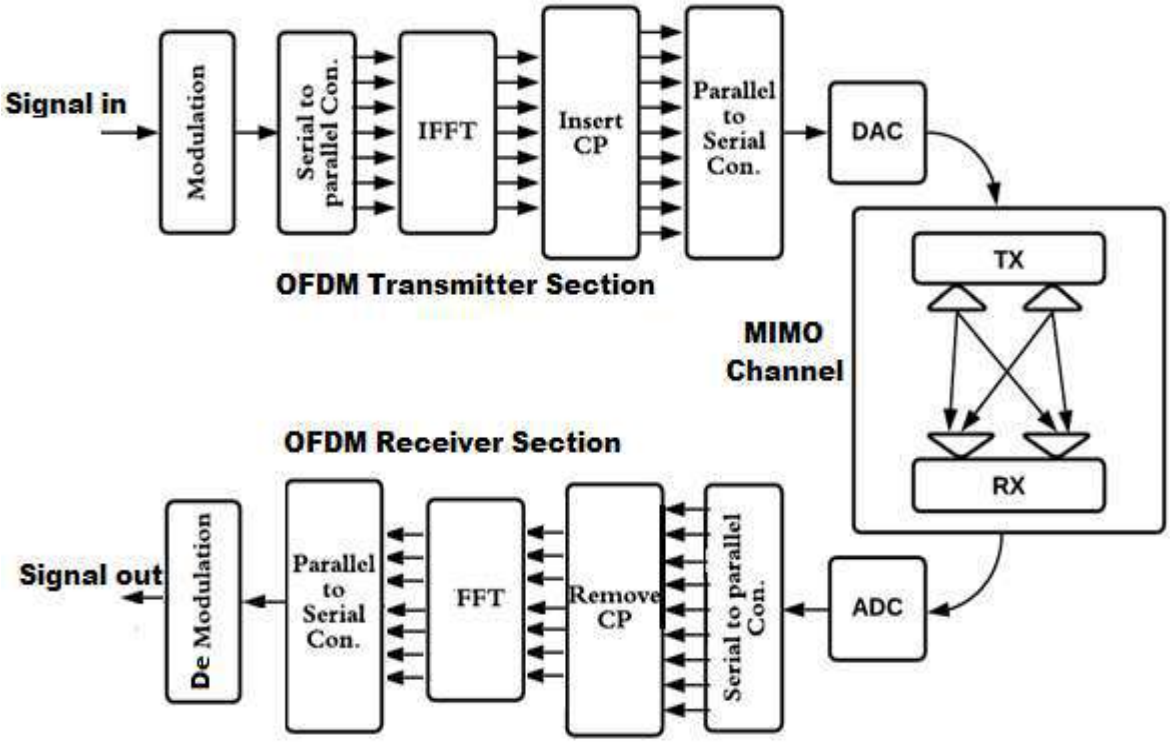

Fig. 3.9 A MIMO-OFDM system with $M_T \times M_R$ antenna configuration

Complex equalizers. The MIMO OFDM has been adopted in several standards such as Wi-Fi, 'long term evolution (LTE)', and LTE Advance or 3GPP, Wi-MAX / IEEE 802.16m, WLAN / IEEE802.11n, etc., [11], [14], [16].

Chapter 4
Methodology

4.1 PROBLEM IDENTIFICATION.

Considering limitations in wireless network scenario such as bandwidth availability, power constraints, and various challenges faced by a wireless communication network such as hardware and computational complexity, multipath fading environment, carrier frequency offset, etc., it is a very difficult and challenging task to develop such a robust, high speed, a reliable and spectrally efficient wireless system that can fulfill the demands of today's massive number of users and abundant applications like video streaming, electronic mails, internet browsing, bulk data transfer, real-time applications, and many more. Foreseeing the above limitations and challenges many researchers have been attracted towards designing such a reliable wireless communication system, less complex, and low-cost system which doesn't require any extra bandwidth and transmission power to meet today's requirements. In recent scenarios, MIMO-OFDM technology has materialized as a competent technology to fulfill the needs of a next-frontier wireless communication system. However many issues and problems have been identified in the MIMO-OFDM system as listed as follows.

1. An increase in error rates or packet loss due to multipath fading environment.
2. In OFDM systems, there may be an increase in Inter Symbol Interference (ISI) as a result of closely spaced sub-carriers and due to overlapping of delayed replicas arrival at the receiver.
3. High PAPR is the major issue in the OFDM system, which may break the orthogonality of the OFDM system and results in inter-carrier interference (ICI).
4. The overall capacity or data rates of the MIMO-OFDM system can be improved using spatial multiplexing characteristics of the MIMO system without any additional requirement of power and bandwidth and by increasing the transmission power. Choosing the number of transmitting and receiving antennas

to implement spatial diversity is also critical because an increasing number of transmit antennas can significantly increase the data rates but at the cost of high power consumption and increase in complexity of hardware and its cost. In addition, maintaining minimum space between two antennas is a critical issue in handheld devices.

5. An attempt to achieve a very high data rate significantly results in channel distortion. In this scenario, it is very difficult to recover the original information using the simple receiver, which can be mitigated by massive MIMO technology, complex equalization techniques, and perfect channel estimations.

From the literature survey it has been observed that using various modulation schemes, channel coding schemes, and antenna selection and combining schemes the bit error rate over the AWGN channel has been in the range of 10^{-5} to 10^{-6}. On the other hand, the BER values over the Rayleigh fading channel is recorded as in the range of 10^{-2} to 10^{-3}. Here there is a scope to lessen the BER bellow 10^{-6} over AWGN channel and bellow 10^{-3} over Rayleigh fading channel. To get rid of the most deleterious effects of PAPR in the OFDM system different algorithms have been used by many researchers and they have reduced the PAPR to significant value. However, there is further scope for reducing the PAPR without adding complexity and cost of the system and most important without increasing BER significantly, since the attempt to reduce PAPR may increase bit error rates in the OFDM system. So the challenge is to select proper technology which less complex, simple, low cost, and that does not increase BER beyond a certain limit. As far as the capacity of data transfer is concerned it can be enhanced by implementing more antennas at the transmitter and receiver ends of the MIMO system, but this is not a proper solution, since the increase in the number of antennas will definitely increase the power consumption and the cost of the system, which is not good for devices like a cellular phone. So there is a scope to choose such an algorithm and combination of antennas in the MIMO system which not only increases the capacity but also improves the error rate lessening performance of the system.

4.2 METHODOLOGY

Considering the above-listed problem statements, the proposed methodology can be categorized as:

1. **Analysis of error rates in MIMO-OFDM system:** Understanding formulation for error rates (BER / SER) and their minimization using different constellation methods, spatial multiplexing, and different space-time coding techniques.
2. **Analysis of PAPR in OFDM system:** Formulation and investigation of PAPR using different algorithms and schemes used for PAPR reduction. Comparative analysis of proposed PAPR reduction scheme with other techniques. ISI reduction by adding cyclic prefix and ICI elimination by maintaining orthogonality.
3. **Channel capacity analysis in MIMO-OFDM system:** Understanding **f**ormulation of capacity or data rates for MIMO system and analyzing channel capacity using a different set of transmitting and receiving antennas as well as by implementing MIMO channel codlings such as STBC, STTC, Alamouti STBC coding, and MRC scheme.

4.2.1 Performance evaluation of BER

Bit error rates (BER) are defined as the ratio of the number of bits received with error N_e to the total number of bits N transmitted through wireless channel.

$$BER = {}^{N_e}/_{N} \quad \text{... (4.1)}$$

If ‘a’ is the transmitted bit and ‘a^’ is the received bit then the probability of BER incurred is the probability that the received bit ‘a^’ not equal to transmitted bit ‘a’. BER is always analyzed against SNR and it is observed that BER decreases with increasing SNR. Considering continuous-time AWGN channel, if p be the transmitted signal power, ${}^{N_0}/_{2}$ be the ‘power spectral density (PSD)’ of noise and bandwidth equals ‘2W’ then the continuous-time SNR

$$SNR = \frac{p}{psd\ .BW} = \frac{p}{N_0 W} \quad \text{... (4.2)}$$

For the discrete time SNR, if the symbol period $T = {}^{1}/_{2W}$, symbol energy $E_s = p.T = {}^{p}/_{2W}$ and the noise energy equals noise variance $\sigma^2 = {}^{N_0}/_{2}$ then,

The discrete-time SNR is given by

$$SNR = \frac{E_s}{\sigma^2} = \frac{p}{N_0 W} \quad \text{... (4.3)}$$

4.2.1.1 BER in wired communication for BPSK modulation over AWGN channel

Symbol energy in BPSK modulation $E_s = \frac{(1)^2+(-1)^2}{2} = 1$ and Noise power or variance $=\sigma^2$. Therefore SNR for BPSK $= {}^{1}/_{\sigma^2}$. Now the BER for wired line for BPSK modulation on AWGN channel is given by

$$BER = Q\left({}^{1}/_{\sigma}\right) = Q\sqrt{SNR} \quad \text{... (4.4)}$$

$$\text{Where Q function} = (x) = 0.5\, erfc\left({}^{x}/_{\sqrt{2}}\right). \quad \text{... (4.5)}$$

The above BER equation can be approximated as,

$$BER \cong \frac{1}{2}\, e^{-\frac{1}{2}SNR} \quad \text{... (4.6)}$$

4.2.1.2 BER in wireless communication for BPSK modulation over Rayleigh fading channel

Consider a wireless channel model in a multipath fading environment as shown in fig 4.1

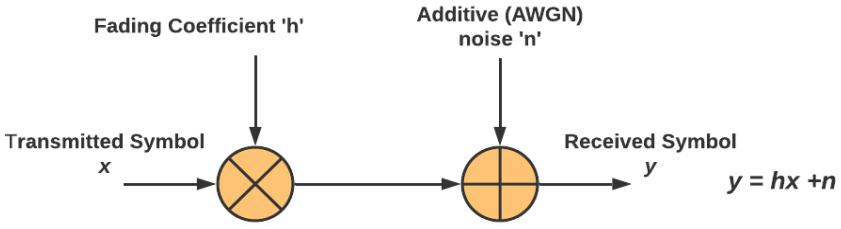

Fig. 4.1 Wireless channel model with multipath fading

The channel model of wireless system in multipath fading environment is given by,

$$y = hx = n \quad \text{... (4.7)}$$

Where ‘y’ is received symbol, ‘x’ is transmitted symbol, ‘h’ is fading coefficient, and ‘n’ is the additive white Gaussian noise (AWGN)

If ‘p’ is transmitted power then the received power in Rayleigh fading channel is $|h|^2.p$, and $h = ae^{j\emptyset}$, where ‘a’ is Rayleigh distributed magnitude of fading

coefficient *h*. There fore received power = $\frac{a^2 p}{\sigma^2}$ and we know that SNR = p/σ^2, therefore Fading SNR is

$$SNR_F = a^2 SNR \quad \text{... (4.8)}$$

Now for BPSK modulation over the Rayleigh fading channel, the BER is given by

$$BER = Q\sqrt{SNR_F} = Q\sqrt{a^2 SNR} \quad \text{... (4.9)}$$

Since 'h' is random the magnitude a is also random and Rayleigh distributed. Therefore to determine the average BER above equation has to be averaged concerning the distribution of 'a' that is Rayleigh distribution.

$$F_A(a) = 2a.e^{-a^2} \quad \text{... (4.10)}$$

Therefore,

$$average\ BER = \int_0^\infty Q\left(\sqrt{a^2 SNR}\right).F_A(a)da \quad \text{... (4.11)}$$

$$average\ BER = \int_0^\infty Q\left(\sqrt{a^2 SNR}\right).2a.e^{-a^2}da \quad \text{... (4.12)}$$

Putting $SNR = \mu$ we have

$$Avg.BER = \int_0^\infty Q\left(\sqrt{a^2\mu}\right).2a.e^{-a^2}da \quad \text{... (4.13)}$$

Now we know that the Q function is given by

$$Q(v) = \int_v^\infty \frac{1}{\sqrt{2\pi}} e^{\frac{-t^2}{2}}\, dt \quad \text{... (4.14)}$$

Substituting the Q function in equation (4.14) we have

$$Avg.BER = \int_0^\infty \int_{\sqrt{a^2\mu}}^\infty \frac{1}{\sqrt{2\pi}} e^{\frac{-t^2}{2}}\, dt\, .2a.e^{-a^2}da \quad \text{... (4.15)}$$

Solving inner and outer integral with respect to 't' and 'a' respectively in equation (4.15), we get a final exact expression of average BER in a wireless communication system for BPSK modulation over a Rayleigh fading channel,

$$Avg.BER = \frac{1}{2}\left[1 - \sqrt{\frac{SNR}{2+SNR}}\right] \quad \text{... (4.16)}$$

At very high SNR, the equation (4.16) can be approximated as,

$$BER \cong \frac{1}{2SNR} \quad \text{... (4.17)}$$

From equation (4.17) it is clear that the average BER in a wireless system decreases with increasing the SNR. The analytical result of BER Vs SNR is shown in fig. 4.2

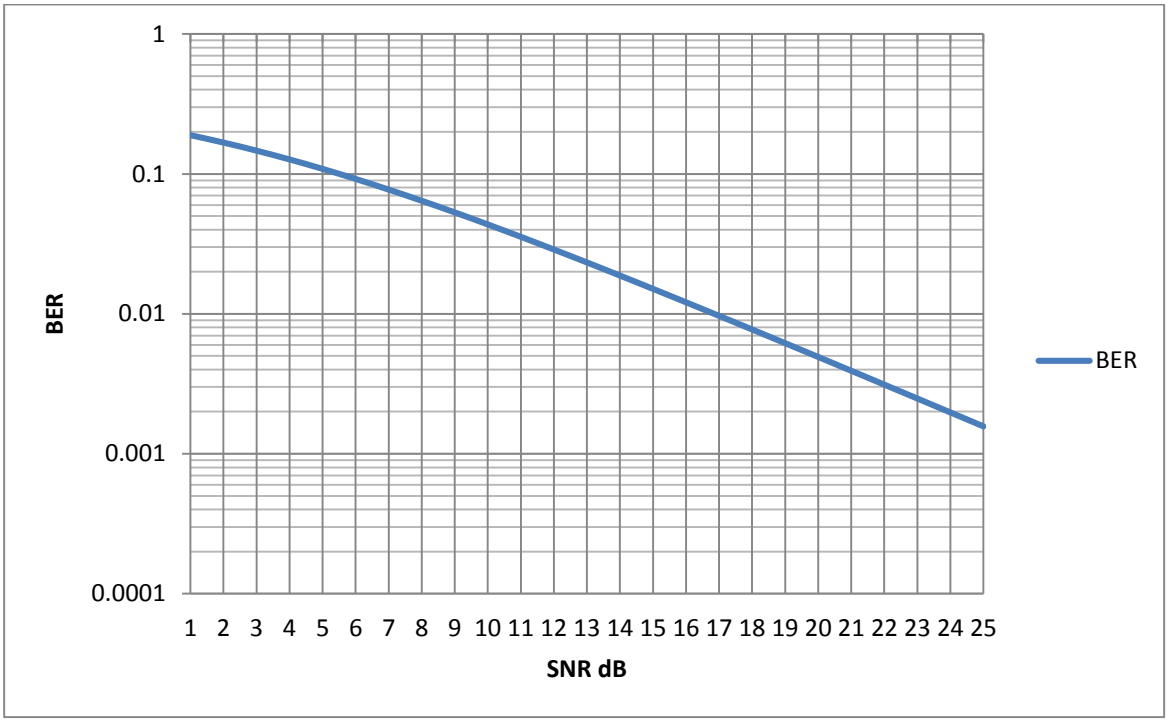

Fig. 4.2 Analytical result of BER Vs SNR

4.2.1.3 Error probability in BPSK modulation over AWGN channel

Figure 4.3 shows a constellation plot for BPSK modulation.

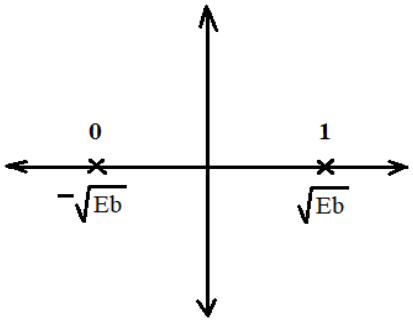

Fig. 4.3 BPSK constellation plot

Assuming symbols '1' and '0' are equally likely and uniform, the probability of occurrence of symbols is 50% or ½. Let 'x' be the transmitted symbol and 'y' be the received symbol. At any instant say x=0 is transmitted, then the function of the received symbol

$$f(y=0) = \frac{1}{\sqrt{\pi N_0}} exp\left[\frac{-1}{N_0}\left(y - \left(-\sqrt{E_b}\right)\right)^2\right] \quad \text{... (4.18)}$$

$$= \frac{1}{\sqrt{\pi N_0}} exp\left[\frac{-1}{N_0}\left(y + \sqrt{E_b}\right)^2\right] \quad \text{... (4.19)}$$

Now the probability that the symbol received as '1' when '0' was transmitted is nothing but error probability for symbol '0' and is given by

$$P_e(0) = \frac{1}{\sqrt{\pi N_0}} \int_0^{\infty} \frac{1}{\sqrt{\pi N_0}} exp\left[\frac{-1}{N_0}\left(y + \sqrt{E_b}\right)^2\right] dy \quad \text{... (4.20)}$$

Putting $z = \frac{1}{\sqrt{N_0}}\left(y + \sqrt{E_b}\right)$, equation (4.20) becomes

$$P_e(0) = \frac{1}{\sqrt{\pi}} \int_{\sqrt{\frac{E_b}{N_0}}}^{\infty} exp[-z]^2 \, dz \quad \text{... (4.21)}$$

The equation (4.21) can be modified as

$$P_e(0) = \frac{1}{2}\frac{2}{\sqrt{\pi}} \int_{\sqrt{\frac{E_b}{N_0}}}^{\infty} exp[-z]^2 \, dz \quad \text{... (4.22)}$$

$$P_e(0) = \frac{1}{2} \, erfc\left(\sqrt{\frac{E_b}{N_0}}\right) \quad \text{... (4.23)}$$

Since $erfc(x) = 2Q\left(\sqrt{2}\, x\right)$

$$P_e(0) = Q\left(\sqrt{\frac{2E_b}{N_0}}\right) \quad \text{... (4.24)}$$

Similarly, the probability for symbol '1' transmitted and '0' received can be written as

$$P_e(1) = \frac{1}{2} \, erfc\left(\sqrt{\frac{E_b}{N_0}}\right) \quad \text{... (4.25)}$$

Since '0' and '1' symbols are equally likely with 50% probability, the average probability of symbol error is

$$P_e = \frac{1}{2}[P_e(0) + P_e(1)] \quad \text{... (4.26)}$$

$$P_e = \frac{1}{2} \, erfc\left(\sqrt{\frac{E_b}{N_0}}\right) \quad \text{... (4.27)}$$

Equation (4.27) represents the symbol error performance of BPSK modulation/demodulation over the AWGN channel. Since there are only two symbols, the probability of SER is equal to the probability of BER in BPSK modulation.

4.2.1.4 Error probability in QPSK (4-QAM) modulation over AWGN channel

Figure 4.4 shows a constellation plot for QPSK modulation. There are 4 decision zones (I to IV). All four signal points are positioned at equidistance from the origin.

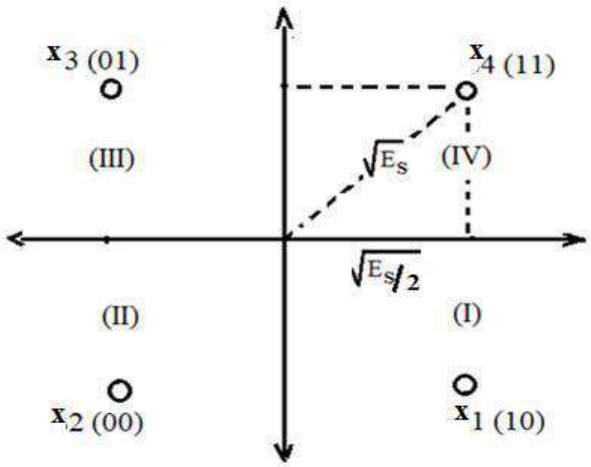

Fig. 4.4 QPSK constellation plot

The QPSK modulated signal in the time domain is

$$X_i(t) = \sqrt{\frac{2E_s}{T}}\, cos\left[(2i-1)\frac{\pi}{4}\right] \cos W_c t - \sqrt{\frac{2E_s}{T}}\, sin\left[(2i-1)\frac{\pi}{4}\right] \sin W_c t \quad ...(4.28)$$

Where $1 \leq i \leq 4$ and the received signal $y(t) = X_i(t) + W(t)$ for, $0 \leq t \leq T$. Where W(t) is additive noise and 'T' is the symbol period. Now the received vector y has two components, that is in-phase (I) and quadrature (q) component and given by

$$y_I = \sqrt{E_s}\, cos\left[(2i-1)\frac{\pi}{4}\right] + W_I \text{ , and} \quad ... (4.29)$$

$$y_q = \sqrt{E_s}\, sin\left[(2i-1)\frac{\pi}{4}\right] + W_q \quad ... (4.30)$$

$y_{I>0}$, implies that the received vector y is either in zone I or zone IV and $y_{q>0}$, implies that the received vector y is either in zone III or zone IV. Here W_I and W_q are the noise components with zero mean and $\frac{N_0}{2}$ variance are Gaussian random variables. And thus y_I and y_q are also random variable with $\frac{N_0}{2}$ variance and the mean of $\sqrt{E_s}\, cos\left[(2i-1)\frac{\pi}{4}\right]$ and $-\sqrt{E_s}\, sin\left[(2i-1)\frac{\pi}{4}\right]$. Now assume that $x_4(t)$ is transmitted and received. The probability that $x_4(t)$ received is $P_{x4(t)} =$ combined probability of $y_{I>0}$ and $y_{q>0}$, therefore means for y_I and y_q is

$$y_I = \sqrt{E_s}\, cos\left[(7)\frac{\pi}{4}\right] = \sqrt{\frac{E_s}{2}} \text{ , and} \quad \text{... (4.31)}$$

$$y_q = \sqrt{E_s}\, sin\left[(7)\frac{\pi}{4}\right] = \sqrt{\frac{E_s}{2}} \quad \text{... (4.32)}$$

Therefore,

$$P_{x4(t)} = \int_0^{\infty} \frac{1}{\sqrt{\pi N_0}} e^{\frac{-\left(Y_I - \sqrt{\frac{E_s}{2}}\right)^2}{N_0}}\, dy_I \,.\, \int_0^{\infty} \frac{1}{\sqrt{\pi N_0}} e^{\frac{-\left(Yq - \sqrt{\frac{E_s}{2}}\right)^2}{N_0}}\, dy_q \quad \text{... (4.33)}$$

Putting $\frac{Y_j - \sqrt{\frac{E_s}{2}}}{\sqrt{N_0}} = z$, we have,

$$P_{x4(t)} = \left[\frac{1}{\sqrt{\pi}} \int_{-\sqrt{\frac{E_s}{2N_0}}}^{\infty} e^{-z^2}\, dz\right]^2 \quad \text{... (4.34)}$$

Since, $\frac{1}{\sqrt{\pi}} \int_{-a}^{\infty} e^{-z^2}\, dz = 1 - \frac{1}{2} erfc(a)$, we have,

$$P_{x4(t)} = \left[1 - \frac{1}{2} erfc\left(\sqrt{\frac{E_s}{2N_0}}\right)\right]^2 \quad \text{... (4.35)}$$

$$P_{x4(t)} = 1 - erfc\left(\sqrt{\frac{E_s}{2N_0}}\right) + \frac{1}{4} erfc^2\left(\sqrt{\frac{E_s}{2N_0}}\right) \quad \text{... (4.36)}$$

Therefore from the equation (4.36) the probability of erroneous decision for $x_4(t)$ is

$$Pe_{x4(t)} = 1 - P_{x4(t)} \quad \text{... (4.37)}$$

$$Pe_{x4(t)} = erfc\left(\sqrt{\frac{E_s}{2N_0}}\right) - \frac{1}{4} erfc^2\left(\sqrt{\frac{E_s}{2N_0}}\right) \quad \text{... (4.38)}$$

Since all the 4 symbols are equidistance from the origin and equally likely, the probability of erroneous decision for $x_1(t)$ to $x_4(t)$ is equal. Thus the average probability of symbol error is

$$Pe = \frac{1}{4}\left[Pe_{x1(t)} + Pe_{x2(t)} + Pe_{x3(t)} + Pe_{x4(t)}\right] \quad \text{... (4.39)}$$

$$Pe = erfc\left(\sqrt{\frac{E_s}{2N_0}}\right) - \frac{1}{4} erfc^2\left(\sqrt{\frac{E_s}{2N_0}}\right) \quad \text{... (4.40)}$$

For large $\left(\frac{E_b}{N_0}\right)$, the second term can be neglected, hence

$$Pe = erfc\left(\sqrt{\frac{E_s}{2N_0}}\right) \quad \text{... (4.41)}$$

In QPSK modulation there are two bits per symbol, so the energy per symbol E_s is twice the energy per bit ($E_s = 2E_b$), therefore

$$Pe = erfc\left(\sqrt{\frac{E_b}{N_0}}\right) \quad \text{... (4.42)}$$

Approximation of BER equation for QPSK modulation:

In QPSK one decision error about the QPSK symbol may cause an error in one bit or both bits of a QPSK symbol. If (11) is detected as (10), that means 1-bit error and if it is detected as (00), that means 2-bit error. The total number of information bits transmitted is twice the number of transmitted symbols, therefore average BER is given by

$$Average\ BER = \frac{1}{2}Pe \cong \frac{1}{2}\ erfc\left(\sqrt{\frac{E_b}{N_0}}\right) \quad \text{... (4.43)}$$

The BER equation (4.43) is almost similar to the average BER of BPSK modulation. Thus error performance of QPSK is as good as BPSK and it requires half bandwidth for transmission compared to BPSK.

4.2.1.5 Error performance of M-QAM modulation over AWGN channel [86]

For (M=4) 4 QAM or 4 phase QAM constellation, fig. 4.5 shows 4 points single amplitude and two amplitude QAM constellation with radii A and $\sqrt{3}$ A. The minimum distance between two adjacent constellation points is 2A. In both case the minimum average transmission power is

$$P_{avg} = 2A^2 \quad \text{... (4.44)}$$

Thus in both cases, the error performance remains the same. Now let us consider 8-QAM (M=8) constellation with the minimum distance between two adjacent constellation points equals to 2A. Figure 4.6 shows different types of 8 point circular and rectangular 8 QAM constellations. In fig 4.6 (a) and (c) signal points are falling on a rectangular grid hence the minimum average transmission power in this case is $P_{avg} = 6A^2$. For the signal set shown in 4.6 (b) and (d) the minimum average transmission power (P_{avg}) is $6.83\ A^2$ and $4.73\ A^2$ respectively.

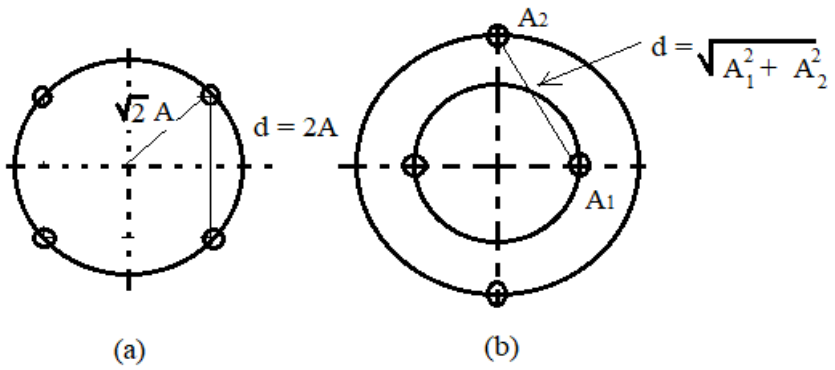

Fig. 4.5 Four phases (4-QAM) signal constellations (a) single (b) Two amplitude 4-point QAM constellation

From the above values of average transmission power, it is clear that to achieve the same error performance the 8 point constellation signal set shown in fig 4.6 (d) is the best since it requires minimum average transmission power for a given minimum distance between adjacent signal points.

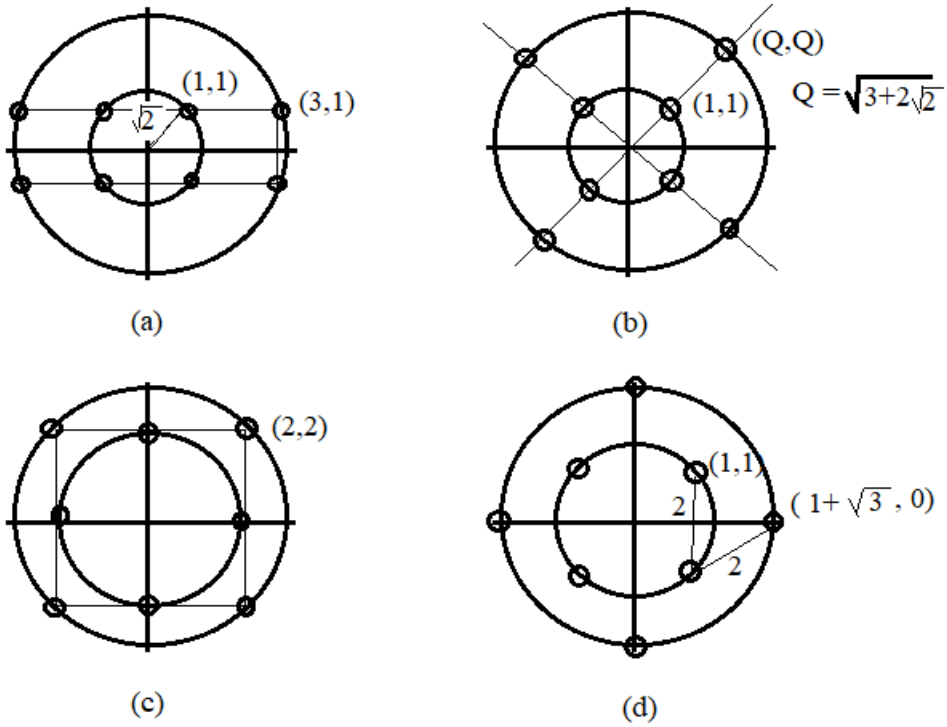

Fig. 4.6 Eight point 8 QAM constellation (a) and (c) Rectangular 8 QAM constellation. (b) and (d) circular 8 QAM constellation.

Let's examine error performance for the 16 QAM constellations. The 8 QAM constellations can be generalized for 16 QAM constellations, but the circular 16

QAM signal constellation performance is not satisfactory compared to the rectangular 16 QAM signal constellation. Hence we consider the rectangular 16 QAM constellation for investigating the error performance in 16 QAM modulations. For M ≥ 16, rectangular M array constellation to achieve the best error performance for the minimum distance between constellation pinpoints the required average transmission power is a little bit more than the best M array QAM constellation. Thus rectangular M array constellations are frequently used. The rectangular M-QAM constellation where $M = 2^k$ (k is even) is alike the two signals on quadrature carriers. Each Pam signal having $\sqrt{M} = 2^{\frac{k}{2}}$ signal points and the probability of error in QAM can be evaluated using the error probability in PAM. The probability of errors detected at the receiver for QAM constellation is,

$$P = \left(1 - P\sqrt{M}\right)^2 \quad \text{... (4.45)}$$

Where, $P\sqrt{M}$ is the probability of error in $\sqrt{M}$ array PAM modulation and it is given by

$$P\sqrt{M} = 2\left(1 - \frac{1}{\sqrt{M}}\right).Q\left(\sqrt{\frac{3.E_s}{(M-1).N_0}}\right) \quad \text{... (4.46)}$$

where, $\frac{E_s}{N_0}$ is the SNR per symbol. Therefore the probability of symbol error in M-QAM is,

$$P_e = 1 - \left(1 - P\sqrt{M}\right)^2 \quad \text{... (4.47)}$$

This is the exact expression for probability of the symbol error for M-QAM constellation. For the optimum demodulator, the probability of symbol error for the M-QAM constellation is tightly upper bounded as

$$P_e \leq 1 - \left\{1 - 2Q\left(\sqrt{\frac{3.E_s}{(M-1).N_0}}\right)\right\}^2$$

$$\leq 4Q\left(\sqrt{\frac{3.k.E_s}{(M-1).N_0}}\right) \quad \text{... (4.48)}$$

The above expression is true for any even k≥ 1 and average SNR of E_s/N_0.

Now for the non-rectangular QAM constellation, where, d_{min} is the minimum Euclidean distance between signals points, the symbol error probability may be upper bound by using union bound is

$$P_e < (M-1).Q\left[\sqrt{\frac{(d_{min})^2}{2N_0}}\right] \quad \text{... (4.49)}$$

4.2.2 Performance Evaluation with PAPR Reduction

In an OFDM system with bandwidth 'W', the high rate data stream is divided into 'N' sub-bands with the bandwidth of 'W/N' where each sub-band experiences flat fading. For each sub-bands the symbol period, $T_s = {}^{N}/_{W}$. Sub-bands are orthogonal to each other and closely spaced with a minimum spacing $({}^{1}/_{T_s})$ between two adjacent subcarriers. Even though there are chances of overlapping and occurrence of ISI. The symbol period can be increased more than the multipath spread to avoid ISI [8]. Each of the sub-bands with a low data rate signals stream is independently modulated and transmitted using 'N' independent sub-carriers of N-point IFFT, where the frequency domain signals are transformed into the time domain. At the IFFT all the sub-carriers in the same phase are added coherently in the time domain which results in high peak signal power. The ratio of this high peak signal power to the average signal power is called as peak to average power ratio (PAPR).

$$\text{PAPR}=\frac{max\{|x(k)|^2\}}{E\{|x(k)|^2\}} \quad \text{... (4.50)}$$

In general when all the 'N' subcarriers are having equal amplitude and phase when coherently added using N-point IFFT in the time domain results in PAPR of value N. Therefore the peak signal power is 'N' times that of average power in OFDM. The high peak signal power in OFDM demands highly dynamic power amplifier (HPA) circuits in the transmitter. More specifically the power amplifier (PA) in the transmitter should be self-motivated to accommodate such peak power. The PA must be biased properly otherwise the PA enters into saturation and cause non-linear amplification of high peak signals [82]. Even highly linear amplifiers enforce

distortion in their outputs when applied input is much greater than its normal value, due to saturation characteristics of such amplifiers [15].

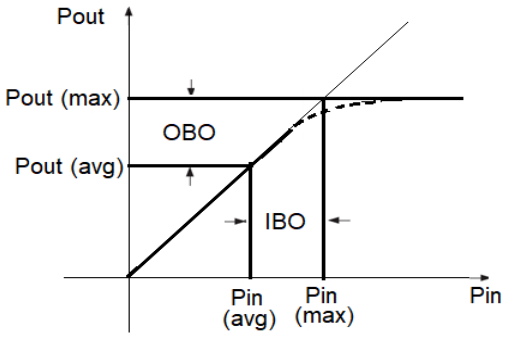

Fig. 4.7 Input Output Characteristic of HPA

The input-output characteristic that is input power (Pin) versus the output power (Pout) of a 'high-power amplifier (HPA)' is presented in fig 4.7. Due to the saturation condition of HPA the output is restricted to Pout (max) concerning the input Pin (max). From fig. 4.7 it is very clear that I/P power should be moving backward by IBO to run PA in the linear area [87]. The non-linear area of I/O characteristics is given by

$$IBO = 10\ log_{10} \frac{P_{in(\max)}}{P_{in(avg)}} \quad \text{... (4.51)}$$

Or

$$OBO = 10\ log_{10} \frac{P_{out(\max)}}{P_{out(avg)}} \quad \text{... (4.52)}$$

High input signal power when applied to the HPA and it enters in to saturation region; it results in out-of-band radiation which interferes with signals of neighboring bands and in-band distortion in the received signal [80]. Due to non-linear amplification of HPA, the orthogonality of the OFDM system may fail which results in ICI. The high PAPR value in the OFDM system severely affects the efficiency of the HPA of the OFDM transmitter. It degrades the SQNR of highly linear devices like ADC and DAC. Also, the HPA consumes more power which becomes a critical issue in the case of up-linking with battery-operated mobile terminal [15]. Hence it is very essential to reduce the PAPR to the desired level to have trustworthy communication. Assuming information symbols $X(0), X(1), \ldots . X(N-1)$ equals to $\pm a$. The information symbols are loaded onto the

subcarriers and transmitted through N point IFFT. Let the IFFT samples are$x(0), x(1), \ldots . x(N-1)$. The K^{th}symbol from IFFT is,

$$x(k) = \frac{1}{N}\sum_{i=0}^{N-1} X(i)e^{(j2\pi ki/N)} \quad \ldots (4.53)$$

The average power is given by

$$P_{avg} = E\{|x(k)|^2\} \quad \ldots (4.54)$$

$$= \frac{1}{N^2}\sum_{i=0}^{N-1} E\{|X(i)|^2\}\, E\left\{\left|e^{(j2\pi ki/N)}\right|^2\right\}$$

Since, the phase factor $E\left\{\left|e^{(j2\pi ki/N)}\right|^2\right\} = 1$ we have

$$P_{avg} = E\{|x(k)|^2\} = \frac{1}{N^2}\sum_{i=0}^{N-1} E\{|X(i)|^2\} \quad \ldots (4.55)$$

We have assumed that information symbols $X(i) = \pm a$

$$P_{avg} = E\{|x(k)|^2\} = \frac{1}{N^2}\sum_{i=0}^{N-1} a^2$$

$$P_{avg} = \frac{1}{N^2}a^2 \text{ N}$$

$$P_{avg} = \frac{a^2}{N} \quad \ldots (4.56)$$

Now let us find the peak power of the transmitted symbol. From eq. (4.53)

$$x(0) = \frac{1}{N}\sum_{i=0}^{N-1} X(i) \ , for\ k = 0 \quad \ldots (4.57)$$

Since $X(0), X(1), \ldots . X(N-1)$ equals to $\pm a$.

$$x(k) = \frac{1}{N}\sum_{i=0}^{N-1} a \ = \frac{aN}{N} \ = a \quad \ldots (4.58)$$

Hence, the peak power

$$max\{|x(k)|^2\} = a^2 \quad \text{... (4.59)}$$

Therefore PAPR in the OFDM system from eq. (4.50), (4.56), and (4.59) is,

$$PAPR = \frac{a^2}{a^2/_N} = N \quad \text{... (4.60)}$$

The eq. (4.60) represents that the peak power is approximately 'N' times the average transmitted power. And it is also observed that the PAPR in the OFDM system essentially arises due to IFFT transformation. The best way to measure the PAPR is its statistical parameter, CCDF. CCDF is the probability that the PAPR exceeding a certain threshold value of PAPR. Let 'x' be the threshold value of PAPR then the CDF of PAPR of an OFDM signal for N subcarriers is given by

$$CDF(x) = \Pr[PAPR \leq x] = \left(1 - e^{\frac{-x^2}{2\sigma^2}}\right)^N \quad \text{... (4.61)}$$

Therefore, the CCDF of PAPR, CCDF(x) is given by

$$\Pr[PAPR \geq x] = 1 - \left(1 - e^{\frac{-x^2}{2\sigma^2}}\right)^N \quad \text{... (4.62)}$$

Many methods lessening PAPR have been employed including 'iterative clipping and filtering (ICF)', 'selective mapping (SLM)', 'iterative companding transform and filtering (ICTF)', 'partial transmit sequence (PTS)' and so on.

4.2.2.1 Iterative clipping and filtering (ICF)

For the PAPR lessening purpose, the clipping approach is the most accepted technique, which truncates the transmitted signal to a predetermined specific level and thus reduces PAPR conveniently in the transmitted signal. However, this technique is susceptible to in-band distortion which is responsible for degrading the BER performance and the out-of-band radiation which results in ICI. Although the effect of out-of-band radiation is reduced by filtering, this may affect high-frequency components of the in-band signal which was sampled at the Nyquist sampling rate in the time domain. This problem can be efficiently mitigated by oversampling the OFDM signal before low pass filtering in the time domain [15]. Also, the BER performance can be improved by passing the signal through a band-pass filter.

Attempt to reduce the effects of out-of-band radiation by clipping and filtering may result in peak regrowth and may exceed the specified clipping levels [88], [89].

Among different schemes employed for lessening PAPR, the iterative clipping, and filtering of OFDM signal to desire threshold level, ICF is the most prominent PAPR lessening scheme. Clipping and filtering of the OFDM symbol are performed in the time domain and frequency domain respectively. The main application of filtering is to minimize spectral growth. So to have desired PAPR result ICF method employed many iterations [90]. Figure 4.8 shows the ICF scheme for lessening the PAPR, Where 'C0' is the original OFDM symbols, 'N' is the number of subcarriers; 'L' is the oversampling factor; 'x_m' is the OFDM signal before clipping in the time domain; '$\hat{x}_m$' is the OFDM signal after clipping in the time domain; '$\hat{C}_m$' is the clipped signal in the frequency domain; after filtering 'C' is OFDM signal in the frequency domain and 'x' is the original OFDM signal in the time domain.

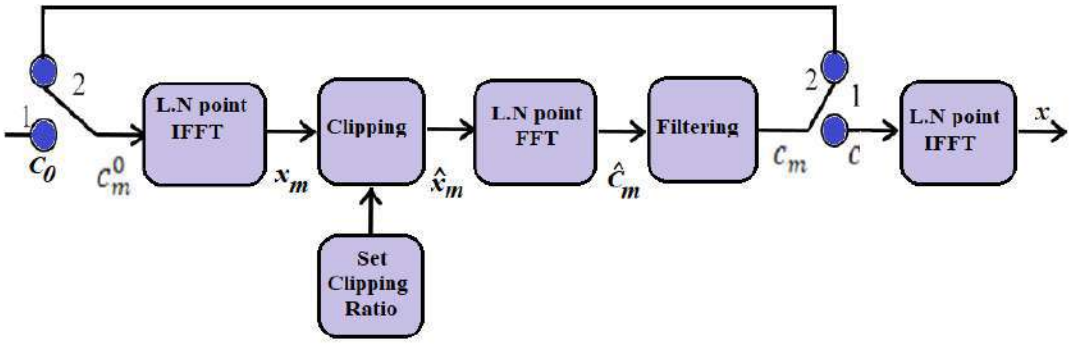

Fig. 4.8 Conventional ICF method for PAPR reduction

The number of iterations is denoted by m = 1, 2….M. The clipped signal in conventional ICF PAPR reduction scheme can be expressed as [34],

$$\hat{x}_m(n) = \begin{cases} Ae^{j\emptyset(n)}, & if\ |x(n)| > A \\ x(n), & Otherwise \end{cases} \quad \text{... (4.63)}$$

Where 'A' is the pre-defined clipping level; $\emptyset(n)$ is the phase angle. The 'clipping ratio (CR)' is the clipping level normalized by the RMS value (ρ) of the OFDM signal, such that

$$\text{Clipping Ratio (CR)} = \gamma = \frac{A}{\rho} \quad \text{... (4.64)}$$

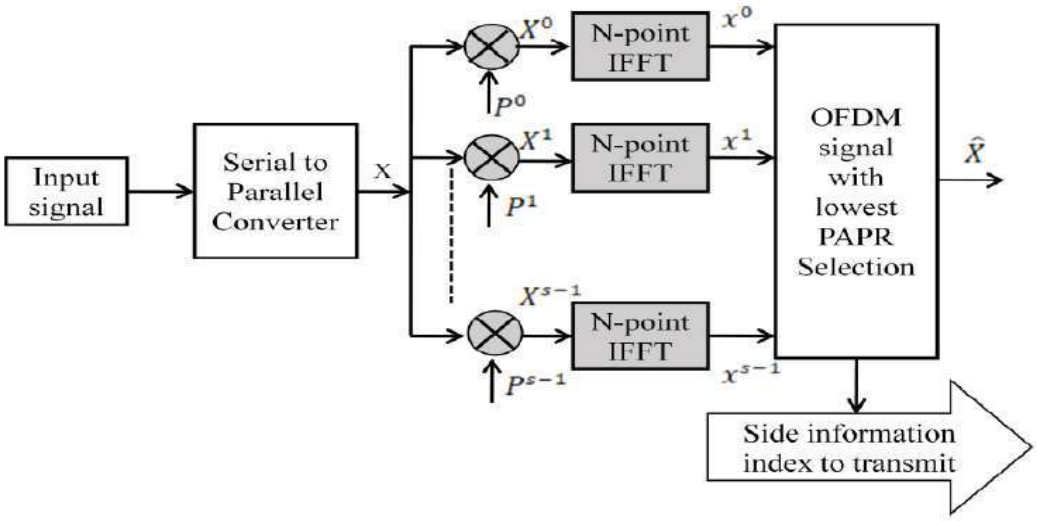

It is known that $\rho = \sqrt{N}$ and $\rho = \sqrt{N/2}$ in the baseband and pass-band OFDM signal respectively [15].

The basic model of OFDM is used for the simulation of PAPR reduction using ICF schemes. Simulation parameters used for the same are; N=256 subcarriers, oversampling factor = 2, 4-iterations, Clipping levels 1 to 6, and QPSK modulation scheme. The performance of the proposed ICF technique for the PAPR reduction method depicts that at the CCDF of 10^{-4} the PAPR is reduced from 11.8 dB (unclipped) to 5dB for the clipping level of 6. The simulation result is shown in the result section.

4.2.2.2 Selective mapping scheme (SLM)

Many methods have been implemented and tested for reducing PAPR from the transmitted OFDM signal. The selective mapping technique has been observed most successful method of PAPR reduction. The SLM can efficiently diminish PAPR at the desired level without introducing distortion in the transmitted OFDM signal [38], [91].

Fig. 4.9 Conventional selective mapping scheme for PAPR reduction

Figure 4.9 depicts the basic block diagram for the conventional SLM method for PAPR reduction, where the input signal $X(n) = X(0), X(1) \ldots\ldots X(N-1)$ is multiplied with S number of phase sequences $P^s = [P_0^s, P_1^s, P_2^s, \ldots\ldots P_{N-1}^s]^T$, where $p = e^{j\emptyset}$ and

$\emptyset \in (0,2\pi)$ for s=1,2…..S, that generate alternative OFDM signal $X^s = [X^s(0), X^s(1), X^s(2), \ldots . X^s(N-1)]^T$. The IFFT of S phase sequences using N-point IFFT is used to produce independent OFDM sequences, $X^s = [x^s(0), x^s(1), x^s(2), \ldots . x^s(N-1)]^T$. Among these X^s independent sequences $\hat{X} = X^{\hat{s}}$ with the lowest PAPR value is chosen for transmission [15].

$$\hat{S} = \underset{s=1,2,\ldots S}{argmin}\left(\underset{n=0,1,2,\ldots N-1}{max}|x^s(n)|\right) \quad \ldots (4.65)$$

In the SLM technique, distinctive phase sequences are chosen for diminishing the PAPR which very complex and monotonous process of locating optimal phase sequences. In the SLM technique, several independent OFDM signals are generated. From several independent data signals, the signal with optimum PAPR is chosen for transmission [92]. The 'side information (SI)' index of the chosen signal with minimum PAPR is transmitted to the receiver section for the recovery of the original data signal. But this results in data rate loss or reduction in throughput [91], [93]. When the set of SI bits are transmitted along with the selected independent signal, the chances of flawed SI index detection have a significant effect on the error performance of the OFDM system. Every time whenever incorrect SI index is detected complete data block is omitted or lost. Hence to protect SI index bits channel coding must be used, but this may result further in a complex system and delay in transmission [93]. One of the disadvantages of the SLM scheme is high computational complexity as a result of the generation of several alternative OFDM signals through IFFT [94].

4.2.3 Performance Evaluation of MIMO System over Multipath fading Channels.

The basics of the MIMO system have been already discussed in chapter 3 (section 3.3). The MIMO systems consist of multiple transmitting and receiving antennas which provides antenna diversity or spatial diversity in a wireless communication system to get better the throughput, and quality of services. The antenna diversity feature of the MIMO system can be employed in wireless systems to combat the deleterious effects of multipath fading in a wireless channel. The multiple receiving

antennas at the receiver provide receiver diversity and receive multiple delayed replicas of the transmitted signal. Each of the receiving antennas experiences different types of impairments, that is at any time when any one receiving antenna experiences deep fade, another receiving antenna may receive better quality signal [8,95]. In a MIMO configuration, each antenna requires an individual RF chain which is very expensive as compared to the cost of antenna elements. Hence the proper number of antenna selection at transmitter and receiver is necessary for the MIMO system [8,96]. Figures 1.4 (b), 1.4 (c), and 3.8 show different antenna configurations such as SIMO, MISO, and MIMO. The channel matrix H for the MIMO antenna system with M_T transmitting and M_R receiving antennas ($M_T \times M_R$) can be written as,

$$H = \begin{bmatrix} h_{11}\, h_{12} \_\_\_\_\_ h_{1M_r} \\ h_{21}\, h_{22} \_\_\_\_\_ h_{2M_r} \\ \quad - \\ \quad - \\ h_{M_{t_1}}\, h_{M_{t_2}} \_\_\_ h_{M_t M_r} \end{bmatrix} \quad \text{... (4.66)}$$

The MIMO system model is given by

$$\hat{Y} = H\hat{S} + \hat{n} \quad \text{... (4.67)}$$

Where, $\hat{Y}$ is output vector $[M_R \times 1]$ at receiver, H represents the channel matrix $[M_T \times M_R]$, $\hat{S}$ is the transmitted symbol vector $[M_T \times 1]$ and $\hat{n}$ is the noise vector $[M_R \times 1]$, each noise element is well thought-out as iid, AWGN noise with variance σ^2 and zero mean. The signal vector $\hat{S}$ can be obtained by weighting the transmitted symbol. All the signals with good SNR are amplified and others are attenuated. The output signal at the receiver will be the product of the transmitted input signal vector and the channel noise AWGN. The received signal without any interference is given by

$$Y = \sqrt{P_0} H W_T S + n \quad \text{... (4.68)}$$

Where, P_0 indicates the average power of desired received signal; W_T indicates the weighted vector; H is the channel matrix for the preferred user. The decision variable to detect the transmitted symbol S is obtained after combining it with a weight vector W_R. Therefore, the resulting received signal is given by

$$Z = W_R^H \ \mathrm{Y} = \sqrt{P_0}\|H^H W_R\|S + \ W_R^H \mathrm{n} \quad \text{... (4.69)}$$

From equation (4.69), the SNR is given by

$$SNR = \frac{P_0\|H^H W_R\|^2}{\sigma_n^2\|W_R\|^2} \quad \text{... (4.70)}$$

To maximize SNR, replacing the received weight vector by $W_R = Hu_{max}$, where u_{max} is a unit norm eigenvector corresponding to maximum Eigen value Λ_{max}. This indicates the strongest path can be selected for the signal transmission through the wireless channel [76].

4.2.3.1 Error rate performance for transmit beamforming in MISO system.

The MISO antenna system with more than one transmitting antennas and a one receiving antenna is shown in fig. 1.4(c). Assuming M_T = 2 transmitting antennas and $M_R = 1$ receiving antenna, we have (2×1) MISO system and its model is given by

$$Y = [h1 \quad h2][x1 \quad x2]^T + w \quad \text{... (4.71)}$$

$$\text{Or } \hat{Y} = H\,\hat{x} + \ \hat{w} \quad \text{... (4.72)}$$

Where, $\hat{Y}$ output (2×1) vector, H is fading coefficient matrix (1×2) , $\hat{x}$ is transmitted signal vector (2×1), and $\hat{w}$ is the noise vector with zero mean and variance σ^2. For the best optimal transmission scheme, let x denotes the single transmit symbol, the transmit vector is given by

$$\hat{x} = \frac{1}{\|\hat{h}\|}\begin{bmatrix} h1^* \\ h2^* \end{bmatrix} x \quad \text{... (4.73)}$$

Where, $\begin{bmatrix} h1^* \\ h2^* \end{bmatrix}$ is a unit vector and $\frac{1}{\|\hat{h}\|}\begin{bmatrix} h1^* \\ h2^* \end{bmatrix}$ is transmit beamformer. Therefore applying transmit beamforming scheme we have

$$\hat{x} = \begin{bmatrix} \frac{h1^*}{\|\hat{h}\|}x \\ \frac{h2^*}{\|\hat{h}\|}x \end{bmatrix} \quad \text{... (4.74)}$$

From equation 4.72 & 4.73 we have

$$Y = [h1 \quad h2]\ \frac{1}{\|\hat{h}\|}\begin{bmatrix} h1^* \\ h2^* \end{bmatrix} x + w \quad \text{... (4.75)}$$

$$= \|\hat{h}\|^2 \frac{1}{\|\hat{h}\|}\, x + w$$

$$= \|\hat{h}\|x + w \quad \text{... (4.76)}$$

The SNR is the ratio of signal power to the noise power, therefore

$$SNR = \frac{\|\hat{h}\|^2 E\{|x|^2\}}{\sigma^2}$$

$$\text{Or } SNR = \frac{\|\hat{h}\|^2 P}{\sigma^2} \quad \text{... (4.77)}$$

The equation (4.77) of SNR is similar to the SNR equation of the MRC (Maximal ratio Combining) scheme. In this case, the challenge is to find the fading coefficients h1 and h2 to form a beamformer, or in another word, we need the CSI at the transmitter.

Bit error rate (BER) for transmit beamforming:

Since the SNR of transmit beamforming is similar to the SNR of MRC scheme, therefore at high SNR the BER equation for transmit beamforming is also equivalent to the BER equation of the MRC scheme, and it is given by

$$BER = \binom{2L-1}{L} \left(\frac{1}{2\,SNR}\right)^L \quad \text{... (4.78)}$$

where L is the number of transmit antennas.

4.2.3.2 Error rate performance for receive beamforming or MRC scheme.

MRC scheme at receiver or 'L' multiple antennas at receiver while single antenna at the transmitter is shown in fig. 4.10. This scheme is also referred to as receive beamforming. If 'x' denotes the transmitted signal, we have a system model for receiver beamforming,

$$\hat{Y} = \hat{H}x + \hat{n} \quad \text{... (4.79)}$$

Where, '$\hat{n}$' is iid AWGN noise with zero mean and variance σ^2 and $(1 \times L)$ vector, $\hat{Y}$ is output $(1 \times L)$ vector, and $\hat{H}$ is the fading coefficient vector $(1 \times L)$. The expected value of noise that is noise power at each receive antenna is,

$$E\{|n_i(k)|^2\} = \sigma_n{}^2 \quad \text{... (4.80)}$$

At the receiver, let $y1, y2, y3, \ldots \ldots yL$ signals received at L antennas. Combining received signal linearly, we have

$$w_1^* y_1 + w_2^* y_2 + w_3^* y_3 + \ldots\ldots\ldots + w_L^* y_L \quad \text{... (4.81)}$$

Therefore beamformer vector is written as

$$[w_1^* + w_2^* + .. + w_L^*][y_1 + y_2 + .. + y_L]^T = \bar{w}^H \bar{y} \quad \text{... (4.82)}$$

$$= \bar{w}^H \bar{h}\, x + \bar{w}^H \bar{n} \quad \text{from eq. (4.79)}$$

which is the sum of the signal component ($\bar{w}^H \bar{h}\, x$)and the noise component ($\bar{w}^H \bar{n}$). Therefore to find SNR, the signal power equals to $\left|\bar{w}^H \bar{h}\right|^2 P$, where 'P' the transmit signal power and the noise power of the beamformer equals to $\sigma_n{}^2 \, \|\bar{\mathrm{w}}\|^2$, where $\bar{\mathrm{w}} = (\bar{\mathrm{w}}^{\mathrm{H}} \bar{\mathrm{w}})$ is the beamforming vector. Therefore,

$$SNR = \frac{\left|\bar{w}^H \bar{h}\right|^2 P}{\sigma_n{}^2 (\bar{\mathrm{w}}^{\mathrm{H}} \bar{\mathrm{w}})} \quad \text{... (4.83)}$$

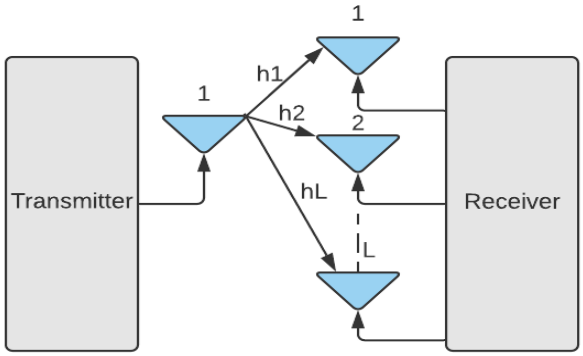

Fig. 4.10 Single input multiple output (SIMO) receiver beamforming

Choosing $\|\bar{w}\|^2 = 1$, that is $\bar{\mathrm{w}}^{\mathrm{H}} \bar{\mathrm{w}} = 1$, eq. (4.83) gives

$$SNR = \frac{\left|\bar{w}^H \bar{h}\right|^2 P}{\sigma_n{}^2} \quad \text{... (4.84)}$$

So, the optimal beamforming vector $\bar{\mathrm{w}}$, that maximizes the received SNR at the output of beamformer is, $\bar{\mathrm{w}}_{\mathrm{opt}} = \frac{\bar{\mathrm{h}}}{\|\bar{\mathrm{h}}\|}$ which is also known as maximal ratio combiner, therefore,

$$SNR = \frac{\left|\frac{\bar{h}^H}{\|\bar{h}\|} \bar{h}\right|^2 P}{\sigma_n{}^2} = \left\|\bar{h}\right\|^2 \frac{P}{\sigma_n{}^2} \quad \text{... (4.85)}$$

BER equation for the MRC scheme or receiver beamforming scheme:

The bit error rates for the MRC scheme with 'L' receive antennas is given by

$$BER = \left(\frac{1-\lambda}{2}\right)^L \sum_{l=0}^{L-1} {}^{L+l-1}C_l \left(\frac{1+\lambda}{2}\right)^l \quad \text{... (4.86)}$$

where, $\lambda = \sqrt{\frac{SNR}{2+SNR}}$

For high SNR, $\frac{1}{2}(1-\lambda) \approx \frac{1}{2SNR}$, and $\frac{1}{2}(1+\lambda) \approx 1$. Substituting in eq. (4.85), we have

$$\text{Average BER} = \left(\frac{1}{2SNR}\right)^L \sum_{l=0}^{L-1} {}^{L+l-1}C_l \,.1$$

$$\text{Average BER} = {}^{2L-1}C_L \frac{1}{2^L}\left(\frac{1}{SNR}\right)^L \quad \text{... (4.87)}$$

This is the equation for average BER for the MRC scheme with 'L' receives antennas. It is clear from the above equation that the BER value is directly proportional to $\frac{1}{(SNR)^L}$. Thus BER decreases at a faster rate with increasing the number of receive antennas.

Probability of deep fade in MRC scheme with 'L' receive antenna:

From eq. (4.85), the SNR at the receiver in the MRC scheme is

$$\|\bar{h}\|^2 \frac{P}{\sigma_n{}^2} = g.\frac{P}{\sigma_n{}^2}$$

where 'g' is an overall gain of channel for MRC and it is 'Chi-Square Random variable' with 2L degree of freedom. The system is said to be in deep fade when $g < \frac{1}{SNR}$. The probability distribution of g is

$$F_g(g) = \frac{g^{L-1}}{(L-1)!}e^{-g} \quad \text{... (4.88)}$$

The probability of deep fade,

$$P_r\left(g < \frac{1}{SNR}\right) = \int_0^{1/SNR} \frac{g^{L-1}}{(L-1)!}e^{-g}\, dg \quad \text{... (4.89)}$$

$$P_r\left(g < \frac{1}{SNR}\right) \approx \int_0^{1/SNR} \frac{g^{L-1}}{(L-1)!}\, dg$$

At high SNR, $1/SNR \approx 1$, therefore

$$P_r\left(g < \frac{1}{SNR}\right) \approx \frac{g^L}{L!}\Big|_0^{\frac{1}{SNR}}$$

$$P_r\left(g < \frac{1}{SNR}\right) \approx \frac{1}{L!}\left(\frac{1}{SNR}\right)^L \quad \text{... (4.90)}$$

This implies the probability of deep fade is directly proportional to $\left(\frac{1}{SNR}\right)^L$, hence by increasing the number of receiving antennas, the probability of the system in deep fade decreases significantly.

4.2.4 Space time coded MIMO systems

In an attempt to increase the SNR value in the case of the AWGN wireless channel the slope of the BER graph is an abrupt fall approach to infinity after some specific value of SNR. Whereas for the Rayleigh fading channel upon increasing the SNR value, the slope of the BER graph becomes linear after a certain value of SNR. This means the BER performance of the MIMO system for the Rayleigh fading channel is showing significant degradation even after increasing SNR to a high value. Due to the above-stated facts, it is recommended to convert the wireless fading channel into an AWGN channel to improve the BER presentation curve. To achieve this antenna diversity scheme can be utilized in the MIMO system. However, there are few drawbacks of the receiver antenna diversity scheme, such as computational complexity, high power consumption, and inter receive antenna space for cellular units specifically in down-linking. The spatial diversity can be obtained by employing multiple transmitting and receiving antennas in the MIMO system. In the case of mobile to base station transmission, due to the availability of multiple antennas with sufficient space between them at the base station, it is very easy to achieve receive diversity using different combing schemes like MRC. But in the case of reverse transmission, because of the limited size of mobile, it is very difficult to employ multiple receive antennas in the mobile sets and hence difficult to achieve receive diversity. Therefore it is enviable to obtain transmit diversity to make use benefits of spatial diversity. Among many available coding schemes, STC in the MIMO system is widely used for improving diversity gain. To achieve the diversity gain STC coding is performed on the transmitter side and a very simple linear processing is employed for STC decoding at the receiver side. To minimize computational complexity at the receiver end differential STC can be utilized

without using CSI at the receiver. The STC coded MIMO system with M_T transmitting and M_R receiving antennas is shown in fig. 4.11. The input sequence is mapped into symbols $x_1, x_2, x_3, \ldots\ldots\ldots x_N$ which is space-time coded into $\{x_i^t\}_{i=1}^{M_T}$, t=1, 2, 3 ...T, where 'i' denotes the index of the antenna and 't' denotes the time slots index of symbols. The STC codeword with N number of symbols is $N = M_T.T$. Thus the rate of the STC MIMO system is $R = {}^{N}/_{T}$ Symbols per channel use. At the receiver end, the received symbols are $\{y_j^t\}_{j=1}^{M_R}$, t=1, 2, 3 ...T. Let $h_{ij}{}^{(t)}$ be Rayleigh distributed channel gain with i^{th} transmit and j^{th} receive antenna over t^{th} symbol time [8], [15], [97].

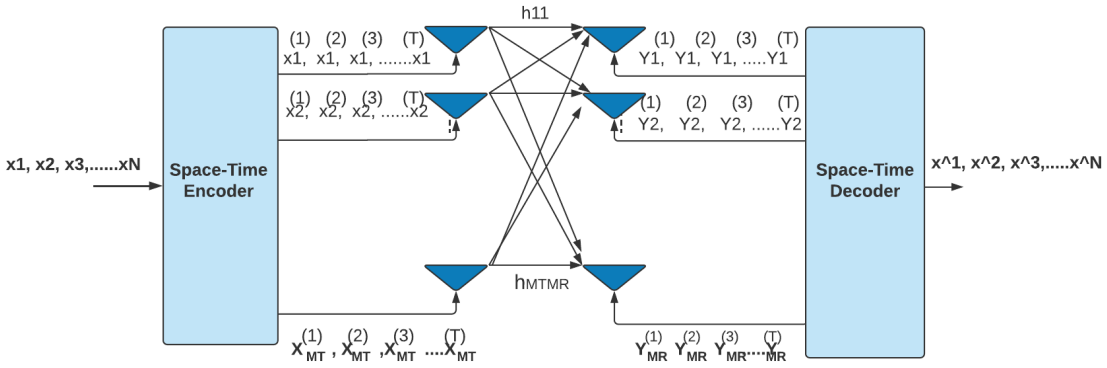

Fig. 4.11 Space time-coded ($M_T \times M_R$) MIMO system

The received signal at j^{th} received antenna is given by,

$$y_j^{(t)} = \sqrt{\frac{E_x}{N_0 M_T}} . \left[h_{j1}^{(t)} h_{j2}^{(t)} \ldots . h_{jMT}^{(t)}\right] . \left[x_1^{(t)} x_2^{(t)} \ldots . x_{MT}^{(t)}\right]^T + z_j^{(t)} \qquad \ldots (4.91)$$

Where, $z_j^{(t)}$ is the noise at j^{th} receive antenna with (t) time slot and E_x is the average symbol energy. The total transmitted power is given as,

$$\sum_{i=1}^{M_T} E\left\{\left|x_i^{(t)}\right|^2\right\} = M_T \qquad \ldots (4.92)$$

Assuming ½ variance for channel gain h_{ij}, the PDF of each channel gain is given by,

$$f_{H_{ij}[hij]} = \frac{1}{\pi} e^{-|h_{ij}|^2} \qquad \ldots (4.93)$$

And the PDF of additive noise is given by,

$$f_{z_j^{(t)}}\left[z_j^{(t)}\right] = \frac{1}{\pi} e^{-\left|z_j^{(t)}\right|^2} \quad \text{... (4.94)}$$

Based on equation (1), for ($M_T \times M_R$) MIMO system, assuming quasi static channel gain of $h_{ij}^{(t)} = h_{ij}$, the system model is modified as

$$\begin{bmatrix} y_1^{(1)} & y_1^{(2)} & & y_1^{(T)} \\ y_2^{(1)} & y_2^{(2)} & \dots & y_2^{(T)} \\ \vdots & \vdots & & \vdots \\ y_{MR}^{(1)} & y_{MR}^{(2)} & & y_{MR}^{(T)} \end{bmatrix} = \sqrt{\frac{E_x}{N_0 M_T}} \begin{bmatrix} h_{11} & h_{12} & & h_{1MT} \\ h_{21} & h_{22} & & h_{1MT} \\ . & . & \dots & . \\ . & . & & . \\ h_{MR1} & h_{MR2} & & h_{MRMT} \end{bmatrix} . \begin{bmatrix} x_1^{(1)} & x_1^{(2)} & & x_1^{(T)} \\ x_2^{(1)} & x_2^{(2)} & \dots & x_2^{(T)} \\ \vdots & \vdots & & \vdots \\ x_{MT}^{(1)} & x_{MT}^{(2)} & & x_{MT}^{(T)} \end{bmatrix} + \begin{bmatrix} z_1^{(1)} & z_1^{(2)} & & z_1^{(T)} \\ z_2^{(1)} & z_2^{(2)} & \dots & z_2^{(T)} \\ \vdots & \vdots & & \vdots \\ z_{MR}^{(1)} & z_{MR}^{(2)} & & z_{MR}^{(T)} \end{bmatrix} \quad \text{... (4.95)}$$

4.2.4.1 Space-Time Block Codes (STBC)

STBC coding techniques are the most efficient method of accomplishing transmits diversity while other methods failed to do so in the case of quasi-static fading channels. STBC coding techniques can be generalized to achieve receive diversity using multiple receive antennas. STBCs can be efficiently decoded at the receiver using simple linear processing of L number of received signals through L receive antenna [8].

4.2.4.2 Performance evaluation of STBC coded MIMO system.

Considering BPSK modulation, the probability of bit error can be written as,

$$P_r(\psi) = Q\left(\sqrt{\frac{2\psi\rho}{M_T}}\right) \quad \text{... (4.96)}$$

where $\psi = \sum_{j=1}^{M_R} \sum_{i=1}^{M_T} d_{i,m} \left|h_{i,j}\right|^2$; ρ is the average SNR at each receive antenna. Assuming all the diagonal elements $\left(d_{i,m} = d_m\right)$ corresponding to m^{th} signal are identical. Therefore, $\psi = d_m \sum_{j=1}^{M_R} \sum_{i=1}^{M_T} \left|h_{i,j}\right|^2$ and it is chi-square distributed with $2M_T M_R$ degree of freedom. Thus the probability of error for large SNR can be approximated as,

$$P_r \approx \binom{2M_T M_R - 1}{M_T M_R} \left(\frac{M_T}{4 d_m \rho}\right)^{M_T M_R} \quad \text{... (4.97)}$$

From the above equation, it is shown that the BER for STBC coded MIMO system over Rayleigh fading channel with the BPSK modulation scheme decays inversely with the $(M_T M_R)^{\text{th}}$ power of the SNR. The diversity order of $M_T M_R$ is achieved

which is the full spatial diversity. In the case of other M-PSK modulation for an AWGN channel, the symbol error rate is given by

$$P_e \approx 2\binom{2M_TM_R-1}{M_TM_R}\left(\frac{M_T}{4d_m sin^2\left(\frac{\pi}{M}\right)}\right)^{M_TM_R}\left(\frac{1}{\rho}\right)^{M_TM_R} \quad \text{... (4.98)}$$

The above equation indicates that diversity advantage can be easily attended using STBC coded MIMO system.

4.2.4.3 Alamouti STBC scheme

The primary challenge of the transmit beamforming is the requirement of CSI at the transmitter. To resolve this issue a new scheme STC is introduced. The most popular scheme in this category is the Alamouti scheme which is also known as the orthogonal STBC scheme. S. M. Alamouti (1998) established a scheme for achieving transmits diversity using STBC with two transmit antennas is shown in fig. 4.12.

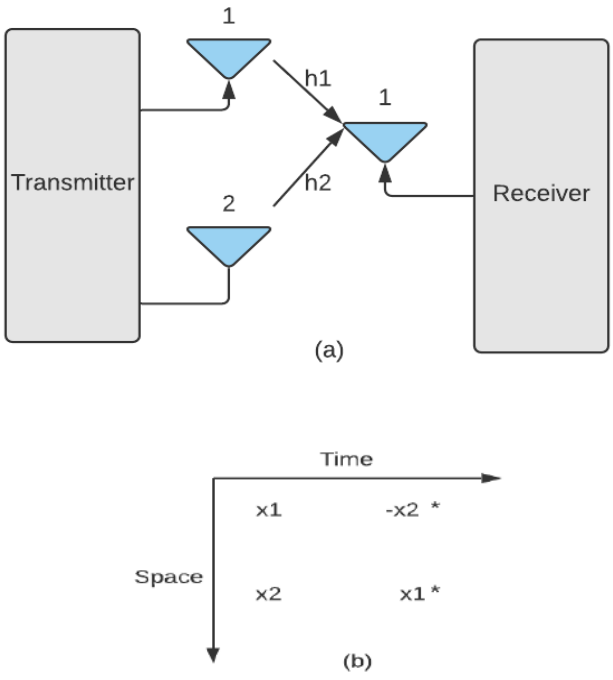

Fig. 4.12 (a) Two Transmit and one Receive Antenna system
(b) 2-Transmit, 1-Receive Alamouti STBC coding

This scheme doesn't require any channel state information or knowledge of channel coefficients. Here two symbols x_1 and x_2 are transmitted through transmitting antennas 1 and 2 in two-time slots. During the first-time slot symbol x_1 and x_2 are transmitted through transmit antenna 1 and 2 respectively. During the second time slot, $-x2^*$ and $x1^*$ are transmitted through transmit antenna 1 and 2 respectively. This process is shown in figure 2. Since we are grouping symbols and transmitting them in two consecutive time slots, hence there is no data rate loss [62]. The received signal in the first and second-time slot is given in equations (4.98) and (4.99).

$$y_1 = h_1 x_1 + h_2 x_2 + n_1 = [h_1 \quad h_2] \begin{bmatrix} x_1 \\ x_2 \end{bmatrix} + n_1 \qquad \text{... (4.99)}$$

$$y_2 = -h_1 x_2{}^* + h_2 x_1{}^* + n_2 = [h_1 \quad h_2] \begin{bmatrix} -x_2{}^* \\ x_1{}^* \end{bmatrix} + n_2 \qquad \text{... (4.100)}$$

where, y_1, y_2 are the received symbols, x_1, x_2 are the transmitted symbols and n_1, n_2 are the noise in the $1^{st}, 2^{nd}$ time slots respectively. h_1, h_2 are the channel coefficients from $1^{st}$and 2^{nd}transmitting antenna to receiving antenna respectively. Since the noise terms are iid,

$$E\left\{\begin{bmatrix} n_1 \\ n_2{}^* \end{bmatrix} [n_1{}^* \quad n_2]\right\} = \begin{bmatrix} |n_1|^2 & 0 \\ 0 & |n_2|^2 \end{bmatrix} \qquad \text{... (4.101)}$$

The above equation can be implemented in matrix notation as,

$$\begin{bmatrix} y_1 \\ y_2{}^* \end{bmatrix} = \begin{bmatrix} h_1 & h_2 \\ h_2{}^* & -h_1{}^* \end{bmatrix} \begin{bmatrix} x_1 \\ x_2 \end{bmatrix} + \begin{bmatrix} n_1 \\ n_2{}^* \end{bmatrix} \qquad \text{... (4.102)}$$

Let $H = \begin{bmatrix} h_1 & h_2 \\ h_2{}^* & -h_1{}^* \end{bmatrix}$, to solve for $\begin{bmatrix} x_1 \\ x_2 \end{bmatrix}$. Now let us find the inverse of H. We know, for a general m x n matrix, the pseudo inverse is defined as, $H^p = (H^H H)^{-1} H^H$. Now the term $(H^H H)$ is given by,

$$(H^H H) = \begin{bmatrix} h_1{}^* & h_2 \\ h_2{}^* & -h_1 \end{bmatrix} \begin{bmatrix} h_1 & h_2 \\ h_2{}^* & -h_1{}^* \end{bmatrix}$$

$$= \begin{bmatrix} |h_1|^2 + |h_1|^2 & 0 \\ 0 & |h_1|^2 + |h_1|^2 \end{bmatrix} \qquad \text{... (4.103)}$$

For the diagonal matrix the inverse of matrix is the inverse of the diagonal elements itself,

$$\begin{bmatrix}\widehat{x_1}\\ x_2\end{bmatrix} = (H^H H)^{-1} H^H \begin{bmatrix}y_1\\ {y_2}^*\end{bmatrix}$$

$$= (H^H H)^{-1} H^H \left(H \begin{bmatrix}x_1\\ x_2\end{bmatrix} + \begin{bmatrix}n_1\\ {n_2}^*\end{bmatrix}\right)$$

$$= \begin{bmatrix}x_1\\ x_2\end{bmatrix} + (H^H H)^{-1} H^H \begin{bmatrix}n_1\\ {n_2}^*\end{bmatrix} \quad \text{... (4.104)}$$

The equation with the estimated symbol following equalization in the MRC is identical to the above solution.

4.2.4.4 Error performance for Alamouti STBC scheme.

In this case, there are two transmitting vectors x_1, and x_2, therefore the total transmitting power 'P' is equally divided 'P/2' for each transmitting symbol. Therefore, $E\{\|x_1\|^2\} = E\{\|x_2\|^2\} = {}^{P}/_{2}$.

Now SNR for Alamouti scheme,

$$SNR = \frac{\|\bar{h}\|^2 {}^{P}/_{2}}{\sigma^2} = \frac{1}{2}\frac{\|\bar{h}\|^2 P}{\sigma^2} \quad (4.105)$$

This expression of SNR for the Alamouti scheme is similar to the MRC scheme except for the factor of ½. That is we get ½ SNR in the Alamouti scheme compared to the MRC scheme. Thus Alamouti scheme doesn't require CSI at the cost of ½ SNR.

BER performance of Alamouti scheme:

As the SNR and the BER expression for the Alamouti scheme is equivalent to the MRC scheme with two transmit (L=2) and one receive antenna, Therefore BER at high SNR form eq. (4.87), we have

$$\text{Average BER} = \binom{2L-1}{L} \frac{1}{2^L} \left(\frac{1}{SNR}\right)^L$$

Putting L=2, we have

$$\text{Average BER} = \quad {}^{3}C_{2} \quad \frac{1}{2^2}\left(\frac{1}{\frac{1}{2}SNR}\right)^{L} = \frac{3}{(SNR)^2}$$

$$\text{Average BER} = \frac{3}{(SNR)^2} \qquad \text{... (4.106)}$$

Eq. (4.92) represents the BER expression for the Alamouti scheme under the assumption that channel coefficients are IID Rayleigh fading coefficients with average power equals unity.

4.2.5 Channel Capacity of wireless communication.

Channel capacity or data rate is defined as the maximum rate of information transmission between transmitter and receiver with lower probability of error [8]. The Channel capacity can be expressed as the maximum mutual information between transmitter and receiver over all possible distribution at the source. Consider the Gaussian channel, as shown in Fig. 4.13.

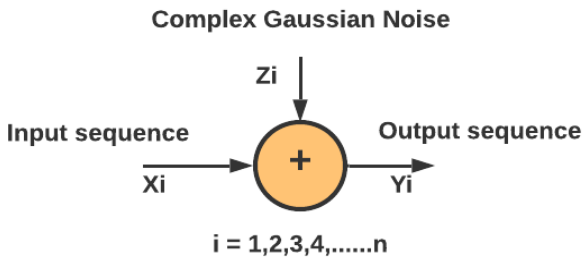

Fig. 4.13 Gaussian channel

The channel model for the wireless channel is written as, $y_i = x_i + z_i$ with average power constraint, $\frac{1}{n}\sum_{i=1}^{n} {x_i}^2 \leq p$. That means a limited amount of power is available at the transmitter. There are many types of power constraints; the average power constraint is most commonly used. In 1948 Shannon demonstrated that the capacity is the maximum shared information between input and output $\mathrm{I(X;Y)}$, over the noisy channel as the blcok length $\mathrm{n} \to \infty$.

$$C = \lim_{n\to\infty} \frac{1}{n} \max_{\mathrm{p(x_1,x_2,\ldots x_n)}} \mathrm{I}(X_{1,}X_{2,\ldots.}X_N\ ;\ Y_{1,}Y_{2\ldots..}Y_N) \text{... (4.107)}$$

The simplified expression can be written as

$$C = \max_{p(x)} \; I(X,Y) \qquad \text{... (4.108)}$$

Where, $I(X,Y)$ is shared information between X and Y and it is given by

$$I(X,Y) = h(y) - h(y|x)$$

$$I(X,Y) = h(y) - h(x+z|x) \qquad \text{... (4.109)}$$

'z' is noise independent of x source, $(x|x) = 0$, therefore

$$I(X,Y) = h(y) - h(z) \qquad \text{... (4.110)}$$

$$h(z) = \frac{1}{2}\log_2 2\pi eN \qquad \text{... (4.111)}$$

This is derived as the entropy of a gaussian distribution of noise with power *N* and mean zero. The variance of power is given by,

$$E(y^2) = E(x+z)^2 = E(x^2) + E(z^2) + 2E(x)E(z) \qquad \text{... (4.112)}$$

E(x) = E(z) = 0, for AWGN channel with mean zero, so we have

$$E(y^2) = E(x^2) + E(z^2) = p + N \qquad \text{... (4.113)}$$

Therefore, $h(y) \leq \frac{1}{2}\log_2 2\pi e(p+N)$, and the mutual information $I(X,Y)$ is given by

$$I(X,Y) = \frac{1}{2}\log_2 2\pi e(p+N) - \frac{1}{2}\log_2 2\pi eN \qquad \text{... (4.114)}$$

$$I(X,Y) = \frac{1}{2}\log_2 \frac{2\pi e(p+N)}{2\pi eN}$$

$$I(X,Y) = \frac{1}{2}\log_2 \frac{p+N}{N} \quad \text{or}$$

$$I(X,Y) = \frac{1}{2}[\log_2(1 + {}^{p}/_{N})] \qquad \text{... (4.115)}$$

This is the expression for the Capacity of the Gaussian frequency flat MIMO channel. Now the expression for capacity of complex Gaussian channel $y_i = x_i + z_i$ is given by

$$I(X,Y) = \log_2\left(1 + {}^{p}/_{N}\right) \quad \text{... (4.116)}$$

This is the expression of the capacity of the SISO channel.

4.2.5.1 Capacity of frequency flat deterministic MIMO Channel.

Let M_T be the transmitting and M_R be the receiving antennas respectively, channel bandwidth B = 1Hz and assuming frequency flat band. If H is the ($M_T \times M_R$) channel matrix, 'y' is the received vector ($M_R \times 1$), 'x' is the signal vector ($M_T \times 1$), and 'n' is the noise vector ($M_R \times 1$), then the MIMO system model can be written as

$$y = \sqrt{{}^{E_s}/_{M_T}}\ H.x + n \quad \text{... (4.117)}$$

The component $\sqrt{{}^{E_s}/_{M_T}}$ indicates the input signal power is uniformly distributed among M_T transmitting antennas. The covariance matrix of source 'x', $R_{ss} = E[xx^H]$ and because $E[x] = 0$, we put the constraint Trace (R_{ss}) = M_T. Now let us assume H is known at the receiver or perfect CSI is available only at the receiver. The channel capacity for the MIMO system is given by

$$C = \max_{p(x)}\ I(X,Y)$$

$$I(X,Y) = h(y) - h(y|x)$$

For AWGN channel,

$$I(X,Y) = h(y) - h(n|x)$$

$$I(X,Y) = h(y) - h(n)$$

To maximize this expression we have to maximize h(y), since we can't do anything with h(n). The covariance matrix of 'y' is R_{yy},

$$R_{yy} = E[yy^H] = E\left\{\left[\sqrt{{}^{E_s}/_{M_T}}\ H.x + n\right]\left[\left[\sqrt{{}^{E_s}/_{M_T}}\ H.x + n\right]\right]^H\right\}$$

$$= E\left\{\left[\sqrt{E_s/M_T}\ H.x + n\right]\left[\sqrt{E_s/M_T}\ H^H.x^H + n^H\right]\right\}$$

$$R_{yy} = \left\{\frac{E_s}{M_T}\ H.x.x^H.H^H + \sqrt{E_s/M_T}\ H.x.n^H + \sqrt{E_s/M_T}\ H^H x^H.n + nn^H\right\}$$

Since E is operated on variables 'x' and 'n' not on deterministic 'H' and as $E[x] = E[n] = 0$, middle two terms are zero and $R_{xx} = E[xx^H]$, we have

$$R_{yy} = \frac{E_s}{M_T} HE[xx^H]H^H + E[nn^H]$$

$$R_{yy} = \frac{E_s}{M_T} HR_{xx}H^H + E[nn^H] \quad \text{... (4.118)}$$

The component $E[nn^H]$ matrix is written as

$$E[nn^H] = E\left[\begin{bmatrix} n_1 \\ n_2 \\ \cdot \\ \cdot \\ n_{M_R} \end{bmatrix}\left[n_1^*, n_2^* \ldots \ldots n_{M_R}^*\right]\right] \quad \text{... (4.119)}$$

$E[nn^H] = E\begin{bmatrix} E[n_1]^2 & 0 & 0 & 0 \ldots 0 \\ 0 & E[n_2]^2 & 0 & 0 \ldots 0 \\ & \cdot & & \\ & \cdot & & \\ 0 \quad 0 & 0 & 0 & 0\ E[n_{M_R}]^2 \end{bmatrix}$ is a diagonal matrix, as $E[n_i n_j] =$ $0\ ; if\ i \neq j$

So we have, $[nn^H] = N_0 I_{M_R}$, where I_{M_R} is the identity matrix of size ($M_T \times M_R$). Therefore

$$R_{yy} = \frac{E_s}{M_T} HR_{xx}H^H + N_0 I_{M_R} \quad \text{... (4.120)}$$

$$\text{Now, } h(y) = \log_2\left[\det\left(\pi e R_{yy}\right)\right]$$

$$= \log_2\left[\pi e^{M_R} \det\left(R_{yy}\right)\right] \quad \text{... (4.121)}$$

$$h(n) = \log_2\left[\det\left(\pi e N_o I_{M_R}\right)\right]$$

$$= \log_2\left[\pi e^{M_R} \det\left(N_o I_{M_R}\right)\right] \quad \text{... (4.122)}$$

Now the expression for mutual exchange of information between input and output is wrtten as,

$$I(X,Y) = h(y) - h(n)$$

$$= \log_2\left[\pi e^{M_R} \det\left(R_{yy}\right)\right] - \log_2\left[\pi e^{M_R} \det\left(N_o I_{M_R}\right)\right]$$

$$I(X,Y) = \log_2\left[\frac{\pi e^{M_R} \det\left(R_{yy}\right)}{\pi e^{M_R} \det\left(N_o I_{M_R}\right)}\right] \quad \text{... (4.123)}$$

Putting R_{yy} in above expression we have the solution as

$$I(X,Y) = \log_2\left[\det\left(I + \frac{E_s}{M_T N_0}.H.R_{xx}.H^H\right)\right] \quad \text{... (4.124)}$$

Therefore the expression for capacity of frequency flat deterministic MIMO channel

$$C = \max_{\mathrm{Tr}(R_{xx}) = \mathrm{M_R}} \left\{\log_2\left[det\left(I_{M_R} + \frac{E_s}{M_T N_0}.H.R_{xx}.H^H\right)\right]\right\}$$

Rewriting above equation

$$C = \log_2\left[det\left(I_{M_R} + \frac{E_s}{M_T N_0}.HH^H\right)\right] \quad \text{... (4.125)}$$

4.2.5.2 Capacity of MIMO channel with and without channel information available at the transmitter.

Consider a MIMO system as shown in fig. 4.14;

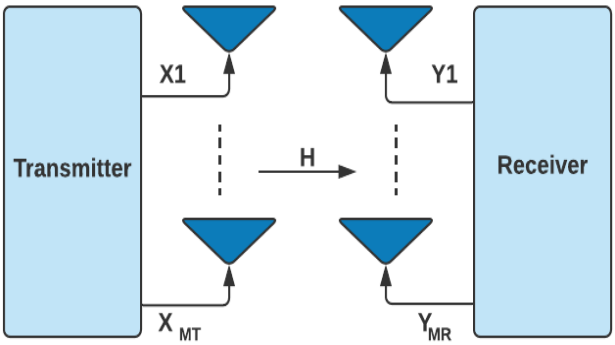

Fig. 4.14 $(M_T \times M_R)$ MIMO System

1) No CSI at the transmitter.

Means ideal estimation of perfect channel knowledge is available at the receiver. In this case, channel has no preferred direction. So, $x = [x_1, x_2, \ldots . x_{M_T}]^T$ is non-preferential. $R_{xx} = I_{M_T} = E[xx^H]$; $E[x] = 0$; $E[x_i x_j] = 0$, if $i \neq j$. Signals are evenly powered and independent at the transmitter. The MIMO channel capacity is given by Eq. (4.124)

$$C = \log_2 \left[det \left(I_{M_R} + \frac{E_s}{M_T N_0} . HH^H \right) \right]$$

Since HH^H is the positive semi-definite with Eigenvalues as the squares of the non-zero singular values of H (i.e., $\lambda_1 = \sigma_1^2, \lambda_2 = \sigma_2^2, \ldots\ldots \lambda_{M_R} = \sigma_{M_R}^2$)), the square matrix HH^H can be diagonalized as $HH^H = Q \wedge Q^H$ where Q is the unitary matrix where '$\wedge'$ is a diagonal matrix of eigenvalues $\lambda 1, \lambda 2, \ldots, \lambda_{M_R}$. Rewriting expression for the capacity

$$C = \log_2 \left[det \left(I_{M_R} + \frac{E_s}{M_T N_0} . Q \wedge Q^H \right) \right] \quad \ldots (4.126)$$

Now using identity, det[AB] = det[BA], let A=Q and B=$\wedge Q^H$, we have $Q \wedge Q^H = \wedge Q^H Q = \wedge$, since $Q^H Q$ is identity matrix $I_{MR.}$ So capacity expression becomes

$$C = \log_2 \left[det \left(I_{M_R} + \frac{E_s}{M_T N_0} . \wedge \right) \right]$$

Where, $I_{M_R} = \begin{bmatrix} 1 & 0 \cdots 0 & 0 \\ \vdots & 1 & \vdots \\ 0 & 0 \cdots 0 & 1 \end{bmatrix}$ and $\wedge = \begin{bmatrix} \lambda_1 & 0 \cdots 0 & 0 \\ \vdots & \lambda_2 & \vdots \\ 0 & 0 \cdots 0 & \lambda_{M_R} \end{bmatrix}$, therefore capacity expression can be rewritten as (r is the rank of the matrix)

$$C = \sum_{i=1}^{r} \log_2 \left(1 + \frac{E_s}{M_T N_0} . \lambda_i \right) \quad \ldots (4.127)$$

The above expression implies that the MIMO channel capacity is the sum of 'r' number of SISO channels or links, each having transmit power (E_s / M_T), power gain of λ_i (i=1,2,3,…r) and N_0 noise power. Now to find the best value of capacity 'C'

let total channel power $\|H\|_F^2 = \sum_{i=1}^{r} \lambda_i = \xi$. Assuming $M_T = M_R = M$; r = M full rank

$$C = \sum_{i=1}^{r=M} \log_2\left(1 + \frac{E_s}{MN_0}.\lambda_i\right)$$

The capacity is maximized subject to the constraint $\sum_{i=1}^{M} \lambda_i = \xi$; $\lambda_i = \lambda_j = \frac{\xi}{M}$ and if H is an orthogonal matrix i.e. $HH^H = H^H H = \frac{\xi}{M} I_M$, so we have

$$C = \sum_{i=1}^{M} \log_2\left(1 + \frac{E_s}{MN_0}.\frac{\xi}{M}\right)$$

Since there is no dependence of any term on sub-index 'i' , therefore $\sum_{i=1}^{M} = M$, hence

$$C = M.\log_2\left(1 + \frac{E_s}{N_0}.\frac{\xi}{M^2}\right)$$

Now if we have $\left\|H_{ij}\right\|^2 = 1$, each element of H have the power of unity; $\|H\|_F^2 = M^2 = \xi$, so we have an expression for the capacity

$$C = M.\log_2\left(1 + \frac{E_s}{N_0}\right) \quad \text{... (4.128)}$$

Thus the capacity of an orthogonal MIMO deterministic channel is 'M' times the capacity of the SISO channel.

2) The CSI is available at the transmitter (Water-filling).

When the transmitter has access to the CSI, by applying the water-filling principle the best possible solution is obtained [8]. If 'P_i' is the power of transmitted symbol on the 'ith' parallel channel, the capacity is given by

$$C = \max_{P:\sum_{j=1}^{r} P_j \leq 1} \sum_{i=1}^{r} \log_2\left(1 + \frac{E_s}{N_0}\lambda_i P_i\right) \quad \text{... (4.129)}$$

The above expression of capacity is true for the independent complex Gaussian inputs.

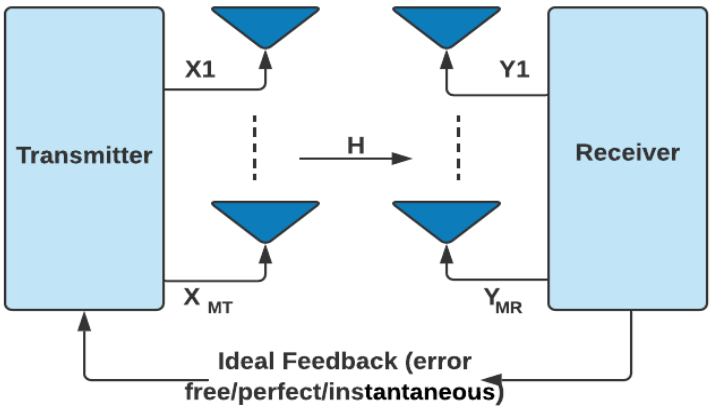

Fig. 4.15 $(M_T \times M_R)$ MIMO System with feedback

This optimization problem gives up the well-accepted solution,

$$P_{i,opt} = \left(\mu - \frac{1}{\frac{E_S}{N_0}\lambda_i}\right)^+,$$

where $(z)^+ = max(z, 0)$ and μ is the solution of

$$\sum_{i=1}^{r}\left(\mu - \frac{1}{\frac{E_s}{N_0}\lambda_i}\right)^+ = 1$$

And the capacity is given by

$$C = \sum_{i=1}^{r}\left(\log_2\left(\mu\frac{E_s}{N_0}\lambda_i\right)\right)^+ \quad \text{... (4.130)}$$

This expression implies that the scheme for providing optimal solution exploits only few of the equivalent parallel channels with optimal SNR. The parallel channels with more SNR or best gain are selected for transmission and hence making beam forming optimal.

4.2.5.3 Capacity of Ergodic MIMO Channels (Shannon Capacity)

The channel coefficients of ergodic MIMO channels are time-varying. When the channel is ergodic, employing a long block code length, all possible channel states are monitored for a long time. For the ergodic channel, the capacity is determined by taking the expected value of the capacity for an AWGN channel. Consider a channel

matrix 'H' which is random but ergodic. Here we assume channel information is available at only the receiver and not at the transmitter, signals are complex Gaussian, equally powered, and independent at the transmitter. Therefore taking an expectation over random matrix 'H', the channel capacity for ergodic MIMO channel

$$C = E\left\{\log_2\left[det\left(I_{M_R} + \frac{E_S}{M_T N_0}.HH^H\right)\right]\right\} \quad \text{... (4.131)}$$

The CSI observed at the receiver is classified according to channel coefficient realizations. The capacity is determined for each realization since inputs are still independent Gaussian. Finally, overall capacity is computed by taking the average of all quantities.

4.2.5.4 Capacity of Non-Ergodic MIMO Channels (Outage Capacity)

For a non-ergodic channel, it is assumed that fading coefficients remain constant over the length of the codeword. Here Shannon capacity of the MIMO system is simply zero since there is a non-zero probability that the shared information between input and output is less than any fixed information rate. So instead of ergodic capacity or Shannon capacity, we should define another type of capacity, which is outage capacity. In this scenario for a low SNR, it is not suggested to allocate power equally among all transmit antennas. Because this may result in that at the receiver end we will not be able to distinguish between real signal and noise. Hence it is suggested that instead of considering all transmit antennas, we should manage all transmit antennas into a smaller subset with independent Gaussian input and high power allocation [98]. Assuming 'k' transmit antennas ($k \leq M_T$) and independent Gaussian input with k/2 variance is used. For a given SNR (ρ) the capacity is a arbitrary variable and it is given by

$$C(\rho) = \log.\det\left(I_{M_R} + \rho H^H R_x(k) H\right) \quad \text{... (4.132)}$$

Where, $R_x(k) = \frac{1}{k}\text{diag}\{1,1,\ldots 1,0,0,\ldots..0\}$

If 'R' is the rate of transmission then,

$$P_{out} = \min_{k=1,2,\ldots.M_T} P\left(\log.\det\left(I_{M_R} + \rho H^H R_x(k) H\right) \leq R\right) \quad \text{... (4.133)}$$

This is the expression for the outage probability in MIMO-OFDM system.

4.3 ALGORITHMS FOR THE SIMULATION OF VARIOUS METHODOLOGIES USING MATLAB

Algorithms with sensitive parameters for capacity enhancement, PAPR, and error rate reduction are depicted in this section. The capacity, PAPR, and error rate results can be extended with various sensitive parameters of the algorithm.

4.3.1 Algorithm for PAPR reduction using SLM scheme

1. Initialize;
   - FFT size (64,128,256,512....etc)
   - Number of selection (4 or 8)
   - Symbol sets and the modulation technique used
   - Number of symbols to be transmitted
2. Different phase sequences are multiplied to input signal.
3. For each signal the OFDM signal is generated.
4. OFDM signal having lowest PAPR is selected
5. Plot PAPR Vs SNR

4.3.2 Algorithm for PAPR reduction using ICF scheme

1. Initialize;
   - OFDM Symbol size (64, 128,256,512.....etc)
   - Interpolation factor (Oversampling factor) L=2,4...
   - Size of FFT=OFDM symbol size×Interpolation factor
   - Clipping Ratio (CR=2,3,4,5...)
   - Number of iterations (3,4,5,6...)
   - Maximum number of symbols to be transmitted
2. Initialize modulation type and the symbol sets
3. Padding OFDM signal (frequency domain) with (L-1) ×N zeros, .
4. Transform OFDM signal into Time domain using IFFT
5. Clip the signal to some threshold value
6. Determine clipping noise which is the difference of original and clipped signal.
7. Transform the noise in frequency domain using FFT
8. Apply filter to remove out of band radiation
9. Compute time domain signal by applying IFFT
10. Determine peak signal power and mean signal power and thus compute PAPR
11. Go back for next iteration to step 5, repeat for the set number of iterations
12. Plot CCDF of PAPR

4.3.3 Algorithm for Ergodic Capacity for MIMO system

1. Initialize;
   - Antenna configurations (Receive diversity schemes: 1×1, 1×2, 1×3, 1×4, 1×5) or (spatial diversity schemes: 1×1, 2×2, 3×3, 3×4, 4×5.....etc)
   - AWGN noise power
   - SNR range
   - Number of iteration in the range of 10^5
2. Assign channel matrix
3. Assign number of antenna elements
4. Assign number of SNR vector elements
5. allocate memory for capacity
6. allocate memory for singular value decomposition
7. Determine SNR for this iteration
8. Calculate transmit power (tx-Power = noise Power×snr）
9. loop over number of iterations
10. generate channel coefficients
11. calculate singular value decomposition SVD
12. store values of lambda in SVD
13. find carrier to noise rations
14. find allocated power based on water filling algorithm
15. Calculate the capacity
16. Plot capacity versus SNR
17. Repeat for next configuration of antennas

4.3.4 Algorithm for error rates using STTC scheme

1. Initialize;
   - Number of iteration for simulation of error rates
   - Choose number of transmit and receive antennas (Tx=2; Tx=2)
   - Range of SNR
2. Identity matrix for Rx = 1 and 2
3. Generate 1st and 2nd parameters for STTC
4. Employ modulation technique
5. Generate random integer data
6. Employ STTC encoding
7. Add AWGN Noise
8. Receive the signal and employ STTC decoder
9. Compute probability of error rates (BER, SER, FER, and PEP)
10. Plot probability of error (Pe) versus SNR

4.3.5 Algorithm for BER of OFDM system at different symbol length over AWGN channel

1. Initialize
   - Symbol length (L= 64,128,256.....1024 etc)
   - FFT size N=L×0.0625
   - Random integer data generation for transmission
   - Range of SNR for simulation of BER
2. Employ modulation type
3. Convert complex serial data into parallel
4. Convert frequency domain signal into time domain using IFFT
5. Convert Parallel signal to series
6. Add Cyclic prefix
7. Transmit the signal in time domain
8. At receiver remove CP and convert signal serial to parallel
9. Employ FFT and covert signal into frequency domain
10. Convert Parallel signal to series
11. Demodulate the signal to obtain original one
12. Compute error rate on received signal
13. Plot BER Vs SNR

4.3.6 Algorithm for BER of MRC scheme with (1×2) and (1×4) antenna configuration

1. Initialize;
   - Frame length (100 to 150)
   - Number of bits/packets (10000 to 100000)
   - Range of SNR in dB
2. Generate random binary sequence
3. Choose number of transmit antenna Tx=1 and Receive antenna Rx=2 or 4
4. Transmit symbols
5. Multiply each symbol with channel coefficient
6. Add AWGN noise
7. Select receiving path
8. Equalize received symbols
9. Using hard decision decoding determine BER
10. Repeat process for multiple values of SNR
11. Plot the BER Vs SNR

4.3.7 Algorithm for BER of receive diversity

1. Initialize;
   - Number of symbols (10000 to 100000)
   - Random integer data generation for transmission
   - Range of SNR for simulation of BER
   - Modulation scheme
   - Choose transmit antenna Tx=1 and receive antenna Rx = 1 to 4
2. Add AWGN Noise
3. Employ equalizing technique
4. Employ hard decision decoding at receiver
5. Compute error rates
6. Repeat for multiple values of SNR
7. Choose different number of receiving antennas
8. Compute BER for each configuration in the same way
9. Plot BER Vs SNR for each configuration providing receive diversity.

4.3.8 Algorithm for BER of Alamouti Space Time Block coding with (2×2) antenna configuration

1. Initialize;
   - Number of symbols or bits (10000 to 100000)
   - SNR range
   - Choose number of receive antennas (Rx 1 or 2)
2. Generate random integers values (0s and 1s)
3. Employ modulation scheme on random sequence of bits
4. Rearrange modulated bits into Alamouti code words
5. Add white Gaussian noise
6. Transmit through Rayleigh fading channel
7. Repeat the same channel for two symbols
8. Receive symbols and apply equalization
9. Using hard decision decoding at receiver decode the code words
10. Compute error rates
11. Repeat for multiple SVR values
12. Plot BER versus SNR

Chapter 5
Results and Discussion

As per discussion in methodology section , here we consider OFDM system with various parameter such as, number of FFT points 64,128 ,,number of subcarriers per resource block 52,cyclic prefix length in samples 16, no of bits per symbol 52, modulation BPSK with 20 MHz ,100 MHz frequency. The said parameters have been used for simulation with MATLAB platform. Simulation parameters is depicted in table no. 5.1

Table 5.1 Simulation parameters for OFDM spectrum at different frequencies

Parameters	**Value**
FFT Size	64 and 128
Subcarriers per resource block	52
Length of Cyclic prefix	16
Symbol size (bits per symbol)	52
Frequency	20 MHz and 100 MHz
Modulation type	BPSK

The figure 5.1 and figure 5.2 depicted OFDM spectrums for 20MHz and 100 MHz respectively the power spectral density limited to -55 to -25 and -75 to -35 respectively. In OFDM, multiple closely spaced orthogonal subcarrier signals with overlapping spectra are transmitted to carry data in parallel. The fast Fourier transform algorithm is adopted to demodulate the input signal; same has been represented by figure 5.3

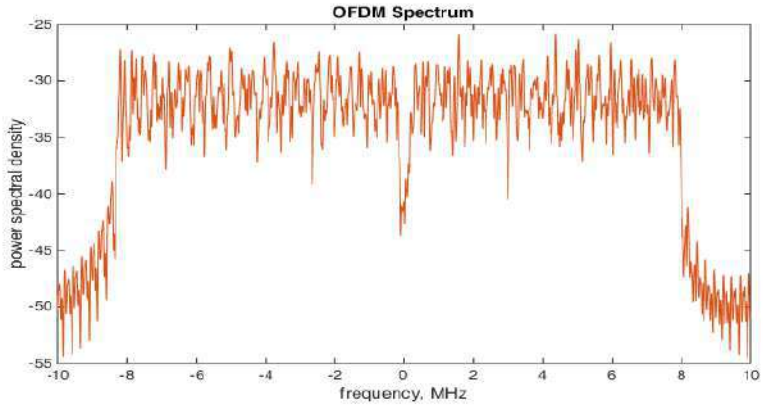

Fig. 5.1 Spectrum of OFDM transmitter at frequency 20MHz

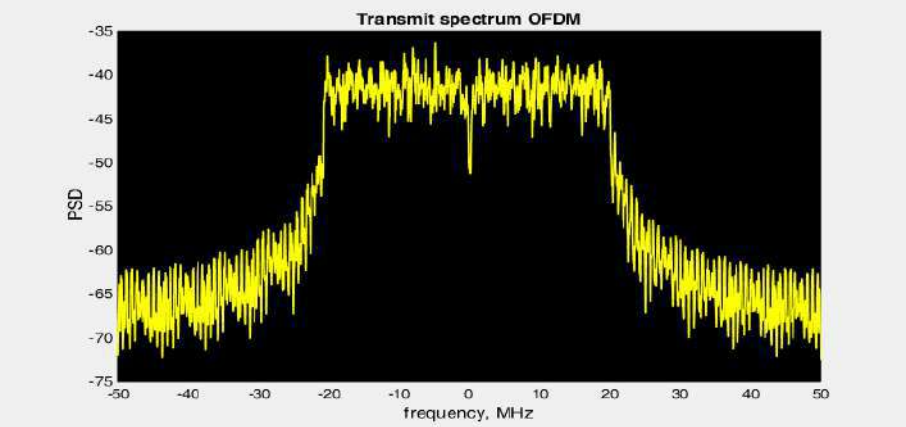

Fig. 5.2 Spectrum of OFDM transmitter at frequency 100MHz

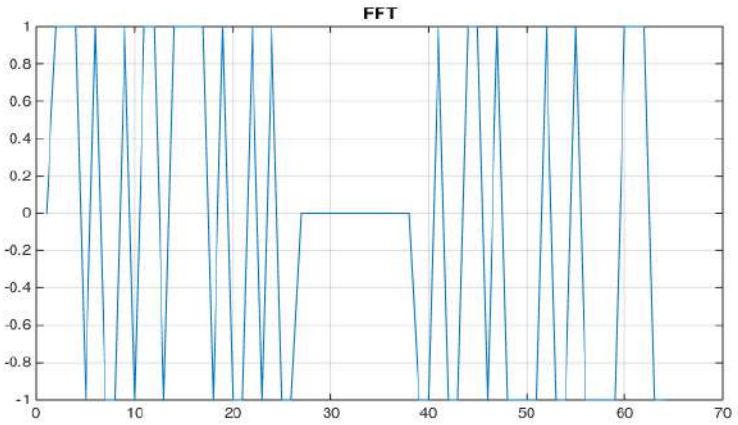

Fig. 5.3 Input FFT signal of OFDM system

Sinusoidal signals of different frequencies, and their discrete Fourier transforms (DFTs) have been represented in figure 5.4. The first five ($x_1, x_2, x_3, x_4,$ and x_5) sinusoidal signals (figure 5.4 LHS) it is clear that their frequencies are integer multiple of fundamental frequency and these five signal are mutually orthogonal to each other. But the first five signals and last two signals (x_6 and x_7) are not mutually orthogonal since the frequencies of last two signals are not multiple of fundamental frequency. It can be also very clear from the DFT of these seven sinusoidal signal (figure 5.4 RHS) that the DFTs for first five signals (for k = 1, 2, 3, 4, 5) are very clear, but for sixth and seventh signal DFTs are not clear due to spectral leakage.

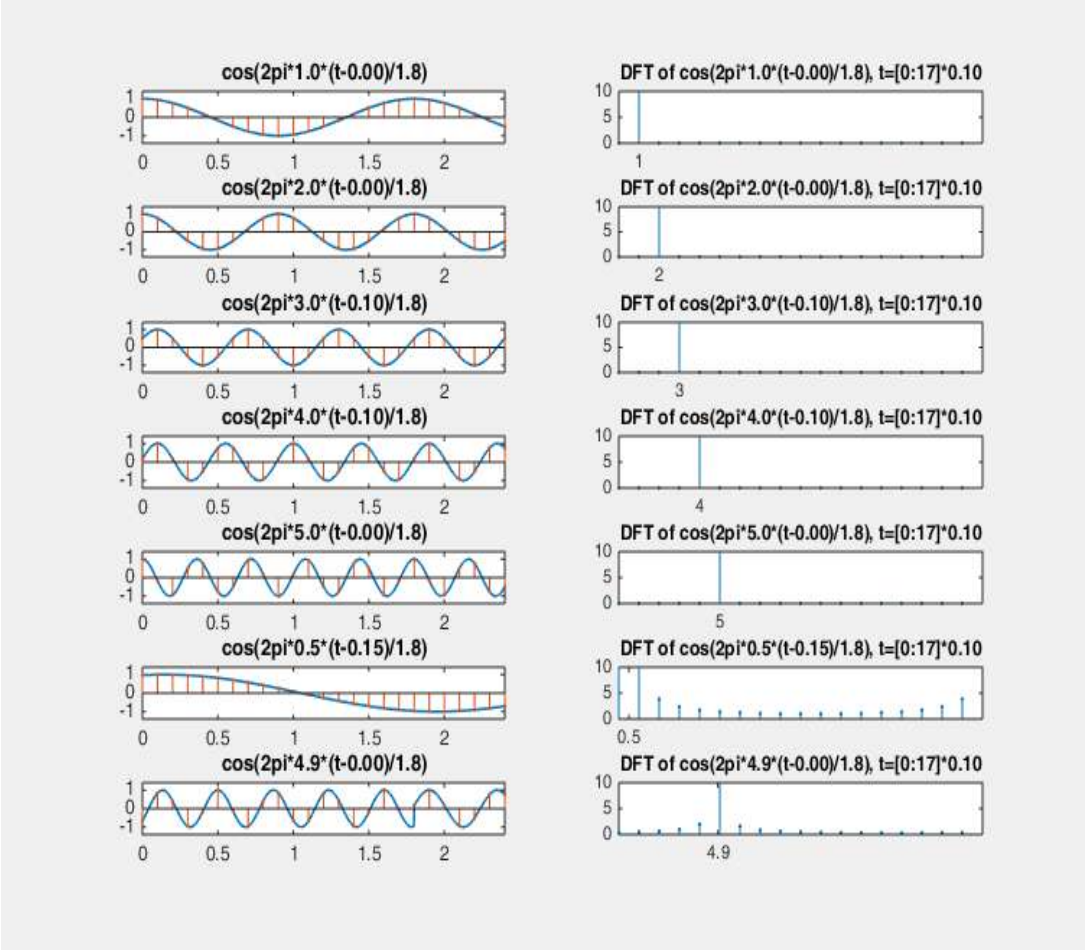

Fig. 5.4 Sinusoidal signals with different frequency and their DFT

5.1 MIMO-OFDM SYSTEMS PERFORMANCE ANALYSIS

5.1.1 Channel Capacity

Shannon Capacity- The channel capacity can be expressed as the maximum mutual information between transmitter and receiver considering the power constraint on the total transmitting power of the source, that is

$$Tr\ (K_C) \leq P \qquad \ldots (5.1)$$

Where;

K_C = Covariance of the input matrix

Tr (K_C) =Trace of a matrix K_C.

P = Transmit power

So, the channel capacity is given by

$$C = \underset{Tr(K_c)\leq Tx}{max}\ log_2\left\{det\left[I_{Rx} + \left(\frac{\gamma}{Tx}\right) H.K_c.H^H\right]\right\} \quad \text{... (5.2)}$$

The unit for capacity of channel is bits/s/Hz indicates that at any channel bandwidth 'W' the maximum rate of transmission is the product of capacity 'C' and band width W bits/s/Hz. In the case of equal number of transmitting and receiving antenna configuration of MIMO system the increase in capacity is almost linear with respect to increase in number of antennas at transmitter and receiver section. It is observed that at high SNR, after 3 dB increase in SNR, the capacity C grows linearly with $\min(\mathrm{M_T}, \mathrm{M_R})$ bits/s, where $\mathrm{M_T}, \mathrm{M_R}$ are number of transmitting and receiving antennas.

Ergodic Capacity- The channel coefficients of ergodic MIMO channels are time-varying. When the channel is ergodic, employing a long block code length, all possible channel states are monitored for a long time. For the ergodic channel, the capacity is obtained by taking the expected value of the capacity of an AWGN channel. Consider a channel matrix 'H' which is random but ergodic. Here we assume channel information is available at only the receiver and not at the transmitter, signals are complex Gaussian, equally powered, and independent at the transmitter. Therefore taking an expectation over random matrix 'H', the channel capacity for ergodic MIMO channel

$$C = E\left\{\log_2\left[det\left(I_{M_R} + \frac{E_S}{M_T N_0}.HH^H\right)\right]\right\} \quad \text{... (5.3)}$$

The channel state information observed at the receiver is classified according to channel coefficient realizations. The capacity is determined for each realization since inputs are still independent Gaussian. Finally, overall capacity is computed by taking the average of all quantities.

Outage capacity- In the case of a non-ergodic channel, it is assumed that fading coefficients remain constant over the length of the codeword. Here Shannon capacity of the MIMO channel is simply zero since there is a non-zero probability that the mutual information between input and output is less than any fixed information rate. So in this case instead of ergodic or Shannon capacity, we should define another

type of capacity, which is outage capacity. For capacity *C*, if the outage capacity is *'C_0'* at the outage probability of *'r_0'*, then

$$P_r\,(C < C_0) = r_0 \qquad \text{... (5.4)}$$

Figure 5.5 and 5.6 represents algorithm/flowchart for the estimation of ergodic and outage capacity respectively.

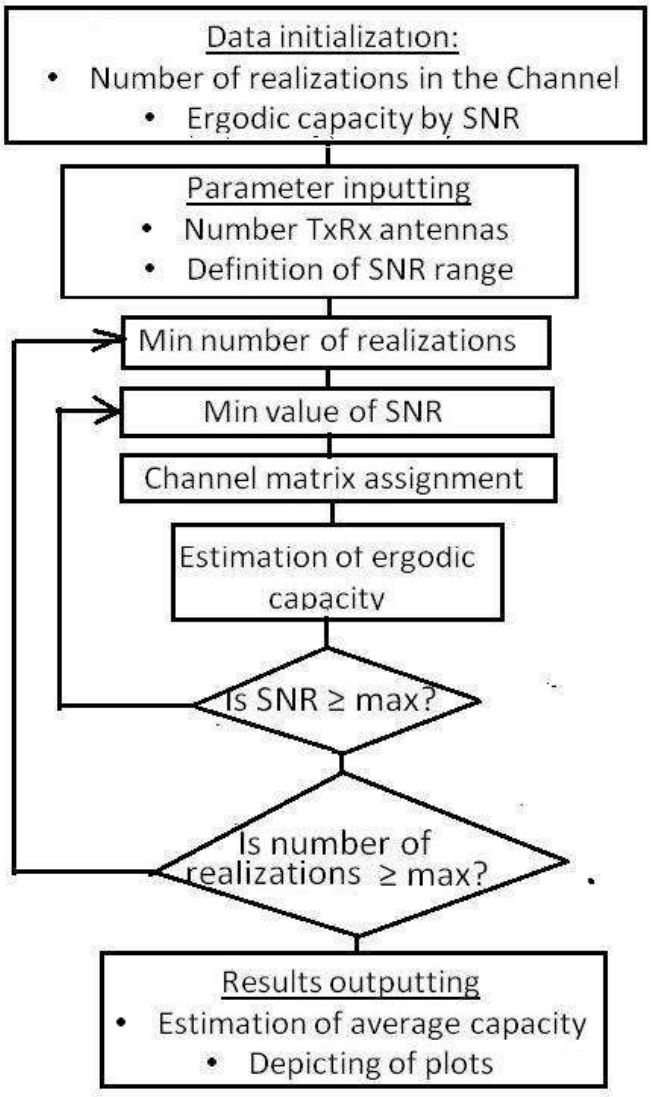

Fig. 5.5 Flowchart for the estimation of ergodic capacity

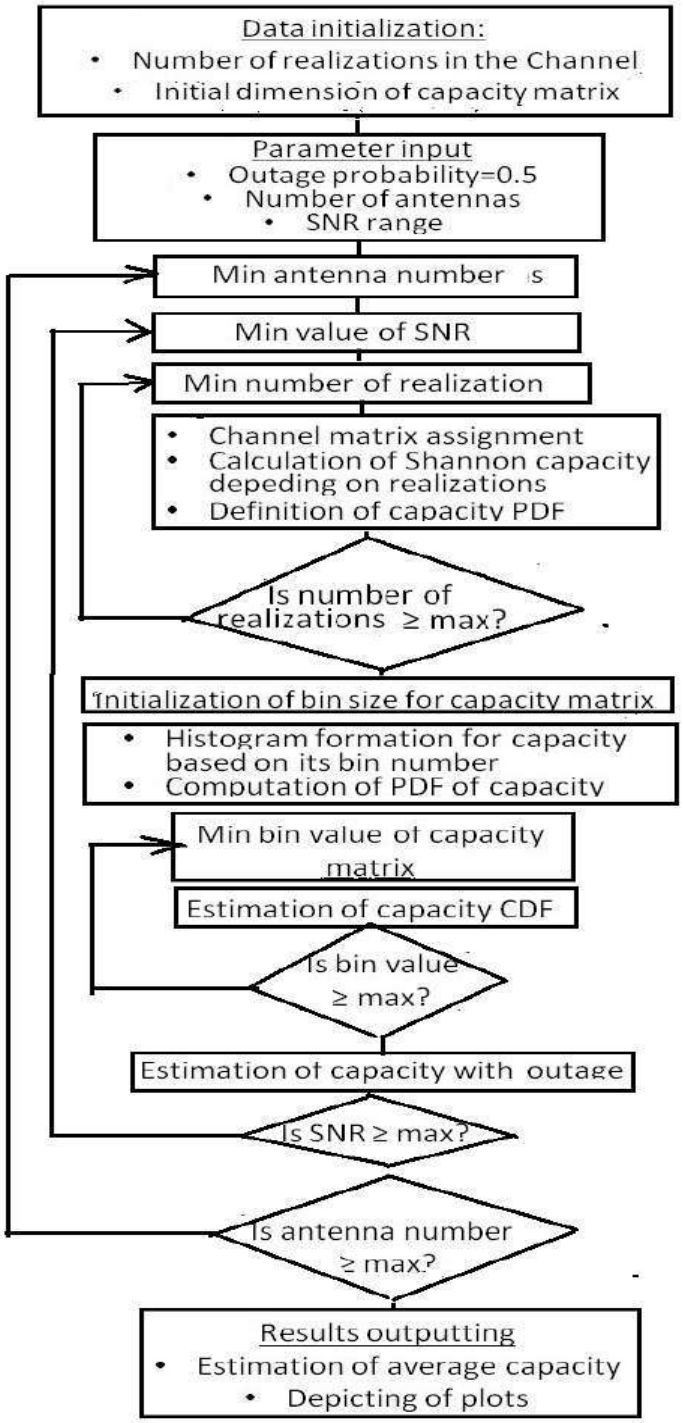

Fig. 5.6 Flowchart for the estimation of outage capacity

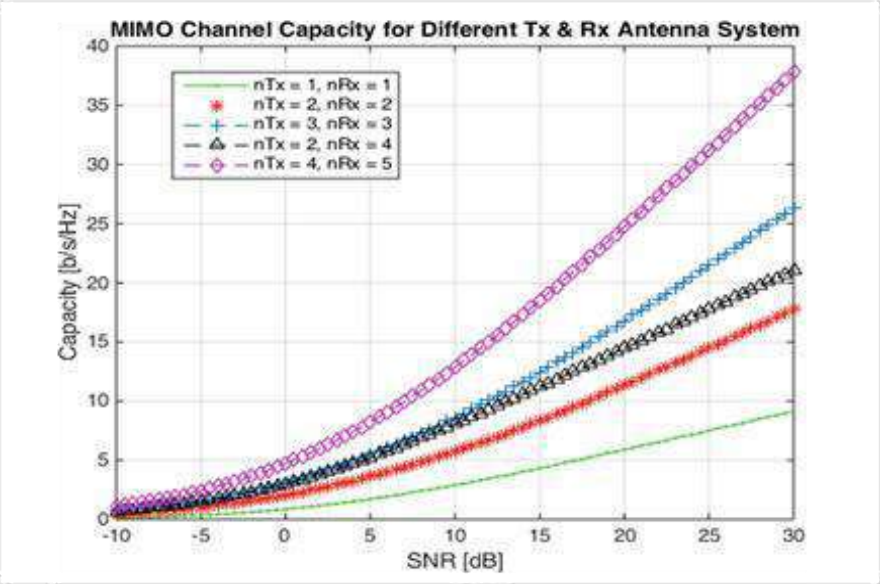

Fig. 5.7 MIMO ergodic channel capacity for different antenna systems

Figure 5.7 shows MIMO channel capacity for different combination of number of transmitting and receiving antennas. It is observed that the statement given in section 5.1.1 that the channel capacity increases linearly with increasing the number of transmitting and receiving antenna is found true. From the fig 5.7, it is seen that after SNR of 20 dB, the increase in capacity is almost linear. At 20 dB SNR the channel capacity for $(M_T \times M_R) = (4 \times 5)$ the capacity is estimated of 24.7 bits/s/Hz. Similarly at 25 dB and 30 dB it is recorded about 31.5 and 37.5 bits/s/Hz respectively. From above capacity values at high SNR the statement "at high SNR, after 3 dB increases in SNR, the capacity grows linearly with $\min(M_T, M_R)$ bits/s," also found true. The estimation of ergodic capacity with different combination of antennas in MIMO system is also depicted clearly in fig 5.8 and table 5.2.

Table 5.2 Estimation of ergodic capacity with different combination of antennas

Sr. No.	No. of Transmit Antennas M_T	No. of Receive Antennas M_R	Capacity Bits/s/Hz		
			SNR =20 dB	SNR =25 dB	SNR =30 dB
1	1	1	5.9	7.6	9.4
2	2	2	11.3	14.5	16.1
3	2	4	14.5	17.8	21.0
4	3	3	16.8	21.5	26.3
5	4	5	24.7	31.5	37.5

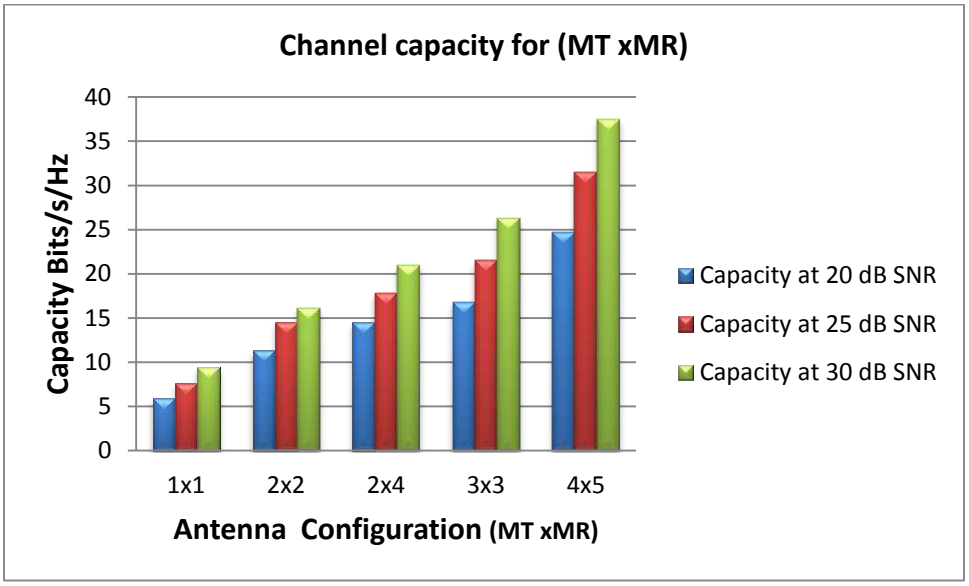

Fig. 5.8 MIMO channel capacity chart for different antenna systems

Figure 5.9 portrays the CDF of the random $(1 \times 1), (2 \times 2), (2 \times 4), (3 \times 3)$ and (4×5) channel capacities without any selection at the SNR of 8 dB in which 10% outage is considered. It is observed that the average probability of capacity for the entire antenna configurations is equal and that are 50%. It is clear from the CDF that data rates increases when the numbers of transmitting and receiving antennas are increases.

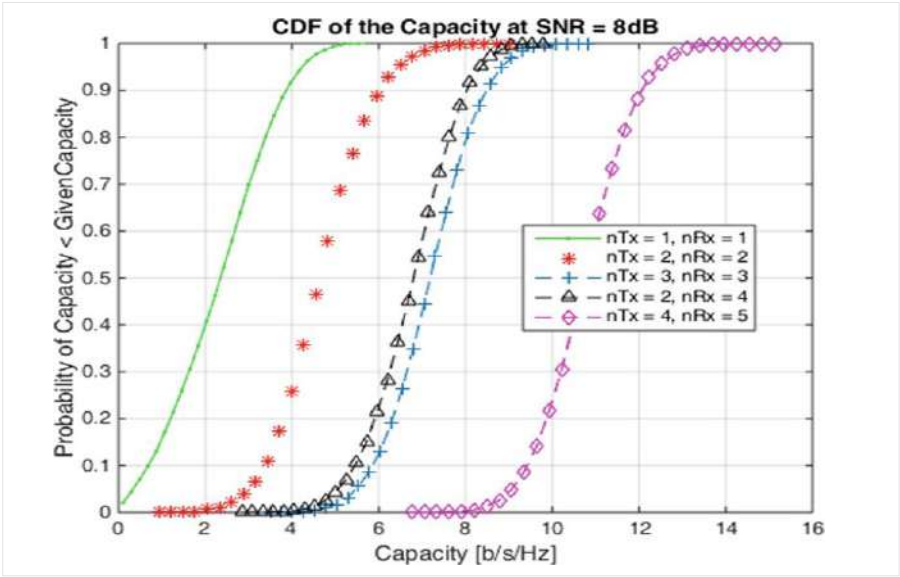

Fig. 5.9 Outage probability at 8dB SNR

90% of the time the channel capacities for $(2 \times 2), (2 \times 4), (3 \times 3)$ and (4×5) random channel at 8 dB SNR are greater than 3.4 Bits/s/Hz, 5.5 Bits/s/Hz, 5.9 Bits/s/Hz and 9.4 Bits/s/Hz respectively.

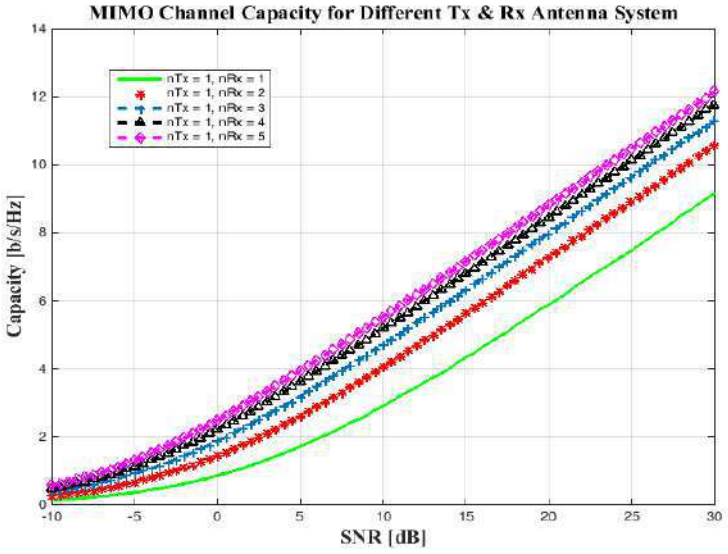

Fig. 5.10 Channel capacity for receiver diversity

Figure 5.10 portrays the channel capacity for receive diversity $(1 \times M_R)$ where one transmit and 1 to 5 receive antennas are used. It is observed from the simulated results that capacity increases with increasing receiving antennas but at slow rate. At 30 dB SNR maximum capacity for(1×5) is 12.16 bits/s/Hz. Also figure 5.11 presents CDF of capacity for the receive diversity at the constant SNR of 5 dB.

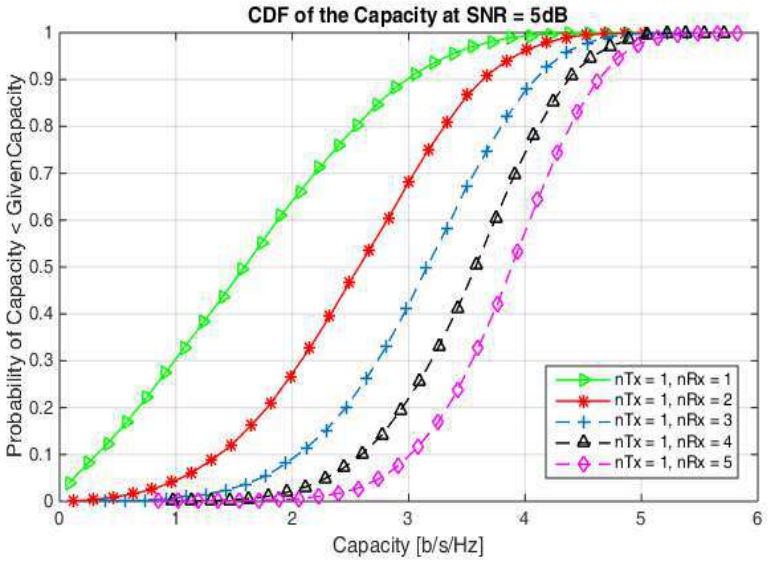

Fig. 5.11 CDF of capacity for receiver diversity at 5dB SNR

5.1.2 PAPR Reduction Scheme Analysis

In this book the iterative clipping and filtering method of PAPR reduction have been proposed. This section deals with the PAPR analysis using ICF method, where its PAPR performance is compared with SLM method of PAPR reduction. The simulation parameter for the same is shown in table 5.3.

5.1.2.1 PAPR analysis using ICF and SLM schemes

The multicarrier OFDM system experiences high 'peak-to-average power ratio (PAPR'), which is the major issue in the OFDM scheme; it causes the breakdown in the orthogonality of OFDM symbols and hence undergo inter carrier interference (ICI).

Table 5.3 Simulation parameter table for PAPR reduction

Parameters	**Value**
Bandwidth (BW)	1 MHz
Oversampling factor (L)	8
Sampling frequency, fs = BW*L	8 MHz
Carrier frequency, fc	2 MHz
Symbol length (K)	128
Cyclic Prefix / GI size	32
Modulation Format	BPSK and QPSK
Clipping Ratio (CR)	1.0, 1.2, 1.4, 1.8, 2, 3 & 4
Clip and filter levels	1 to 6

It is also observed that an attempt to reduce the PAPR causes an increase in BER. Many schemes have been introduces by different researchers for diminishing the PAPR, such as ICF, ICTF, SLM, PTS, Bayesian approach and many more. Still the effect on error rates due to reduction in PAPR is the significant issue in OFDM scheme. In this thesis the conventional ICF techniques is used and its performance in terms of PAPR and BER is analyzed. It is found that the suggested scheme is working better as compared to other schemes.

The figure 5.12 and 5.13 represented the ICF and SLM scheme based result respectively. The basic parameters included in the simulation as, QPSK modulation techniques, size of OFDM symbol K=128, subcarriers N=4 for ICF schemes,

Clipping ratio up to 6.

It is observed from the fig 5.12 that, in case of ICF method upon increasing the clipping and filtering level there is considerable reduction in PAPR. At the beginning up to clipping and filtering level 4, the PAPR is rapidly reduces but after level 5 the PAPR is reduced at the slow rate. In case of SLM technique the simulation is carried out for symbol size K = 64, number of subcarriers N=4 with QPSK modulation scheme. It is found that the PAPR is reduced by 3 dB compared to original signal. The PAPR reduced to 7.8 dB using SLM scheme, whereas in case of ICF method for the clipping and filtering levels 4, 5, and 6, the PAPR is observed as 5.5 dB, 5.1 db and 5.0 dB respectively.

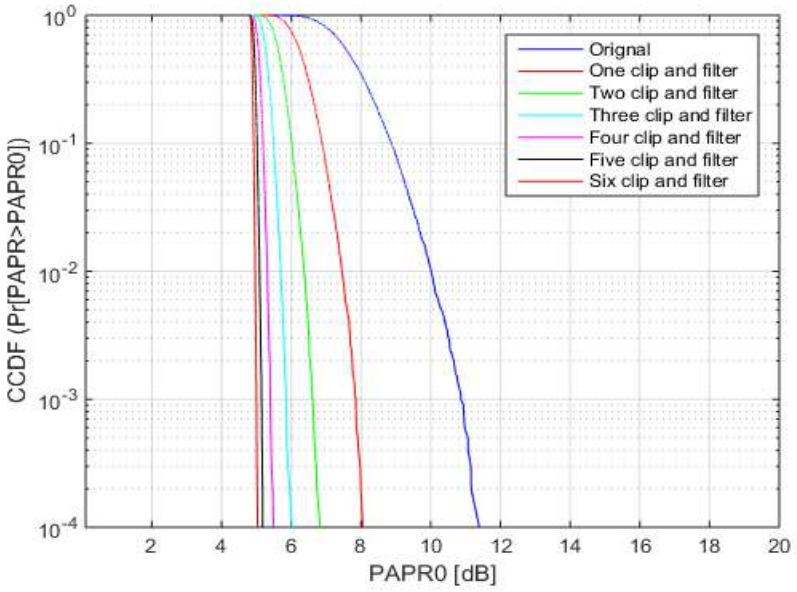

Fig. 5.12 Error performance of clipping and filtering (ICF) method

This means the ICF method outperforms conventional SLM method by PAPR gain of 2.8 dB at the clipping and filtering level of 6. At the CCDF of 10^{-4} the clipping and filtering method with six clips and filter level the PAPR of 5 dB is achieved, where as SLM method achieved PAPR of 7.8 dB. Thus from simulation results it is clear that the proposed ICF technique is more suitable for effectively minimizing the PAPR without affecting BER. Also, maintaining the simplicity of the system. Figure 5.14 indicates the OFDM signal after clipping and filtering.

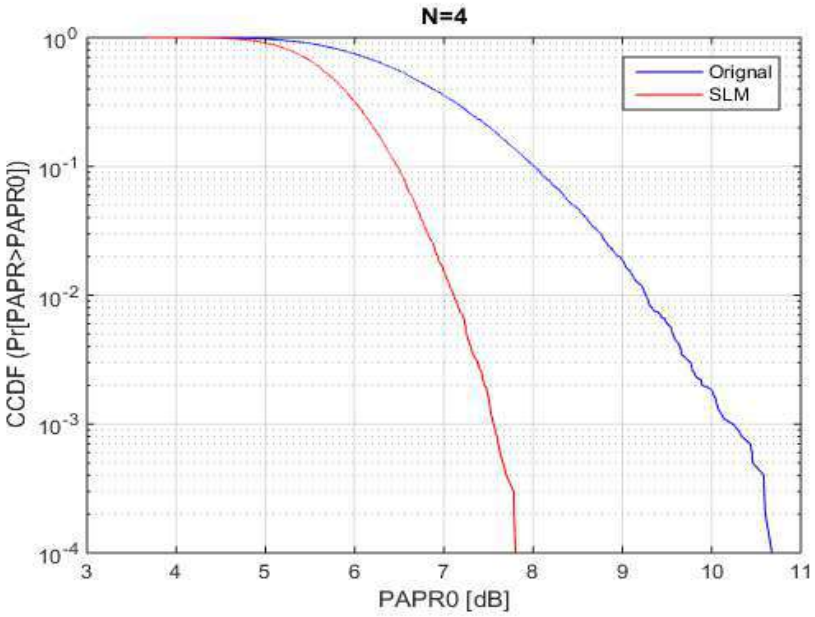

Fig. 5.13 Error performance for Selective Mapping (SLM) scheme

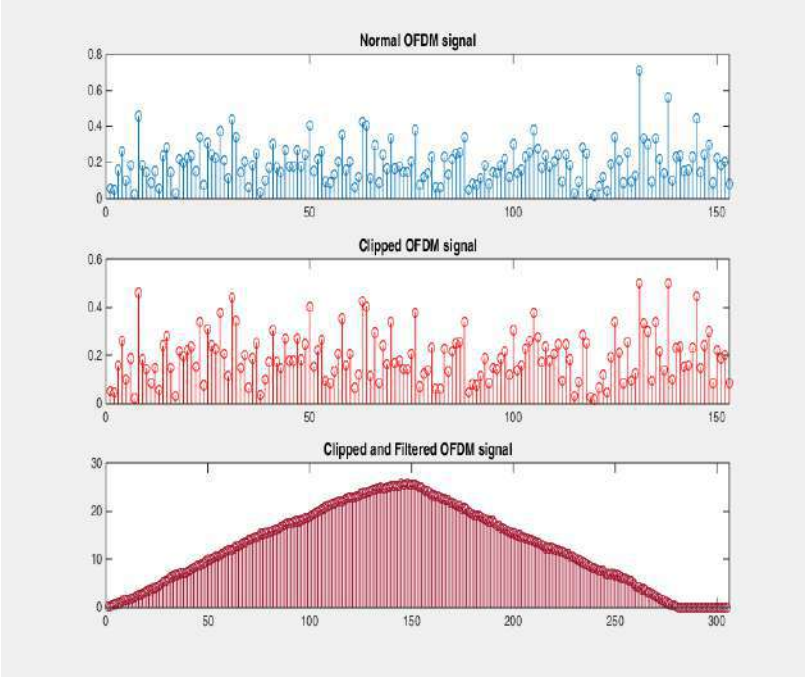

Fig. 5.14 Clipped and filtered OFDM signal

5.1.2.2 Error rate (BER) performance of ICF scheme

The error rate performance of proposed ICF scheme has been presented in figure 5.15 with the OFDM symbol length of K= 128 over sampling factor 8 (L) and different clipped ratio. The simulation parameters have been portrayed in table 5.3.

It is seen from the BER result shown in fig 5.15 that the BER performance is seriously degraded due to clipping compared to unclipped signal. At 12 dB SNR, the BER value for unclipped signal is 3.5×10^{-5}, whereas for clipped signal for clipping ratio (CR) of 1, 1.2, 1.4, 2, 3, and 4 the BER values are 2.4×10^{-2}, 8.7×10^{-3}, 1.5×10^{-2}, 5.7×10^{-3}, 8.7×10^{-3}, and 2.6×10^{-3} respectively. It is seen that for the clipped signal at CR of 4, the BER value of 10^{-3} is achieved at SNR of 15 dB, whereas for the unclipped signal it is achieved at the SNR of 9.8 dB. Thus there is an SNR loss of 5.2 dB using clipping at CR of 4.

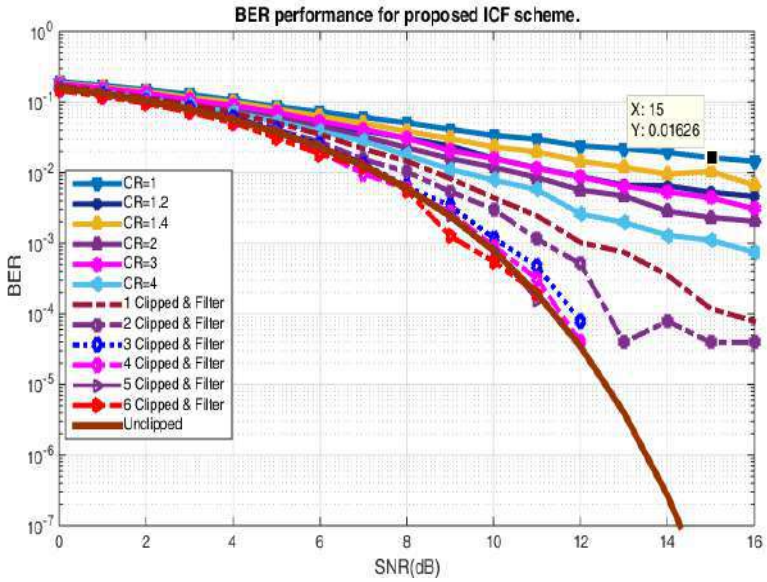

Fig. 5.15 Error performance for different clipped ratio and clipping & filtering levels

The BER values for different clipping ratio at SNR of 10 dB, 12 dB and 15 dB is depicted in table 5.4.

Table 5.4 Comparative error performance for different CR

Symbol length (K)	over sampling factor (L)	Clipped Ratio (CR)	BER Performance (SNR=10dB)	BER Performance (SNR=12dB)	BER Performance (SNR=15dB)
128	8	1	0.033366	0.0239	0.01626
128	8	1.2	0.02323	0.008661	0.05276
128	8	1.4	0.01587	0.01457	0.01039
128	8	2	0.01587	0.005669	0.002323
128	8	3	0.01193	0.008658	0.004409
128	8	4	0.007874	0.002598	0.001102

After applying clipping and filtering (ICF) method the BER is maintained very near to unclipped signal for the clipping and filtering levels of 4, 5, and 6. At 12 dB SNR for the clipping and filtering levels of 4, the BER values is 4.0×10^{-5} ,and for the level of 5 and 6 it is about 3.7×10^{-5} which is very close to that of unclipped signal. Table 5.5 shows the BER performance of clipping and filtering scheme for different clipping and filtering levels from 1 to 6.

Table 5.5 Comparative error performances for different clipping and filtering level

Symbol length (K)	over sampling factor (L)	Clip& filter	BER Performance (SNR=10dB)	BER Performance (SNR=12dB)
128	8	1clip&filter	0.004409	0.001024
128	8	2clip&filter	0.003031	0.0005118
128	8	3clip&filter	0.001181	7.874E-05
128	8	4clip&filter	0.0009055	3.937E-05
128	8	5clip&filter	0.0007827	3.673E-05
128	8	6clip&filter	0.0005512	3.722E-05

5.1.3 Error rate performance of MIMO-OFDM system

Figure 5.16 shows bit error rates (BER) presentation of MIMO-OFDM system for various symbol lengths. The length of symbols varied from L=32 to 512.

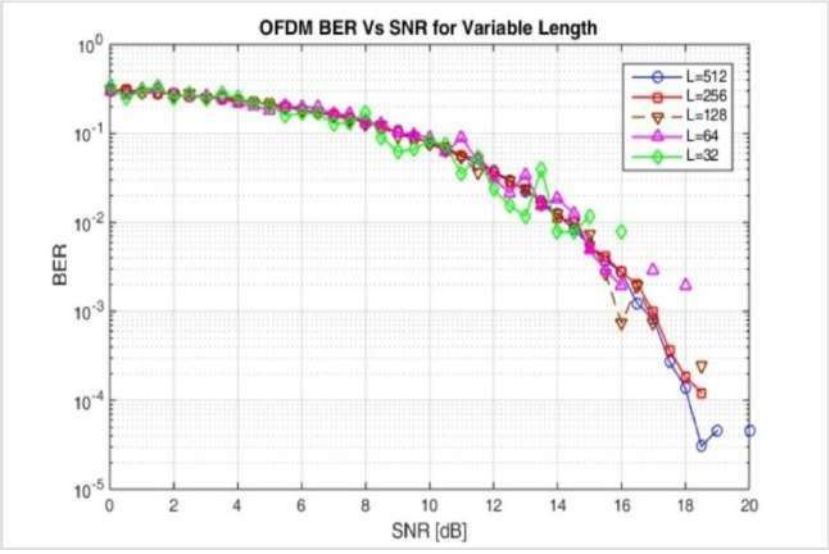

Fig. 5.16 Bit error performance with variable Symbol length

For all the symbol length the BER performance is found similar. After 14 dB of SNR the BER decreases rapidly compared to that of for SNR less than 14 dB at AWGN channel. After 18 dB SNR the BER value is almost less than 10^{-4} for all the symbol lengths.

5.1.3.1 Error rate performance of MRC scheme

MRC scheme at receiver or 'L' multiple antennas at receiver while single antenna at the transmitter. This scheme is also referred to as receive beamforming. The bit error rates for the MRC scheme with 'L' receive antennas is given by

$$\text{Average BER} = \binom{2L-1}{L} \frac{1}{2^L} \left(\frac{1}{SNR}\right)^L \quad \text{... (5.5)}$$

This is the equation for average BER for the MRC schemes with L receive antennas. It is clear from the above equation that the BER value is directly proportional to $\frac{1}{(SNR)^L}$. Thus BER decreases at a faster rate with increasing the number of receive antennas. This has been also proved from the simulation result shown in fig 5.17

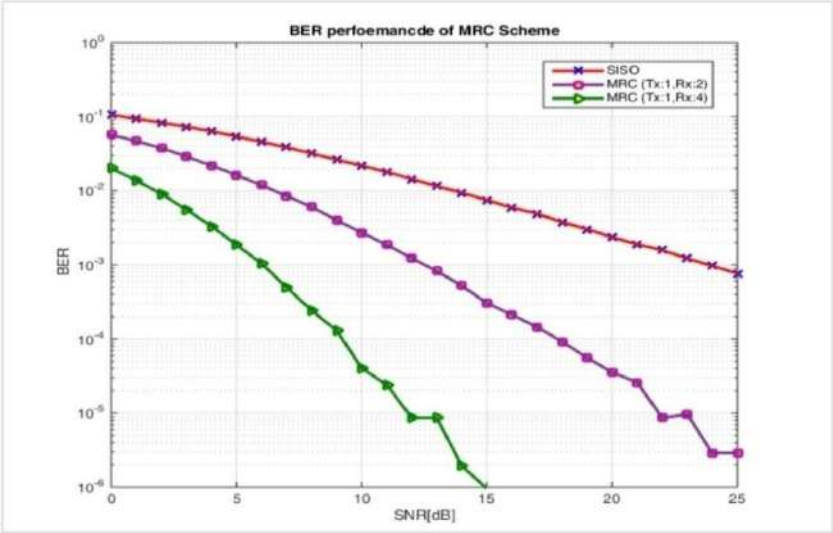

.

Fig. 5.17 Error performance of MRC scheme with (1×2) and (1×4) antenna configuration

Using MRC scheme at the receiver with ($M_T = 1$ and $M_R = 2$) at the 15 dB, 20 dB and 25 dB SNR the BER values are found to be 3×10^{-4}, 3×10^{-5} and 3×10^{-6} respectively. And for the MRC scheme with ($M_T = 1$ and $M_R = 4$), BER values of the order of 10^{-6} is obtained at the SNR of 15 dB only. By doubling the number of receiving antennas SNR gain of 10 dB is achieved.

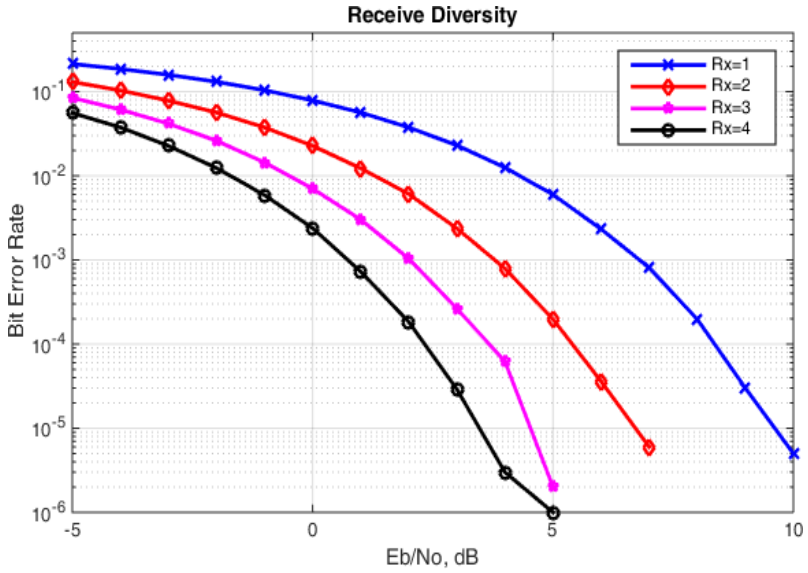

Fig. 5.18 Error performance for receive diversity

Figure 5.18 depicts the BER performance with receive diversity with selection of antenna. For the SISO system without antenna selection gives BER value of 5.0×10^{-6} at 10 dB SNR. By increasing the number of receive antennas (Rx= 2,3,4) the BER performance is significantly improved.

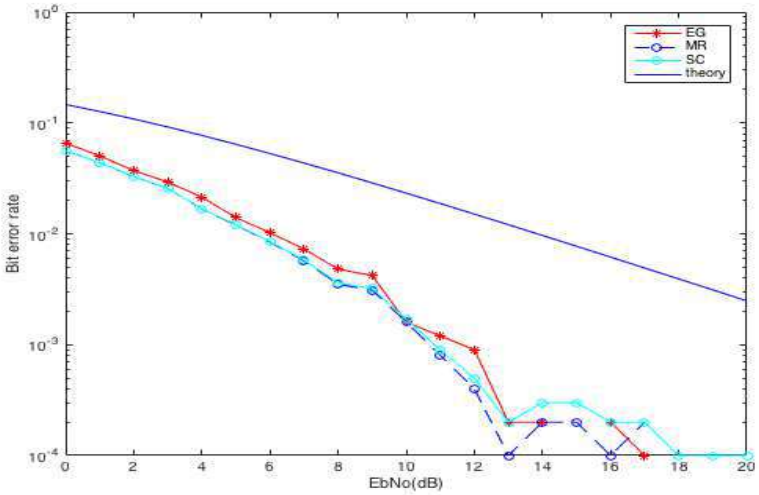

Fig. 5.19 BER Performance for Equal gain, MRC and selection combining scheme

Figure 5.19 represents the BER performance comparison for EGC (Equal gain combing), MRC and SC (selection combining) scheme at 12 dB SNR is depicted in table 5.6. The BER performance for EGC, MRC and SC scheme is 9.0×10^{-4}, 4.0×10^{-4}, and 5.0×10^{-4} respectively.

5.1.3.2 Performance based on space time coded system

Alamouti scheme is transmit diversity scheme with two transmitting antennas and a single receiving antenna. The Alamouti STBC scheme can be used to improve error performance successfully. Figure 5.20 shows the stepwise Alamouti-STBC scheme simulation flowchart.

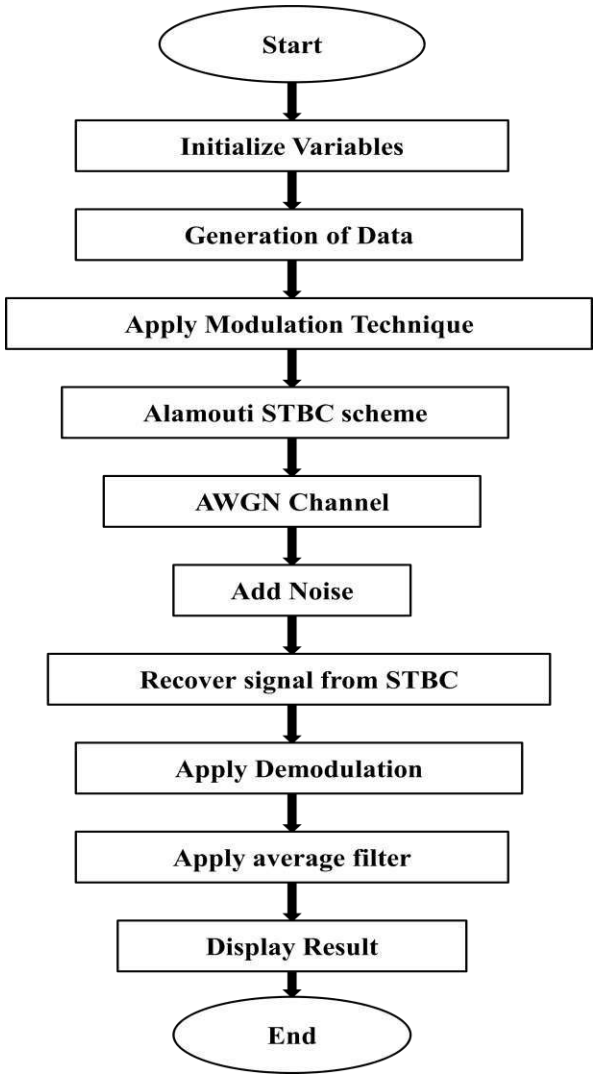

Fig. 5.20 Alamouti STBC simulation flowchart

Figure 5.21 portrays the comparative error presentation for the MIMO-OFDM system using BPSK modulation. The simulation results of MRC scheme with (1×2) and (1×4) is compared with Alamouti-STBC with (2×1) and (2×2) antenna system. From the observation it is clear that, the MRC with (1×4) provide

the best result compared to all others schemes. The comparison of BER performance is given in table 5.7.

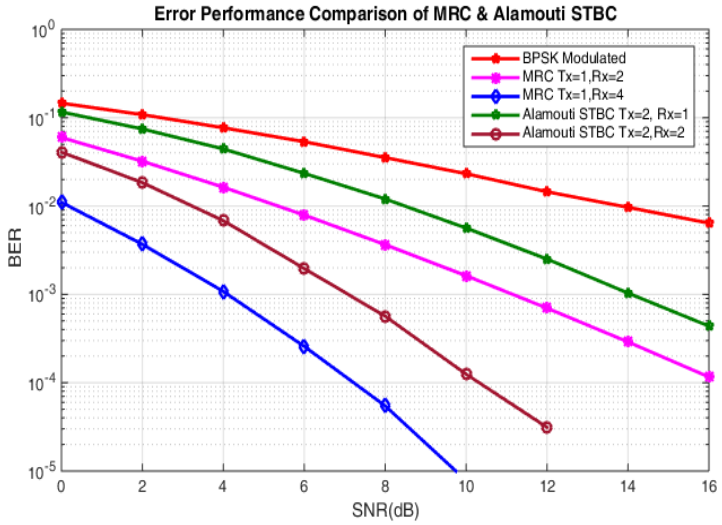

Fig. 5. 21 Error Performance Comparisons of MRC & Alamouti STBC

Figure 5.22 represents the comparative error analysis for the MIMO-OFDM system using BPSK modulation. The simulation results of MRC scheme with (1×4), Alamouti-STBC with (2×2) and STTC scheme with (2×2) antenna system are compared and portrayed in table 5.8. From the fig 5.21 it is found that, the MRC (1×4) gives best BER result compared Alamouti STBC and STTC schemes.

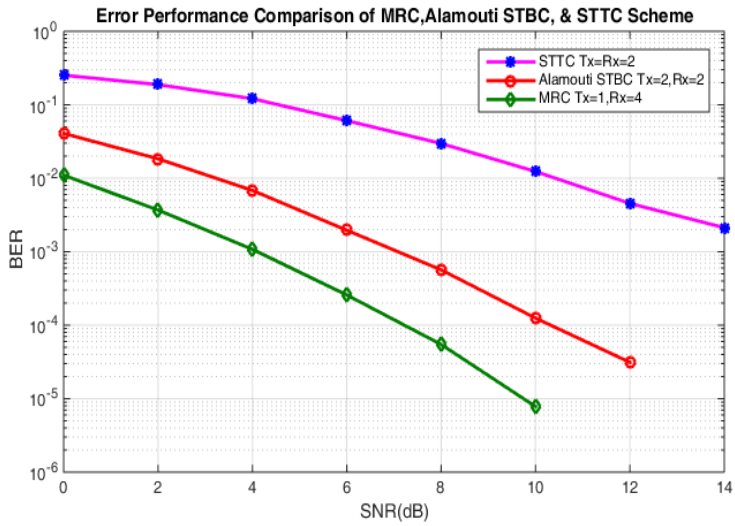

Fig. 5.22 Error Performance Comparison of MRC, Alamouti STBC and STTC scheme

Figure 5.23 represents BER, SER, FER and probability error rate for STTC scheme with (2×2) antenna system. The STBC and STTC schemes are comparable with

respect to spatial diversity for a given number of transmitting and receiving antennas. The STBC provide only diversity gain where as STTC provide coding gain. After analyzing the comparative performance, STTC is found better for both coding as well as spatial diversity gain. Using STTC scheme with (2×2) antenna system, the simulation result for error rates such as BER, SER, FER and PE are depicted in table 5.9. It is clear that STTC offers better coding for spatial diversity but the best error performance is offered by Alamouti STBC coding using the same antenna configuration.

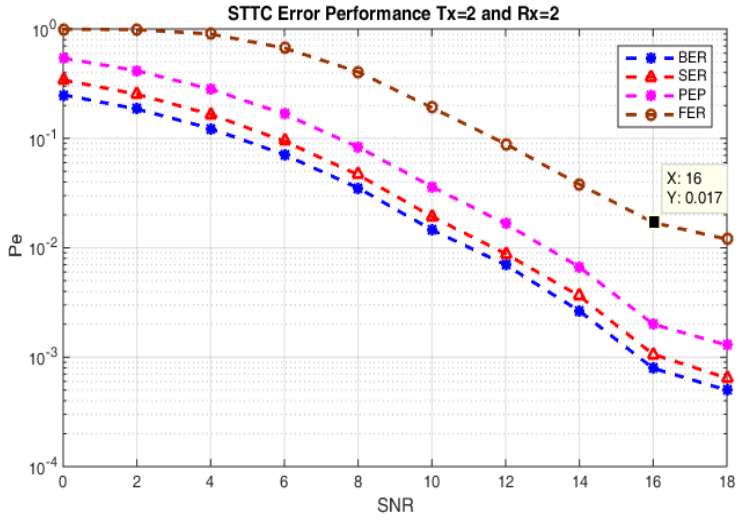

Fig. 5.23 Error performance for STTC with (2×2) antenna system

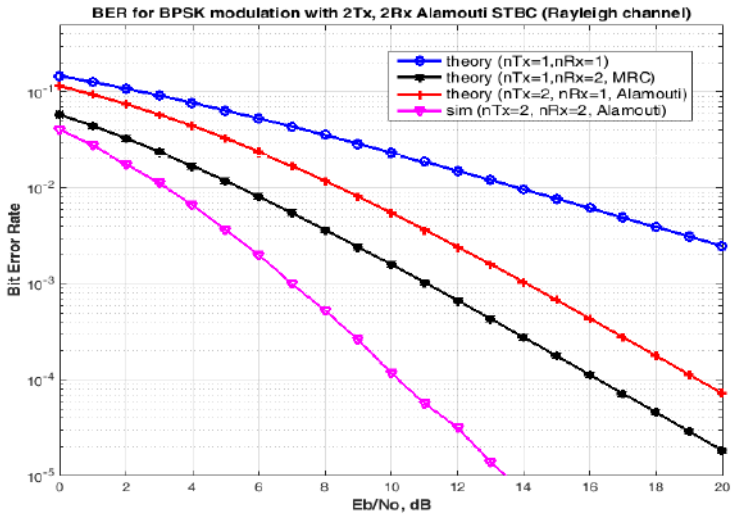

Fig. 5.24 Error performance of AL-STBC 2x2 scheme over Rayleigh fading channel

Figure 5.24 shows error rate of 1.22×10^{-4} for Alamouti-STBC scheme using BPSK modulation, hard decision coding and equalization at receiver, 2×2 antenna system over Rayleigh fading channel.

Table 5.6 BER performance comparison for EG, MRC and SC schemes

Antenna selection schemes	**BER value at SNR=12 dB**
Equal gain combining	9.0×10^{-4}
Maximal ratio combining	4.0×10^{-4}
Selection combining	5.0×10^{-4}

Table 5.7 Comparative error performance of different scheme with antenna selection

Scheme	**Tx**	**Rx**	**BER at SNR=10 dB**	**BER at SNR=12 dB**	**BER at SNR=15 dB**
MRC	1	2	1.7×10^{-3}	6.5×10^{-4}	1.9×10^{-4}
MRC	1	4	7.5×10^{-6}	1.0×10^{-6}	$--$
Al-STBC	2	1	5.6×10^{-3}	2.5×10^{-3}	6.5×10^{-4}
Al-STBC	2	2	1.3×10^{-4}	3.2×10^{-5}	4.0×10^{-6}
SISO	1	1	2.3×10^{-2}	1.3×10^{-2}	7.5×10^{-3}

Table 5.8 Comparative error performance of MRC, Al-STBC and STTC scheme

Scheme	**Tx**	**Rx**	**BER at SNR=10 dB**	**BER at SNR=12 dB**	**BER at SNR=14 dB**
MRC	1	4	7.5×10^{-6}	1.0×10^{-6}	---
Al-STBC	2	2	1.3×10^{-4}	3.2×10^{-5}	---
STTC	2	2	1.23×10^{-2}	4.5×10^{-3}	2.0×10^{-3}

Table 5.9 Error performance for STTC (2×2) antenna system

Scheme	**Error rates**	**BER at SNR=10 dB**	**BER at SNR=12 dB**	**BER at SNR=14 dB**
MIMO-OFDM with STTC coding 2×2	BER	1.6×10^{-2}	7.0×10^{-3}	2.65×10^{-3}
	SER	1.9×10^{-2}	8.5×10^{-3}	3.8×10^{-3}
	FER	1.9×10^{-1}	8.9×10^{-2}	3.9×10^{-2}
	PEP	3.5×10^{-2}	1.7×10^{-2}	6.3×10^{-3}

5.2 COMPARATIVE PERFORMANCE ANALYSIS OF THE SYSTEM

This section deals with the comparative analysis of the proposed system performance with the best performance results from the other schemes used in recent years.

5.2.1 Comparative analysis of MIMO channel capacity

From table 5.10, it is observed that the best performance of capacity in the range of 6.0 to 9.9 bits/s/Hz for IEEE802.11, 3 Gpp, and I-METRA channels is offered by the scheme proposed by Madhusmita Sahoo and Harish Kumar Sahoo (2019). But, this performance is achieved at the cost of a complex DLMS algorithm and STBC diversity code over the AWGN channel. Whereas the proposed MIMO-OFDM scheme for (2×2) antenna configuration without any antenna selection or perfect CSI over AWGN channel offers a significant capacity of 6.2 bits/s/Hz.

Table 5.10 comparative capacity analysis of proposed MIMO-OFDM system

Name of Authors	**Year**	**Scheme detail**	**Antenna Configuration**	**Capacity bits/s/Hz at 10 dB SNR**
Kelvin Anoh et al.	2019	QO-STBC-MIMO; Standard STBC; standard SVD bases detection ; beamforming using 16-QAM constellation; 2 × 1; 4×1 antenna system	2×1	6.2
			4×1	6.8
Madhusmita Sahoo and Harish Kumar Sahoo	2019	MIMO channel; DLMS algorithm; 2 × 2 configuration; 16 QAM, AWGN channel, STBC code diversity	2×2	6.0 to 9.9
Donghun Lee	2018	MRC scheme over imperfect channel estimation; 2 × 1 MIMO system	2×1	3.7 to 4.25
Lopamudra Kundu and Brian L. Hughes	2017	Broadband MIMO-OFDM systems; antenna configurations 2 ×2 and 4 ×4; No. of subcarriers= 64	2×2	4.5 to 5.0
			4×4	7 to 8
Capacity bits/s/Hz of proposed MIMO-OFDM system		MIMO ergodic channel capacity, without antenna selection, imperfect CSI, water-filling algorithm, SNR range of -10 dB to 30 dB; over AWGN channel.	2×2	6.2
			3×3	8.2
			2×4	8.2
			4×5	13

With (3×3) or (2×4) the proposed system offers the capacity of 8.2 bits/s/Hz which is very good and satisfactory since the system is less complex and doesn't need any complex optimization algorithm. Similarly, with the antenna configuration (4×5) the proposed system gives the capacity of 13 bits/s/Hz which is the highest in the table.

5.2.2 Comparative PAPR performance analysis of OFDM system

Table 5.11 comparative PAPR performance analysis of proposed OFDM system

Name of Authors	**Year**	**Scheme detail**	**At 10 dB SNR**	
			PAPR	**BER**
Zhitong Xing. et al.	2020	A low complexity companding schemes; AWGN channel; QPSK modulation	3.4 to 5.1 dB	1×10^{-4} and 4×10^{-4}
Bo Tang et al.	2020	ICF method with ENC scheme, 256 subcarriers , 16 QAM modulation; oversampling factor =4; clipping ratio 1.5 to 1.8; clipping level 3;	4.25 to 5.4 dB	7×10^{-3} and 4×10^{-3}
Ahmad M. Rateb and Mohamed Labana	2019	SLM, PTS and ICF for PAPR reduction are analyzed over AWGN channel, 16-QAM and 64-QAM modulations , and 1024 subcarriers	SLM = 9.8 dB , PTS = 8.3 dB, ICF = 7.2dB	NA
Kee-Hoon Kim	2019	OFDM-IM scheme; ICF; Modulation 16-QAM; clipping ratio 5; iteration=2; subcarrier N=128; length of sub-block = 4; Number of active subcarriers k= 2	6.7 dB	7×10^{-2}
Bo Tang	2019	Clipping-noise compression technique with μ-law algorithm; Number of subcarriers 256; modulation = 16 QAM; over sampling factor =4; Number of iteration =3 ; clipping ratio = 3 & 6, ICF Method	4.8 & 7.1 dB	3.8×10^{-2} and 2.8×10^{-3}
Kelvin Anoh et al.	2017-1	Clipping and filtering (ICF) method; AWGN channel, QPSK modulation, 128 samples, 512 subcarriers, No CP, without optimization, 3 clip	4.5 dB	9×10^{-2}
	2017-2	Root-based μ -law companding (RMC) method; Number of subcarriers 512; symbols =128, QPSK modulation, oversampling factor=4; μ=30;	3.2 dB	1.2×10^{-2}
Proposed method of PAPR reduction		ICF scheme , QPSK modulation , size of OFDM symbol K=128, FFT size 256, interpolation factor 2, active subcarriers N=4 , CR=3 or 4 and Clipping level 6	ICF = 5 dB	2.6×10^{-3} to 5.5×10^{-4}

From the above table, 5.11 it is seen that the proposed system reduces the PAPR up to 5 dB and it is 1.8 dB greater than the PAPR performance offered by the Root-based μ -law companding (RMC) scheme suggested by Kelvin Anoh et al. (2017). But the proposed system maintains the BER performance at a satisfactory level of 5.5×10^{-4} compared to the scheme suggested by Kelvin Anoh where BER is 1.2×10^{-2}. So the proposed system performs better than all the schemes listed in table 5.11.

5.2.3 Comparative error rate performance analysis of MIMO-OFDM system

a) BER performance for various modulation techniques and various selection combining schemes as depicted in table 5.12 (a).
b) BER performance for STBC coded schemes (Alamouti-STBC), MRC scheme, and Receiver diversity scheme as depicted in table 5.12 (b).

From table 5.12 (a) and (b), it is observed that many schemes suggested by different authors have achieved BER level from 10^{-4} to 10^{-6}. The proposed schemes such as the MRC scheme with (1×4), Alamouti STBC with (2×2), and Receiver diversity with Rx = 2,3,4 antennas provide better error rate performance compared to other schemes introduced in table 5.12 (a) and (b). The MRC scheme with (1×4) achieves BER value of 7.5×10^{-6}, AL-STBC (2×2) provide BER value of $1.3 \times 10^{-4}$and the receiver diversity scheme achieves the BER value between $10^{-6}$and 10^{-7}. This means the proposed scheme provides the error rate performance compatible or even better than different schemes suggested earlier. It is also observed that when the Alamouti STBC scheme with (2×2) over Rayleigh fading channel using with hard decision coding and equalization at receiver is simulated, the error rate result found similar as in case of AWGN channel that is 1.22×10^{-4} at 10 dB SNR.

Table 5.12 (a) comparative error rate performance analysis of proposed system

Name of Authors	**Year**	**Scheme detail**		Error Rates
				At SNR=10 dB
Gopika Jayan and Aswathy K. Nair	2018	F-OFDM; BPSK modulation; 50 resource blocks.	BPSK	4.0×10^{-6}
Shendi Wang et al.	2017	PCC -OFDM and UFMC techniques; Rayleigh fading channel; BPSK, QPSK modulation, AWGN channel	BPSK	5.0×10^{-6}
			QPSK	4.0×10^{-5}
Mohammed El-Abasi et al.	2015	MIMO-OFDM-IA with antenna selection; CP length 16; the number of subcarriers 64; users 03 and 3×2 antenna system; Per-subcarrier antenna selection scheme at max-sum-rate and max-SNR.	Max Sum-rate	1.5×10^{-4}
			Max SNR	7.5×10^{-5}
Shital N. Raut, Rajesh M. Jalnekar	2019	Hybrid optimization technique, the Dolphin-Rider-Optimization (DRO), STBC-MIMO-OFDM scheme; over the Rayleigh channel; using BPSK, QPSK, and QAM modulation.	BER	2.5×10^{-5}
			SER	6.0×10^{-6}
Sudhir Kumar Mishra and Kishor Damodar Kulat	2018	reduced feedback rate scheme for transmit antenna selection (TAS) scheme; BPSK modulation scheme; BER is analyzed for a different set of transmit antennas Nt = 3, 6	BPSK	1.25×10^{-3} to 5.0×10^{-5}
N. C. Beaulieu and Yixing Zhang	2017	Different combining schemes (SC , EGC, MRC) with unequal power dual branch, over Nakagami-m where m=0.5, BPSK modulation	SC	5.5×10^{-2}
			EGC	5.5×10^{-2}
			MRC	4.5×10^{-2}
Proposed methods of BER reduction		MIMO OFDM system, over AWGN channel, BPSK modulation, 1×2 antenna system for MRC, EG and SC with unequal power dual branch.	SC	1.7×10^{-3}
			EGC	1.7×10^{-3}
			MRC	1.7×10^{-3}

Table 5.12 (b) comparative error rate performance analysis of proposed system

Name of Authors	**Year**	**Scheme detail**			**Error Rates**
					At SNR=10 dB
Lixia Xiao et a	2017	The STBC MIMO DSM (differential spatial modulation) scheme; BPSK, QPSK, modulation and with 4×2	BPSK		7.8×10^{-3}
			QPSK		8.0×10^{-4}
Siavash M. Alamouti	1998	Alamouti scheme with 2×1 and 2×2 antenna configuration; BPSK modulation over Rayleigh fading channel.	Alamouti (2×1)		1.0×10^{-5}
			Alamouti (2×2)		1.3×10^{-4}
			MRRC (1×2)		1.9×10^{-3}
			MRRC (1×4)		6.0×10^{-3}
S Nandi and A Nandi	2017	Alamouti STBC coded MIMO-OFDM system. BPSK, QPSK modulation, MRC and Alamouti scheme presented	BPSK		5.0×10^{-5}
			QPSK		2.0×10^{-4}
			MRC (1×2)		5.5×10^{-3}
			Alamouti (2×1) and (2×2)		1.75×10^{-3} and 1.0×10^{-4}
Thien Van Luong and Youngwook Ko	2018	The OFDM-IM with MRC and greedy detector BPSK and QPSK modulation; 1×2, 1×4; BPSK modulation, 2 Subcarriers and 1 active subcarrier, and QPSK modulation, 4 Subcarriers, and 2 active subcarriers, Imperfect CSI.	BPSK		6.0×10^{-3} and 6.0×10^{-5}
			QPSK		1.8×10^{-2} and 6.0×10^{-4}
			IEP for QPSK with perfect CSI		2.5×10^{-2} and 2.5×10^{-4}
Ms. Manisha Misra et al	2017	EGC and MRC (1x4) over AWGN and (1×3) over Rayleigh channel schemes for the improvement in BER in MIMO-OFDM system; for N=10000 subcarriers, channel taps L = 4, number of transmit antennas = 8	MRC (AWGN)		1.6×10^{-3}
			MRC (Rayleigh)		1.4×10^{-4}
			EGC (AWGN)		1.2×10^{-3}
			EGC (Rayleigh)		2.0×10^{-4}
Proposed methods of BER reduction		STBC coded MIMO OFDM system, AWGN channel, BPSK modulation , frame length 100, MRC scheme with (1×2) and (1×4), Alamouti STBC with (2×1) and (2×2), Receiver diversity with Rx = 2,3,4 antennas. AL-STBC (2×2) over Rayleigh fading channel with hard decision coding and equalization at receiver. STTC coded MIMO system with (2×2), QPSK modulation over AWGN channel.	MRC (1×2)		2.8×10^{-3}
			MRC (1×4)		7.5×10^{-6}
			Rx = 2, 3 and 4		About 10^{-7}
			AL-STBC(2×1)		5.6×10^{-3}
			AL-STBC(2×2)		1.3×10^{-4}
			AL-STBC(2×2) Rayleigh fading		1.22×10^{-4}
			STTC (2×2)	BER	1.6×10^{-2}
				SER	1.9×10^{-2}
				FER	1.9×10^{-1}
				PEP	3.5×10^{-2}

Chapter 6
Conclusion and future scope

6.1 CONCLUSION

The combination of MIMO with OFDM schemes found the best suitable solution for the current as well as a future communication system. This merger has proven powerful against frequency selective fading effects and is capable of the most reliable wireless communication. It is observed from the simulation results that a significant increase in capacity can be achieved by increasing the number of antennas in the MIMO system. An increase in the number of antennas at both ends results in a remarkable increment in outage capacity at any SNR value. However, an increasing number of antennas is not an acceptable solution always, since the overall cost of the system increases due to the requirement of separate RF chains for each antenna. But this issue can be eliminated by using higher carrier frequencies. In this research work, without any antenna selection and channel state information over the AWGN channel, the ergodic capacity has been analyzed and results have been compared with the capacity results from other schemes. It is found that the proposed system with 3x3 gives better results of channel capacity. This scheme doesn't require channel state information and complex algorithms hence reduces the computational complexity and the system cost. A capacity gain of 2 bits/s/Hz has been achieved using the system with a 3×3 antenna configuration compared to the system with a 2×2 antenna configuration. Adding one more antenna at both terminals for achieving the capacity gain of 2 bits/s/Hz is not a big issue. Hence it is better to employ a MIMO system with a 3×3 antenna configuration is desirable.

It is seen that over an AWGN channel the error rate rapidly decreases upon increasing the SNR. However, an increase in SNR needs to increase in signal power of the signal to be transmitted and due to power constraints in battery-operated devices, it is unenviable. Thus it is desirable to employ different schemes and technologies for the improvement in error rates. Using space-time codes like STBC,

STTC, and Alamouti STBC better error rate performance can be achieved. In the proposed MIMO-OFDM system the Alamouti-STBC scheme with (2×1) and (2×2) antenna system was used and analyzed and it is found that this scheme working satisfactorily. It is found that BER is improved in the range of 10^{-3} to 10^{-4} at the SNR of 10 dB. From the simulation result of the AIamouti STBC scheme, it is clear that if the BER is tested over a greater value of SNR up to 20 dB then the BER will be definitely improved up to 10^{-5} to 10^{-6}. The antenna selection and combining schemes like EGC, MRC, SC are also available for improving error rates. Among these schemes, the MRC schemes and receive diversity schemes are doing better and it is also proven from the simulation results. From the simulation results, it has been confirmed that at 10 dB SNR itself the error rates reduce between 10^{-6} to 10^{-7}. Hence it can be concluded that the MRC scheme can be employed to achieve better SNR gain compared to other schemes but at the cost of an increase in receive antennas. Since the MRC scheme with (1×2) performs similar to the Alamouti scheme with (2×1) antenna system. It is observed that the MRC scheme offers the best error rate performance when the number of receiving antennas is more than 3. In this situation, however, there is no issue with the unlinking but in the case of downlink, because of the size and power constraint in handheld devices like cellular phones may face problems. In this situation the Alamouti STBC scheme with (2×2) antenna system will be the best suitable scheme for the improvement of error rates in MIMO-OFDM system. The presence of high PAPR in an OFDM system is a serious issue since it leads to failure of orthogonality and it results in inter-carrier interference (ICI) that affects the quality of services of the communication system. Maintaining orthogonality in OFDM is also important to avoid inter-symbol interference (ISI), however, ISI can be avoided by inserting a cyclic prefix in the OFDM symbol. But the presence of cyclic prefixes may affect the data rates. So it is enviable to reduce the PAPR in the OFDM system. Many schemes and algorithms have been used for this purpose. In this book, ICF and SLM schemes have been tested / analyzed and the results have been compared with the results from other available techniques. From the comparative results, it has been observed that the proposed ICF scheme not only significantly reduces the PAPR but also keeps the

error rates BER at the desired level which is highly recommended for secured wireless communication and to maintain the quality of signal transmission.

From the above discussion, it has been concluded that to get worthy outcomes from the wireless communication system, the Alamouti STBC coded MIMO system with 2×2 antenna configuration can be concatenated with the ICF algorithm incorporated OFDM system. Here we get the satisfactory capacity of 6.2 bits/s/Hz, which will be definitely increased with increasing the SNR (e.g. at 20 dB SNR capacity is recorded around 12 bits/s/Hz, nearly double). Similarly, the error rates for this suggested system is found to be 10^{-5} at 14 dB SNR, which may reduce further with an increase in SNR (e.g. at 20 dB SNR it may reduce up to10^{-7} . The ICF algorithm for reducing PAPR will work efficiently without significantly increasing the BER. With 4 clip and filter and clipping ratio of 4, the ICF method reduces PAPR to 5.5 dB at the CCDF of 10^{-4} and the BER value at 20 dB SNR has been recorded 10^{-4} which is satisfactory. Thus the MIMO-OFDM-based wireless communication system incorporated with 2×2 antenna configuration, Alamouti STBC coding, and ICF algorithm is the best suitable and trustworthy wireless technology to meet today's requirement.

6.2 FUTURE SCOPE

Wireless communication technology has emerged as one of the finest technology for the transmission of digital data or information wirelessly around the world. Today wireless communication is not only the mean of communication between the peoples but also between things, machines, organizations, and countries all over the world. Now the data security and the speed of transmission are remarkable at the end of 4G and the beginning of 5G. Before the advancement in wireless technology, the only measure of any country whether it is an advanced country or backward was based on their GDP, but nowadays it is measured on the speed of the internet and the amount of spectrum the country has access to. Engineers are working on 5G technology for the worldwide deployment of the 5G network. Very few countries have deployed 5G and trying to achieve perfection. The infrastructure requirement for 5G deployments is the main issue in front of developing nations. They are trying their best the deploy

5G so that each and every device can be connected wirelessly through the 5G network.

There is a huge demand for high-speed networks, trustworthy data transmission because of tremendous growth in users and applications and incessant growth in data traffic. There is a need for more research and development to fulfill the aspect of the 5G network. There is a strong need for internet speed over tens of gigabytes and the response time in microseconds. Now the question arises, whether the 5G network fulfills this requirement? If yes, then at which spectrum? Which standard do the makers have to follow? Will the network fulfill the power constraint? and many more. So, rigorous research is required in this direction.

Intelligent Antenna systems are the important and thrust area of research in wireless technology. The smart antenna systems are not only responsible for secured communication but also efficient for using the spectrum intelligently and to keep the cost of utilization minimum. So, there is scope of more research in this area.

Multiuser (MU) MIMO-OFDM system is an important aspect of the 5G network. The maximum utilization of the capacity of the network is possible using the MU MIMO system by scheduling more users simultaneously through the same channel. This becomes possible due to the spatial degree of freedom provided by the MIMO system. To take the advantage of MU MIMO-OFDM system, there is a strong need for additional compatible hardware including more smart antennas and supporting elements. Also, there is a requirement for perfect channel state information for optimum use of the available spectrum. So, this area also can be viewed as an attractive area of research. The proposed research work can be extended in this direction.

References

1. *Alamri, M. A. (2018). An efficient cooperative technique for power-constrained multiuser wireless network. Telecommunication Systems, 69(3), 263-271.*
2. *Czylwik, A. (1997, May). Comparison between adaptive OFDM and single carrier modulation with frequency domain equalization. In 1997 IEEE 47th Vehicular Technology Conference. Technology in Motion (Vol. 2, pp. 865-869). IEEE.*
3. *Khan, U., Baig, S., & Mughal, M. J. (2009, October). Performance comparison of Single Carrier Modulation with frequency domain equalization an OFDM for wireless communications. In 2009 International Conference on Emerging Technologies (pp. 297-300). IEEE.*
4. *Marchetti, N., Rahman, M. I., Kumar, S., & Prasad, R. (2009). OFDM: Principles and challenges. In New directions in wireless communications research (pp. 29-62). Springer, Boston, MA.*
5. *Gao, F., Lu, Y., Peng, Y., Tan, P., & Li, C. (2018, December). A New Novel Improved Technique for PAPR Reduction in OFDM System. In 2018 26th International Conference on Systems Engineering (ICSEng) (pp. 1-4). IEEE.*
6. *Kedia, D., & Modi, A. (2014). Performance analysis of a modified SC-FDMA-DSCDMA technique for 4G wireless communication. Journal of Computer Networks and Communications, 2014.*
7. *Rateb, A. M., & Labana, M. (2019). An optimal low complexity PAPR reduction technique for next generation OFDM systems. IEEE Access, 7, 16406-16420.*
8. *Duman, T. M., & Ghrayeb, A. (2008). Coding for MIMO communication systems. John Wiley & Sons.*
9. *Huo, Y., Dong, X., & Xu, W. (2017). 5G cellular user equipment: From theory to practical hardware design. IEEE Access, 5, 13992-14010.*
10. *Jiang, M., & Hanzo, L. (2007). Multiuser MIMO-OFDM for next-generation wireless systems. Proceedings of the IEEE, 95(7), 1430-1469.*
11. *Alqahtani, A. H., Humadi, K., Sulyman, A. I., & Alsanie, A. (2019). Experimental Evaluation of MIMO-OFDM System with Rateless Space-Time Block Code. International Journal of Antennas and Propagation, 2019.*
12. *Ramteke, S. B., Deshmukh, A. Y., & Dekate, K. N. (2018, March). A review on design and analysis of 5G mobile communication MIMO system with OFDM. In 2018 Second International Conference on Electronics, Communication and Aerospace Technology (ICECA) (pp. 542-546). IEEE.*
13. *Sandoval, F., Poitau, G., & Gagnon, F. (2017). Hybrid peak-to-average power ratio reduction techniques: Review and performance comparison. IEEE Access, 5, 27145-27161.*
14. *Le, N. P., & Safaei, F. (2015). Antenna selection strategies for MIMO-OFDM wireless systems: An energy efficiency perspective. IEEE Transactions on Vehicular Technology, 65(4), 2048-2062.*
15. *Cho, Y. S., Kim, J., Yang, W. Y., & Kang, C. G. (2010). MIMO-OFDM wireless communications with MATLAB. John Wiley & Sons.*
16. *Wu, Y., & McAllister, J. (2013, September). Bounded selective spanning with extended fast enumeration for MIMO-OFDM systems detection. In 21st European Signal Processing Conference (EUSIPCO 2013) (pp. 1-5). IEEE.*
17. *Hisojo, M. A., Lebrun, J., & Deneire, L. (2014, November). Low PAPR and spatial diversity for OFDM schemes by using L2-orthogonal CPM ST-codes with fast decoding. In 2014 IEEE Latin-America Conference on Communications (LATINCOM) (pp. 1-6). IEEE.*
18. *Wu, H., & Li, J. (2019). Analysis and Mitigation of ICI Due to Gain Adjustment in OFDM Systems. IEEE Access, 7, 21807-21815.*

19. *Fu, Y., Krzymien, W. A., & Tellambura, C. (2007). A technique for multiuser and intercarrier interference reduction in multiple-antenna multiuser OFDM downlink. IEEE transactions on wireless communications, 6(10), 3493-3497.*
20. *Yang, M., Chen, Y., & Du, L. (2019). Interference analysis and filter parameters optimization for uplink asynchronous f-OFDM systems. IEEE Access, 7, 48356-48370.*
21. *Jayan, G., & Nair, A. K. (2018, March). Performance analysis of filtered OFDM for 5G. In 2018 International Conference on Wireless Communications, Signal Processing and Networking (WiSPNET) (pp. 1-5). IEEE.*
22. *Nambi, S. A., & Giridhar, K. (2018). Lower order modulation aided BER reduction in OFDM with index modulation. IEEE Communications Letters, 22(8), 1596-1599.*
23. *El-Absi, M., Galih, S., Hoffmann, M., El-Hadidy, M., & Kaiser, T. (2015). Antenna selection for reliable MIMO-OFDM interference alignment systems: Measurement-based evaluation. IEEE Transactions on Vehicular Technology, 65(5), 2965-2977.*
24. *Rahmati, A., Raahemifar, K., Tsiftsis, T. A., Anpalagan, A., & Azmi, P. (2018). OFDM Signal Recovery in Deep Faded Erasure Channel. IEEE Access, 7, 38798-38812.*
25. *Arbi, T., & Geller, B. (2019). Joint BER Optimization and Blind PAPR Reduction of OFDM Systems with Signal Space Diversity. IEEE Communications Letters, 23(10), 1866-1870.*
26. *Bento, P., Pereira, A., Gomes, M., Dinis, R., & Silva, V. (2019). Simplified and accurate BER analysis of magnitude modulated M-PSK signals. IET Communications, 13(10), 1443-1448.*
27. *Giannopoulos, T., & Paliouras, V. (2008, May). Relationship among BER, power consumption and PAPR. In 2008 3rd International Symposium on Wireless Pervasive Computing (pp. 633-637). IEEE.*
28. *Wang, S., Thompson, J. S., & Grant, P. M. (2017). Closed-form expressions for ICI/ISI in filtered OFDM systems for asynchronous 5G uplink. IEEE Transactions on Communications, 65(11), 4886-4898.*
29. *Hao, J., Wang, J., & Pan, C. (2016). Low complexity ICI mitigation for MIMO-OFDM in time-varying channels. IEEE Transactions on Broadcasting, 62(3), 727-735.*
30. *Xing, Z., Liu, K., & Liu, Y. (2020). Low-complexity companding function design for PAPR reduction in OFDM systems. IET Communications, 14(10), 1581-1587.*
31. *Tang, B., Qin, K., & Mei, H. (2020). A hybrid approach to reduce the PAPR of OFDM signals using clipping and companding. IEEE Access, 8, 18984-18994.*
32. *Bao, H., Fang, J., Chen, Z., Li, H., & Li, S. (2016). An efficient Bayesian PAPR reduction method for OFDM-based massive MIMO systems. IEEE Transactions on Wireless Communications, 15(6), 4183-4195.*
33. *Gökceli, S., Levanen, T., Riihonen, T., Renfors, M., & Valkama, M. (2019). Frequency-selective PAPR reduction for OFDM. IEEE Transactions on Vehicular Technology, 68(6), 6167-6171.*
34. *Anoh, K., Tanriover, C., Adebisi, B., & Hammoudeh, M. (2017-1). A new approach to iterative clipping and filtering PAPR reduction scheme for OFDM systems. IEEE Access, 6, 17533-17544.*
35. *Anoh, K., Adebisi, B., Rabie, K. M., & Tanriover, C. (2017-2). Root-based nonlinear companding technique for reducing PAPR of precoded OFDM signals. IEEE Access, 6, 4618-4629.*
36. *Kim, K. H. (2019). PAPR reduction in OFDM-IM using multilevel dither signals. IEEE Communications Letters, 23(2), 258-261.*
37. *Tang, B., Qin, K., Zhang, X., & Chen, C. (2019). A clipping-noise compression method to reduce PAPR of OFDM signals. IEEE Communications Letters, 23(8), 1389-1392.*
38. *Gupta, P., Singh, R. K., Thethi, H. P., Singh, B., & Nanda, S. K. (2019). Discrete cosine transform matrix based SLM algorithm for OFDM with diminished PAPR for M-PSK over different subcarriers. Journal of Computer Networks and Communications, 2019.*

39. *Amhaimar, L., Ahyoud, S., Elyaakoubi, A., Kaabal, A., Attari, K., & Asselman, A. (2018). PAPR reduction using fireworks search optimization algorithm in MIMO-OFDM systems. Journal of Electrical and Computer Engineering, 2018.*
40. *Wang, Y., Yang, C., & Ai, B. (2015). Iterative companding transform and filtering for reducing PAPR of OFDM signal. IEEE Transactions on Consumer Electronics, 61(2), 144-150.*
41. *Wang, J., Lv, X., & Wu, W. (2019). SCR-based tone reservation schemes with fast convergence for PAPR reduction in OFDM system. IEEE Wireless Communications Letters, 8(2), 624-627.*
42. *Ni, C., Ma, Y., & Jiang, T. (2016). A novel adaptive tone reservation scheme for PAPR reduction in large-scale multi-user MIMO-OFDM systems. IEEE Wireless Communications Letters, 5(5), 480-483.*
43. *Tarokh, V., Seshadri, N., & Calderbank, A. R. (1998). Space-time codes for high data rate wireless communication: Performance criterion and code construction. IEEE transactions on information theory, 44(2), 744-765.'*
44. *Ahmed, I., Khammari, H., Shahid, A., Musa, A., Kim, K. S., De Poorter, E., & Moerman, I. (2018). A survey on hybrid beamforming techniques in 5G: Architecture and system model perspectives. IEEE Communications Surveys & Tutorials, 20(4), 3060-3097.*
45. *Raut, S. N., & Jalnekar, R. M. (2019). Hybrid optimisation for priority-based scheduling in multi-user STBC-MIMO-OFDM. IET Communications, 13(20), 3391-3400.*
46. *Luo, H., Xu, D., & Bao, J. (2018). Outage capacity analysis of MIMO system with survival probability. IEEE Communications Letters, 22(6), 1132-1135.*
47. *Zhang, M., Zhou, X., & Wang, C. (2020). Time-Varying Sparse Channel Estimation Based on Adaptive Average and MSE Optimal Threshold in STBC MIMO-OFDM Systems. IEEE Access, 8, 177874-177895.*
48. *Tang, R., Zhou, X., & Wang, C. (2020). Kalman Filter Channel Estimation in 2× 2 and 4× 4 STBC MIMO-OFDM Systems. IEEE Access, 8, 189089-189105.*
49. *Sandoval, F., Poitau, G., & Gagnon, F. (2019). On optimizing the PAPR of OFDM signals with coding, companding, and MIMO. IEEE Access, 7, 24132-24139.*
50. *Dehri, B., Besseghier, M., Djebbar, A. B., & Dayoub, I. (2019). Blind digital modulation classification for STBC-OFDM system in presence of CFO and channels estimation errors. IET Communications, 13(17), 2827-2833.*
51. *Anoh, K., Adebisi, B., Mahama, S., Gibson, A., & Gacanin, H. (2019, November). Interference-free space-time block codes with directional beamforming for future networks. In 2019 IEEE International Conference on Microwaves, Antennas, Communications and Electronic Systems (COMCAS) (pp. 1-6). IEEE.*
52. *Sahoo, M., & Sahoo, H. K. (2019, March). Adaptive Channel Estimation & Capacity Analysis for MIMO OFDM Communication in Urban and Sub-urban Environments Using Sparse Diffusion LMS Algorithm. In 2019 IEEE 5th International Conference for Convergence in Technology (I2CT) (pp. 1-6). IEEE.*
53. *Aggarwal, P., & Bohara, V. A. (2018). Analytical characterization of dual-band multi-user MIMO-OFDM system with nonlinear transmitter constraints. IEEE Transactions on Communications, 66(10), 4536-4549.*
54. *Kundu, L., & Hughes, B. L. (2017). Enhancing capacity in compact MIMO-OFDM systems with frequency-selective matching. IEEE Transactions on Communications, 65(11), 4694-4703.*
55. *Chen, X. (2012). Spatial correlation and ergodic capacity of MIMO channel in reverberation chamber. International Journal of Antennas and Propagation, 2012.*
56. *Choudhury, S., & Gibson, J. D. (2007, November). Information transmission over fading channels. In IEEE GLOBECOM 2007-IEEE Global Telecommunications Conference (pp. 3316-3321). IEEE.*
57. *Torabi, M., Aissa, S., & Soleymani, M. R. (2006, June). MIMO-OFDM systems with imperfect channel information: capacity, outage and BER performance. In 2006 IEEE International Conference on Communications (Vol. 12, pp. 5342-5347). IEEE.*

58. *Adejumobi, B. S., & Pillay, N. (2019). RF mirror media-based space-time block coded spatial modulation techniques for two time-slots. IET Communications, 13(15), 2313-2321.*
59. *Wu, C., Xiao, Y., Xiao, L., Yang, P., Lei, X., & Xiang, W. (2019). Space-time block coded rectangular differential spatial modulation: System design and performance analysis. IEEE Transactions on Communications, 67(9), 6586-6597.*
60. *Shao, Y., Wang, L., & Cao, X. (2019). On the performance of space-time block coded spatial modulation transmission for full-duplex relay networks. IEEE Access, 7, 180976-180985.*
61. *Xiao, L., Xiao, Y., Yang, P., Liu, J., Li, S., & Xiang, W. (2017). Space-time block coded differential spatial modulation. IEEE Transactions on Vehicular Technology, 66(10), 8821-8834.*
62. *Alamouti, S. M. (1998). A simple transmit diversity technique for wireless communications. IEEE Journal on selected areas in communications, 16(8), 1451-1458.*
63. *Coşkun, A. F., & Kucur, O. (2019). Secrecy outage probability of conventional and modified TAS/Alamouti-STBC schemes with power allocation in the presence of feedback errors. IEEE Transactions on Vehicular Technology, 68(3), 2609-2623.*
64. *Roopa, M., & Shobha, B. N. (2019, May). Performance Improvement Of MIMO System Using OSTBC Scheme and ML Detection Technique Under Rayleigh Channel. In 2019 4th International Conference on Recent Trends on Electronics, Information, Communication & Technology (RTEICT) (pp. 1431-1435). IEEE.*
65. *Mishra, S. K., & Kulat, K. D. (2018). Reduced Feedback Rate Schemes for Transmit Antenna Selection With Alamouti Coding. IEEE Access, 6, 10028-10040.*
66. *Dlodlo, B., Xu, H., & Pillay, N. (2018). Bandwidth efficiency improvement for differential Alamouti space-time block codes using M-QAM. SAIEE Africa Research Journal, 109(4), 217-223.*
67. *Kumar, R., & Saxena, R. (2014). Performance analysis of mimo-stbc systems with higher coding rate using adaptive semiblind channel estimation scheme. The Scientific World Journal, 2014.*
68. *Nandi, S., Nandi, A., & Pathak, N. N. (2017, December). Performance analysis of Alamouti STBC MIMO OFDM for different transceiver system. In 2017 International Conference on Intelligent Sustainable Systems (ICISS) (pp. 883-887). IEEE.*
69. *Pattanayak, P., Trivedi, V. K., Chakraborty, S., & Kumar, P. (2017, February). BER performance of multi user scheduling for MIMO-STBC and MIMO-OFDM broadcast network with imperfect CSI. In 2017 4th International conference on signal processing and integrated networks (SPIN) (pp. 66-70). IEEE.*
70. *Lee, D. (2018) Performance analysis of dual selection with maximal ratio combining over nonidentical imperfect channel estimation. IEEE Transactions on Vehicular Technology, 67(3), 2819-2823.*
71. *Van Luong, T., & Ko, Y. (2018). The BER analysis of MRC-aided greedy detection for OFDM-IM in presence of uncertain CSI. IEEE Wireless Communications Letters, 7(4), 566-569.*
72. *Beaulieu, N. C., & Zhang, Y. (2017). Linear diversity combining on correlated and unequal power Nakagami-0.5 fading channels. IEEE Communications Letters, 21(5), 1003-1006.*
73. *Mishra, M., Mishra, B. K., & Bansode, R. S. (2017, February). Performance evaluation of MIMO-OFDM systems using MRC and EGT for wireless channels. In 2017 Fourteenth International Conference on Wireless and Optical Communications Networks (WOCN) (pp. 1-6). IEEE.*
74. *Das, P., & Subadar, R. (2017, July). Performance analysis of QAM for M-MRC receiver over TWDP fading channels. In 2017 8th International Conference on Computing, Communication and Networking Technologies (ICCCNT) (pp. 1-5). IEEE.*
75. *Tiwari, K., & Saini, D. S. (2014, December). BER performance comparison of MIMO system with STBC and MRC over different fading channels. In 2014 International Conference on High Performance Computing and Applications (ICHPCA) (pp. 1-6). IEEE.*
76. *Ahn, K. S. (2009). Performance analysis of MIMO-MRC system in the presence of multiple interferers and noise over Rayleigh fading channels. IEEE Transactions on wireless communications, 8(7), 3727-3735.*

77. *Jiang, T., Chen, D., Ni, C., & Qu, D. (2017). OQAM/FBMC for Future Wireless Communications: Principles, Technologies and Applications. Academic Press.*
78. *Stepniak, G., Schüppert, M., & Bunge, C. A. (2017). Polymer-optical fibres for data transmission. In Polymer Optical Fibres (pp. 217-310). Woodhead Publishing.*
79. *Garg, V. K. (2007). Fourth Generation Systems and New Wireless Technologies. en. Wireless Communications & Networking. Elsevier, 23-1.*
80. *Han, S. H., & Lee, J. H. (2005). An overview of peak-to-average power ratio reduction techniques for multicarrier transmission. IEEE wireless communications, 12(2), 56-65.*
81. *Jaradat, A. M., Hamamreh, J. M., & Arslan, H. (2019). Modulation options for OFDM-based waveforms: classification, comparison, and future directions. IEEE Access, 7, 17263-17278.*
82. *Chiueh, T. D., Tsai, P. Y., Lai. I-Wei, & Chiueh, T. D. (2012). Baseband receiver design for wireless MIMO-OFDM communications. New York: Wiley.*
83. *Abdelgader, A. M. S., & Wu, L. (2015). Design of a multiorder ofdm frequency diversity approach. Mathematical Problems in Engineering, 2015*
84. *Hassan, A. Y. (2015). Code-time diversity for direct sequence spread spectrum systems. Wireless Personal Communications, 84(1), 695-718.*
85. *Humadi, K. M., Sulyman, A. I., & Alsanie, A. (2014). Spatial modulation concept for massive multiuser MIMO systems. International Journal of Antennas and Propagation, 2014.*
86. *Proakis, J. G., Salehi, M., Zhou, N., & Li, X. (1994). Communication systems engineering (Vol. 2). New Jersey: Prentice Hall.*
87. *Litsyn, S. (2007). Peak power control in multicarrier communications. Cambridge University Press.*
88. *Sharma, C., Sharma, P. K., Tomar, S. K., & Gupta, A. K. (2011, April). A modified Iterative Amplitude clipping and filtering technique for PAPR reduction in OFDM systems. In 2011 International Conference on Emerging Trends in Networks and Computer Communications (ETNCC) (pp. 365-368). IEEE.*
89. *Zhu, X., Pan, W., Li, H., & Tang, Y. (2013). Simplified approach to optimized iterative clipping and filtering for PAPR reduction of OFDM signals. IEEE Transactions on Communications, 61(5), 1891-1901.*
90. *Armstrong, J. (2002). Peak-to-average power reduction for OFDM by repeated clipping and frequency domain filtering. Electronics letters, 38(5), 246-247.*
91. *Badran, E. F., & El-Helw, A. M. (2011). A novel semi-blind selected mapping technique for PAPR reduction in OFDM. IEEE Signal Processing Letters, 18(9), 493-496.*
92. *Gupta, P., & Singh, R. K. (2015, December). Highly optimized Selected Mapping based peak to average power ratio reduction OFDM system using different modulation schemes. In 2015 Third International Conference on Image Information Processing (ICIIP) (pp. 261-264). IEEE.*
93. *Le Goff, S. Y., Al-Samahi, S. S., Khoo, B. K., Tsimenidis, C. C., & Sharif, B. S. (2009). Selected mapping without side information for PAPR reduction in OFDM. IEEE Transactions on Wireless Communications, 8(7), 3320-3325.*
94. *Heo, S. J., Noh, H. S., No, J. S., & Shin, D. J. (2007, September). A modified SLM scheme with low complexity for PAPR reduction of OFDM systems. In 2007 IEEE 18th International Symposium on Personal, Indoor and Mobile Radio Communications (pp. 1-5). IEEE.*
95. *Zaidi, A., Athley, F., Medbo, J., Gustavsson, U., Durisi, G., & Chen, X. (2018). 5G Physical Layer: principles, models and technology components. Academic Press.*
96. *Konar, A., & Sidiropoulos, N. D. (2018). A simple and effective approach for transmit antenna selection in multiuser massive MIMO leveraging sub-modularity. IEEE Transactions on Signal Processing, 66(18), 4869-4883.*
97. *Jafarkhani, H. (2005). Space-time coding: theory and practice. Cambridge university press.*
98. *Telatar, E. (1999). Capacity of multi‐antenna Gaussian channels. European transactions on telecommunications, 10(6), 585-595.*

Citation from Websites:

- *http://www.wirelesscommunication.nl/reference/about.htm*
- *Wireless Communication Reference Website © Jean-Paul M.G. Linnartz*
- *(Editor-in-Chief), 1996-2010.*
- *https://forum.huawei.com/enterprise/en/5g/thread/541471-869*
- *https://www.javatpoint.com/history-of-wireless-communication*
- *https://www.nap.edu/read/5968/chapter/4*
- *https://www.microwavejournal.com/articles/24759-history-of-wireless-communications*
- *https://www.researchgate.net*
- *http://www.dsplog.com*
- *https://www.sciencedirect.com*
- *https://www.dsprelated.com*

About the Authors

Dr. Balram D. Timande is working as an Associate Professor in the Department of Electronics and Telecommunication Engineering at Guru Nanak Institute of Engineering and Technology, Nagpur, Maharashtra, India. He graduated with a B.E. in Electronics Engineering from R.T.M.N.U., Nagpur University (M.S.), and obtained his postgraduate degree (M. Tech.) in Electronics and Telecommunication Engineering from C.S.V.T.U., Bhilai, C.G., India. He was awarded a Ph.D. in Electronics Engineering from MATS University, Raipur, C.G., India. With over 29 years of experience, Dr. Timande has been actively worked in Industry for more than 09 years and has been engaged in research and teaching activities for more than 20 years. He has published over 22 research papers in reputed, Scopus-indexed, and SCI-E international journals, and has presented numerous papers at national journals, National and International conferences. His primary areas of research interest include Embedded System Design, Wireless Communications, Ad-hoc Sensor Networks, and Industrial Instrumentation.

Dr. Hemant Vithalrao Hajare is working as the Principal at Guru Nanak Institute of Engineering and Technology, Nagpur, Maharashtra, India. He graduated with a B.E. in Civil Engineering and earned his postgraduate degree (M.Tech) in Hydraulics from Visvesvaraya Regional College of Engineering (VRCE), affiliated with R.T.M.N.U., Nagpur University (M.S.). He was awarded a Ph.D. in Civil Engineering from NEERI, RTMNU, Nagpur. With over 35 years of teaching experience, he also possesses administrative experience, having served as Principal, Dean of Academics, and Head of Department for more than 35 years.Dr. Hajare has been actively involved with various professional societies and has served on various statutory bodies of different universities. Engaged in research and teaching for over 20 years, he has published more than 40 research papers in reputed, Scopus-indexed, and SCI-E international journals. He has also presented numerous papers at national and international conferences. His primary areas of research interest include Hydraulic Engineering, Water Resources Engineering, and Irrigation Engineering.

Published By

Innovative Scientific Publication
Nagpur (MS), India Email:
ijiesjournal@gmail.com
Ph: 7972481655
http://ijies.net/books

9 788196 873042